Chapter 6

Enhancement of Performance Parameters of JLT

6.1 Introduction

Junctionless transistor posses numerous advantages as compared to conventional MOS devices due to absence of a junction. However, JLT suffers from several drawbacks also, among which the following two are most prominent and causes performance degradation of the device [1-3].

1. higher off-state current
2. carrier mobility degradation

Consequently, in this chapter approaches for mitigation of above two problems has been proposed, modelled and analyzed.

In the JLT for proper switching off of the device, the body region of the device should remain fully depleted and to achieve this condition the work function difference between the gate material and the substrate should be sufficiently high so that the resulting electric field can keep the device in fully depleted condition [4-20]. If this condition is not achieved proper turn off will not be possible. A high-k gate dielectric can also be used to reduce the leakage current[21]. However most of the high-k dielectrics are not compatible with Silicon and use of high-k dielectric reduces the carrier mobility due to excessive lateral electric field. In addition JLT requires high substrate doping concentration for achieving a good conductivity in its on-state. However, high doping concentration results in Coulombic scattering which leads to carrier mobility degradation. Consequently in conjunction with the technique for reduction of leakage current, carrier mobility enhancement techniques have also been developed in this chapter. Some of the techniques proposed here for mobility enhancement can be used for leakage current reduction also.

In addition to the above drawbacks, corner effect is also observed in some non-conventional structures of JLT such as, rectangular, pentagonal, hexagonal etc. In such devices two electric flux lines at the corner are not parallel and mutually crossed at a point

away from the oxide semiconductor interface. At that point the resultant electric field is considerably higher causing premature local turn on of the device [22-26].

In case of cylindrical device although the flux lines are not parallel there is a uniformity throughout the entire periphery. Hence such localized effect is not observed. However, the packing density of circular device is less compared to rectangular or hexagonal device. Consequently, for getting a higher packing density the possible device structures are rectangular or hexagonal. With these structures possibility of device failure is present due to corner effect. In this chapter a new technique for reduction of the corner effect is presented, modelled and analyzed.

6.2 Leakage Current Reduction

Leakage current in any MOS devices imposes limitation on the gate length minimization. In order to find the minimum possible gate length upto which a device can be scaled down the gate leakage as well as drain leakage have to be considered. As discussed in Chapter 3 the scale length is the parameter from which the minimum gate length can be obtained upto which a MOS based device such as JLT can be scaled down. The scale length depends on the following quantities-

1.Channel thickness (t_{si})

2.Gate oxide thickness (t_{ox})

3.Dielectric constant of gate dielectric (ϵ_{ox})

4.Dielectric constant of substrate semiconductor (ϵ_{si})

To find out the minimum possible gate length for a JLT structure the possible combination of t_{si} and t_{ox} has to be found out for which the scale length will be minimum for a particular gate dielectric and substrate material.

Let us consider the gate dielectric to be SiO_2, substrate material to be n-type Silicon with doping concentration 10^{19} /cm^3 , the drain to source voltage to be V_{ds}=0.1 V and work function of gate material is φ_M=5.4eV.

For a Double gate JLT, from the threshold voltage expression, the expression for gate dielectric thickness (t_{ox}) can be obtained as,

$$t_{ox} = \frac{(8 \in_{ox} \in_{si} (V_{ds} + V_{fb} - V_{Th}) - \in_{ox} t_{si}^2 qN_d)}{4t_{si} \in_{si} qN_d} \tag{6.1}$$

The breakdown field of SiO_2 is 0.5 GV/m

Therefore the maximum possible threshold voltage will be

$$V_{Thmax}=0.5\text{x}10^9\text{x}t_{ox} \tag{6.2}$$

Putting (6.2) in (6.1),

$$t_{ox} = \frac{(8 \in_{ox} \in_{si} (V_{ds} + V_{fb} - V_{Th\max}) - \in_{ox} t_{si}^2 qN_d)}{4t_{si} \in_{si} qN_d}$$

$$t_{ox} = \frac{(8 \in_{ox} \in_{si} (V_{ds} + V_{fb} - 0.5\times 10^9 t_{ox}) - \in_{ox} t_{si}^2 qN_d)}{4t_{si} \in_{si} qN_d}$$

or,
$$t_{ox} = \frac{(8 \in_{ox} \in_{si} (V_{ds} + V_{fb}) - \in_{ox} t_{si}^2 qN_d)}{(4\times 10^9 \in_{ox} \in_{si} + 4t_{si} \in_{si} qN_d)} \tag{6.3}$$

Again atomic diameter of Si is 0.333 nm. Hence the minimum possible channel thickness is t_{si}= 0.333 nm

Hence the minimum possible gate oxide thickness will be

t_{ox}=1.7133 nm

The scale length will be

$$\lambda = \sqrt{\frac{t_{si}(4 \in_{si} t_{ox} + \in_{ox} t_{si})}{8 \in_{ox}}} = 0.91276nm$$

The relationship between minimum gate length and scale length can be obtained from subthreshold current. For a double gate JLT subthreshold current expression can be written as,

$$I_d = \frac{\phi(\Delta L) - \phi(0)}{R_d(V_{gs}, V_{ds})}$$

Where,

$$\phi_0(0) = \left[\frac{V_{ds}(e^{\frac{L+L_d}{\lambda}} - e^{\frac{L+L_d-2L_s}{\lambda}}) + (-\frac{qN_d}{\in_{si}} - \frac{1}{\lambda^2}\phi_{gs})\lambda^2(e^{\frac{L+L_d}{\lambda}} - e^{-\frac{L_s}{\lambda}} - e^{\frac{L+L_d-2L_s}{\lambda}} + e^{\frac{2(L+L_d)-L_s}{\lambda}} - e^{2\frac{L+L_d}{\lambda}} + e^{-2\frac{L_s}{\lambda}})}{(e^{2\frac{L+L_d}{\lambda}} - e^{-2\frac{L_s}{\lambda}})} \right]$$

$$= V_{ds}\frac{(e^{\frac{L+L_d}{\lambda}} - e^{\frac{L+L_d-2L_s}{\lambda}})}{(e^{2\frac{L+L_d}{\lambda}} - e^{-2\frac{L_s}{\lambda}})} - \phi_{gs}\frac{(e^{\frac{L+L_d}{\lambda}} - e^{-\frac{L_s}{\lambda}} - e^{\frac{L+L_d-2L_s}{\lambda}} + e^{\frac{2(L+L_d)-L_s}{\lambda}} - e^{2\frac{L+L_d}{\lambda}} + e^{-2\frac{L_s}{\lambda}})}{(e^{2\frac{L+L_d}{\lambda}} - e^{-2\frac{L_s}{\lambda}})}$$

$$-\frac{qN_d}{\in_{si}}\lambda^2\frac{(e^{\frac{L+L_d}{\lambda}} - e^{-\frac{L_s}{\lambda}} - e^{\frac{L+L_d-2L_s}{\lambda}} + e^{\frac{2(L+L_d)-L_s}{\lambda}} - e^{2\frac{L+L_d}{\lambda}} + e^{-2\frac{L_s}{\lambda}})}{(e^{2\frac{L+L_d}{\lambda}} - e^{-2\frac{L_s}{\lambda}})}$$

$$\phi_0(\Delta L) =$$

$$V_{ds}\frac{(e^{\frac{L+L_d+\Delta L}{\lambda}} - e^{\frac{L+L_d-2L_s-\Delta L}{\lambda}})}{(e^{2\frac{L+L_d}{\lambda}} - e^{-2\frac{L_s}{\lambda}})} - \phi_{gs}\frac{(e^{\frac{L+L_d+\Delta L}{\lambda}} - e^{\frac{-L_s+\Delta L}{\lambda}} - e^{\frac{L+L_d-2L_s-\Delta L}{\lambda}} + e^{\frac{2(L+L_d)-L_s-\Delta L}{\lambda}} - e^{2\frac{L+L_d}{\lambda}} + e^{-2\frac{L_s}{\lambda}})}{(e^{2\frac{L+L_d}{\lambda}} - e^{-2\frac{L_s}{\lambda}})}$$

$$-\frac{qN_d}{\in_{si}}\lambda^2\frac{(e^{\frac{L+L_d+\Delta L}{\lambda}} - e^{-\frac{L_s+\Delta L}{\lambda}} - e^{\frac{L+L_d-2L_s-\Delta L}{\lambda}} + e^{\frac{2(L+L_d)-L_s-\Delta L}{\lambda}} - e^{2\frac{L+L_d}{\lambda}} + e^{-2\frac{L_s}{\lambda}})}{(e^{2\frac{L+L_d}{\lambda}} - e^{-2\frac{L_s}{\lambda}})}$$

$$R_d(V_{gs}, V_{ds}) = \frac{1}{q\mu_p p_n}\frac{\Delta L}{Wt_{si}}$$

$$I_d = \frac{q\mu_p p_n W t_{si}\left\{\begin{array}{l} V_{ds}(e^{\frac{L+L_d+\Delta L}{\lambda}} - e^{\frac{L+L_d-2L_s-\Delta L}{\lambda}} - e^{\frac{L+L_d}{\lambda}} + e^{\frac{L+L_d-2L_s}{\lambda}}) \\ -\phi_{gs}(e^{\frac{L+L_d+\Delta L}{\lambda}} - e^{\frac{-L_s+\Delta L}{\lambda}} - e^{\frac{L+L_d-2L_s-\Delta L}{\lambda}} + e^{\frac{2(L+L_d)-L_s-\Delta L}{\lambda}} \\ -e^{\frac{L+L_d}{\lambda}} + e^{-\frac{L_s}{\lambda}} + e^{\frac{L+L_d-2L_s}{\lambda}} - e^{\frac{2(L+L_d)-L_s}{\lambda}}) \\ -\frac{qN_d}{\in_{si}}\lambda^2(e^{\frac{L+L_d+\Delta L}{\lambda}} - e^{\frac{-L_s+\Delta L}{\lambda}} - e^{\frac{L+L_d-2L_s-\Delta L}{\lambda}} + e^{\frac{2(L+L_d)-L_s-\Delta L}{\lambda}} \\ -e^{\frac{L+L_d}{\lambda}} + e^{-\frac{L_s}{\lambda}} + e^{\frac{L+L_d-2L_s}{\lambda}} - e^{\frac{2(L+L_d)-L_s}{\lambda}}) \end{array}\right\}}{(e^{2\frac{L+L_d}{\lambda}} - e^{-2\frac{L_s}{\lambda}})\Delta L} \tag{6.4}$$

Equation (6.4) can be rearranged as,

$$e^{\frac{2L}{\lambda}}P - e^{\frac{L}{\lambda}}Q - R = 0$$

or, $$e^{\frac{L}{\lambda}} = \frac{Q+\sqrt{Q^2+4PR}}{2P}$$

The minimum gate length and scale length relationship is,

$$\frac{L}{\lambda} = \ln\left\{\frac{Q+\sqrt{Q^2+4PR}}{2P}\right\}$$

Where,

$$P = \left\{\begin{array}{l} I_d e^{\frac{2L_d}{\lambda}}\Delta L + \phi_{gs} q\mu_p p_n W t_{si}(e^{\frac{2L_d-L_s-\Delta L}{\lambda}} - e^{\frac{2L_d-L_s}{\lambda}}) \\ +\frac{qN_d}{\in_{si}} q\mu_p p_n W t_{si}\lambda^2(e^{\frac{2L_d-L_s-\Delta L}{\lambda}} - e^{\frac{2L_d-L_s}{\lambda}}) \end{array}\right\}$$

$$Q=\begin{Bmatrix} q\mu_p p_n W t_{si} V_{ds}(e^{\frac{L_d+\Delta L}{\lambda}} - e^{\frac{L_d-2L_s-\Delta L}{\lambda}} - e^{\frac{L_d}{\lambda}} + e^{\frac{L_d-2L_s}{\lambda}}) \\ -q\mu_p p_n W t_{si}\phi_{gs}(e^{\frac{L_d+\Delta L}{\lambda}} - e^{\frac{L_d-2L_s-\Delta L}{\lambda}} - e^{\frac{L_d}{\lambda}} + e^{\frac{L_d-2L_s}{\lambda}}) \\ -\frac{qN_d}{\in_{si}} q\mu_p p_n W t_{si}\lambda^2(e^{\frac{L_d+\Delta L}{\lambda}} - e^{\frac{L_d-2L_s-\Delta L}{\lambda}} - e^{\frac{L_d}{\lambda}} + e^{\frac{L_d-2L_s}{\lambda}}) \end{Bmatrix}$$

$$R = q\mu_p p_n W t_{si}\begin{Bmatrix} \phi_{gs}(e^{\frac{-L_s+\Delta L}{\lambda}} - e^{-\frac{L_s}{\lambda}}) + \\ \frac{qN_d}{\in_{si}}\lambda^2(e^{\frac{-L_s+\Delta L}{\lambda}} - e^{-\frac{L_s}{\lambda}}) \end{Bmatrix} - I_d e^{-2\frac{L_s}{\lambda}}\Delta L$$

Maximum tolerable leakage current is 100 nA/µm [27]. Therefore, the minimum gate length can be obtained as L_{min}= 3.316xλ= 3.0267 nm

Similarly, for pentagonal JLT, the expression for gate dielectric thickness (t_{oxp}) can be obtained as,

$$t_{oxp} = \frac{(37.85 \in_{ox}\in_{si}(V_{ds}+V_{fb}-V_{Th}) - 3.61\in_{ox} t_{si} qN_d)}{9.5\in_{si} qN_d} \tag{6.5}$$

$$t_{oxp} = \frac{(37.85 \in_{ox}\in_{si}(V_{ds}+V_{fb}) - 3.61\in_{ox} t_{si} qN_d)}{(18.9\times 10^9 \in_{ox}\in_{si} + 9.5\in_{si} qN_d)} \tag{6.6}$$

For a pentagonal JLT,

Diameter of inner circle=1.38t_{si}

Hence minimum possible side length is,

t_{si}=0.333/1.38=0.241 nm

Hence the minimum possible gate oxide thickness will be

t_{ox}=1.6528 nm

The scale length is

λ=0.7574nm

and the minimum gate length= 3.546xλ= 2.6857 nm

for hexagonal JLT, the expression for gate dielectric thickness (t_{oxh}) can be obtained as,

$$t_{oxh} = \frac{((4+2\sqrt{3}) \in_{ox} \in_{si} (V_{ds} + V_{fb} - V_{Th\max}) - \sqrt{3} \in_{ox} t_{si}^{2} qN_d)}{2\sqrt{3} t_{si} \in_{si} qN_d} \quad (6.7)$$

$$t_{oxh} = \frac{(4+2\sqrt{3}) \in_{ox} \in_{si} (V_{ds} + V_{fb}) - \sqrt{3} \in_{ox} t_{si}^{2} qN_d}{(2+\sqrt{3}) \times 10^{9} \in_{ox} \in_{si} + 2\sqrt{3} t_{si} \in_{si} qN_d} \quad (6.8)$$

For a hexagonal JLT,

Diameter of inner circle=1.73t_{si}

Hence minimum possible side length is,

t_{si}=0.333/1.73=0.192 nm

Hence the minimum possible gate oxide thickness will be

t_{ox}=1.6462 nm

The scale length is

λ=0.4314nm

and the minimum gate length= 3.324xλ= 1.434 nm

For octagonal JLT, the expression for gate dielectric thickness (t_{oxo}) can be obtained as,

$$t_{oxo} = \frac{\in_{ox} \in_{si} (V_{ds} + V_{fb} - V_{Th\max}) - 0.6 \in_{ox} t_{si}^{2} qN_d}{0.36 t_{si} \in_{si} qN_d} \quad (6.9)$$

$$t_{oxo} = \frac{\in_{ox}\in_{si}(V_{ds}+V_{fb})-0.6\in_{ox}t_{si}^{2}qN_d}{0.5\times10^9\in_{ox}\in_{si}+0.36t_{si}\in_{si}qN_d} \tag{6.10}$$

For a octagonal JLT,

Diameter of inner circle=2t_{si}

Hence minimum possible side length is,

t_{si}=0.333/2=0.1665 nm

Hence the minimum possible gate oxide thickness will be

t_{ox}=1.6503 nm

The scale length is

λ=0.7246nm

and the minimum gate length= 3.123xλ= 2.2629 nm

For rectangular JLT, the expression for gate dielectric thickness (t_{oxr}) can be obtained as,

$$t_{oxr} = \frac{8\in_{ox}\in_{si}(a_{si}+b_{si})(V_{ds}+V_{fb}-V_{Th\max})-\in_{ox}qN_d b_{si}a_{si}^{2}-\in_{ox}qN_d a_{si}b_{si}^{2}}{4a_{si}b_{si}\in_{si}qN_d} \tag{6.11}$$

$$t_{oxr} = \frac{8\in_{ox}\in_{si}(a_{si}+b_{si})(V_{ds}+V_{fb})-\in_{ox}qN_d b_{si}a_{si}^{2}-\in_{ox}qN_d a_{si}b_{si}^{2}}{4\times10^9\in_{ox}\in_{si}(a_{si}+b_{si})+4a_{si}b_{si}\in_{si}qN_d} \tag{6.12}$$

For a rectangular JLT, the scale length is minimum when width to thickness ratio is one (square). Hence considering a square JLT

Diameter of inner circle=t_{si}

Hence minimum possible side length is,

t_{si}=0.333 nm

Hence the minimum possible gate oxide thickness will be

t_{ox}=1.6469 nm

The scale length is

λ=0.4723nm

and the minimum gate length= 3.47xλ= 1.6389 nm

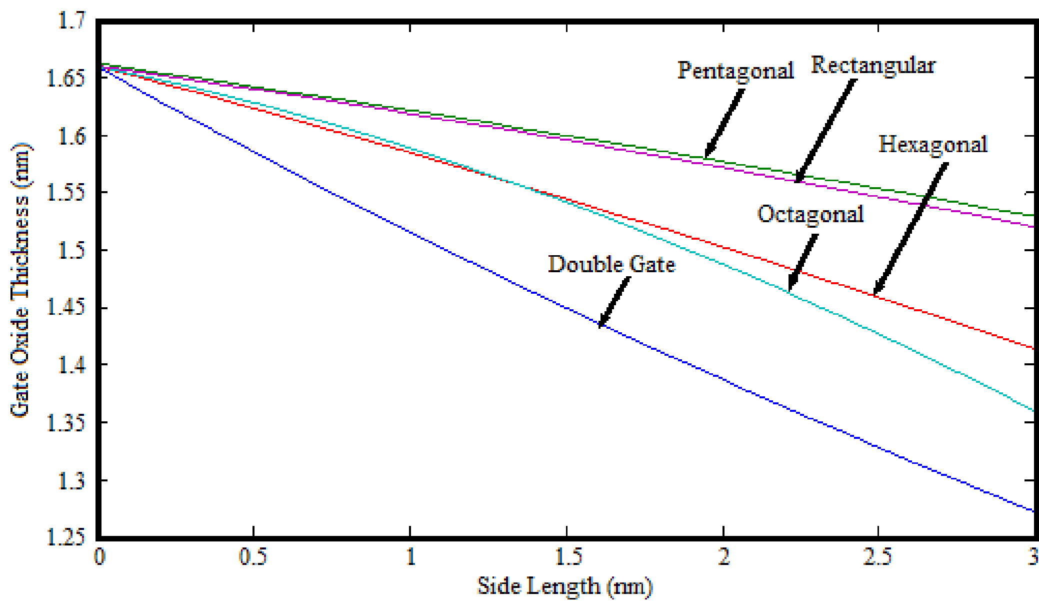

Fig. 6.1: Variation Minimum Possible Gate Oxide Thickness with Channel Thickness

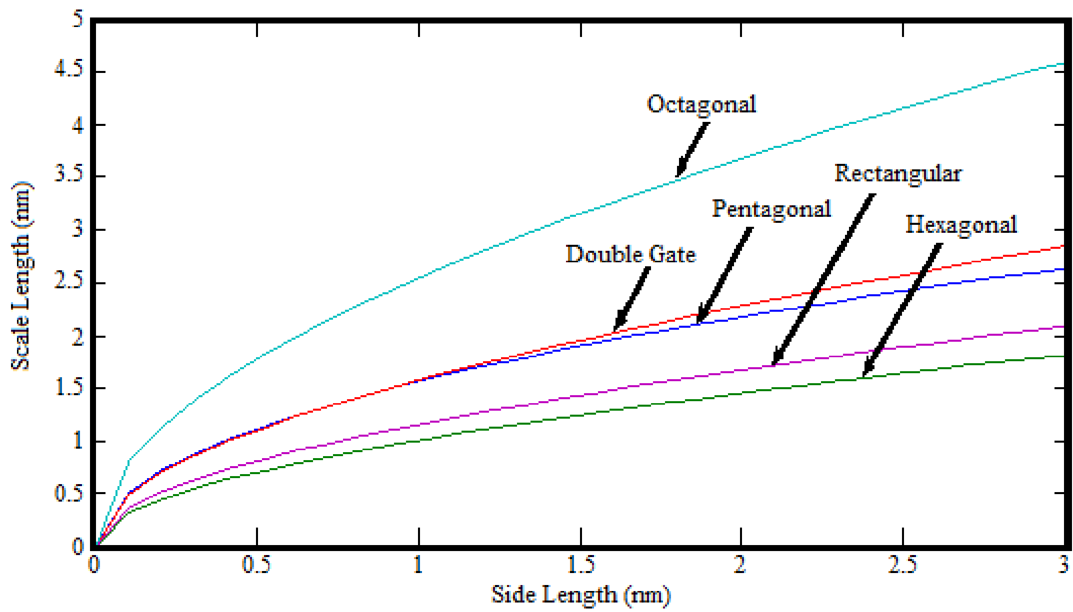

Fig. 6.2: Variation Minimum Possible Scale Length with Channel Thickness

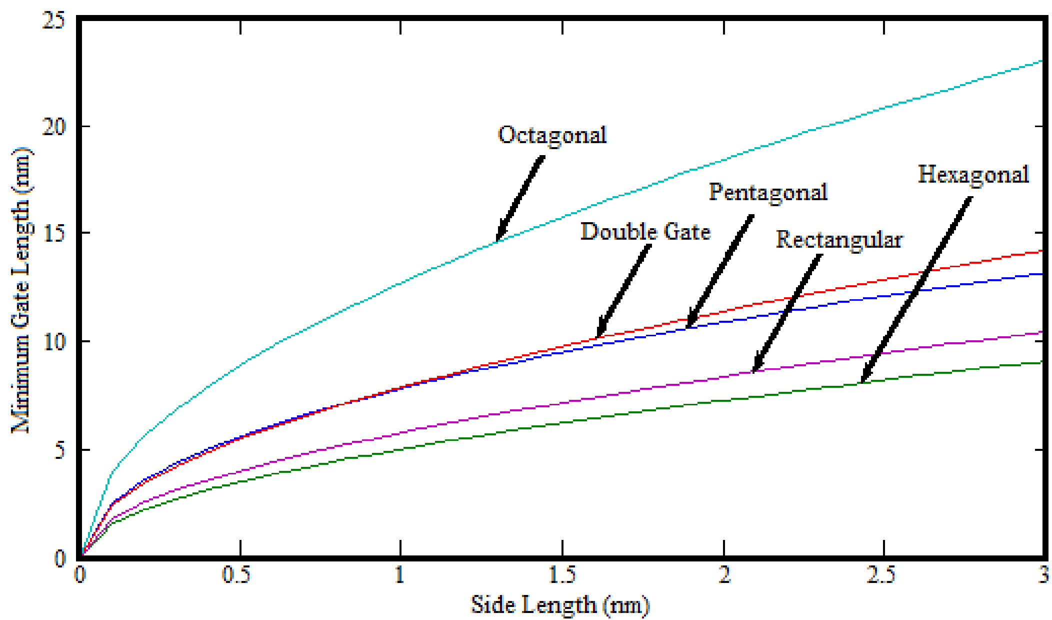

Fig. 6.3: Variation Minimum Gate Length with Channel Thickness

Table 6.1: A comparison of minimum gate length for different materials at breakdown field (0.5 GV/m for SiO_2, 0.2 GV/m for HfO_2)

Structures	Minimum t_{ox} (nm)				Minimum gate length (nm)			
	Si		Ge		Si		Ge	
	SiO_2	HfO_2	SiO_2	HfO_2	SiO_2	HfO_2	SiO_2	HfO_2
Double Gate	1.7133	4.0930	1.6100	4.0932	3.0267	1.2387	2.4926	1.4297
Pentagonal	1.6528	4.1448	1.6528	4.1449	2.6857	1.0117	2.3432	1.0112
Hexagonal	1.6462	4.1342	1.6462	4.1344	1.434	0.5819	1.1832	0.6720
Octagonal	1.6503	4.1358	1.6505	4.1389	2.2629	1.3497	2.5188	1.5579
Rectangular	1.6469	4.1348	1.6470	4.1351	1.6389	0.8874	1.6655	1.0199

Table 6.2: A comparison of minimum gate length for different materials for 0.1GV/m

Structures	Minimum t_{ox} (nm)				Minimum gate length (nm)			
	Si		Ge		Si		Ge	
	SiO_2	HfO_2	SiO_2	HfO_2	SiO_2	HfO_2	SiO_2	HfO_2
Double Gate	7.1887	8.0770	7.1892	8.0775	4.5914	1.5988	4.9820	2.2360
Pentagonal	7.8893	8.2690	8.0835	8.2692	4.6267	1.5328	3.7027	1.6045
Hexagonal	7.9698	8.2384	7.9702	8.2388	2.2796	0.7583	2.1289	0.9089
Octagonal	8.0733	8.2568	8.0739	8.2575	4.6507	1.6170	4.4551	1.9137
Rectangular	7.9897	8.2415	7.9902	8.2421	3.0595	1.0697	2.9022	1.2711

Table 6.3: A comparison of minimum gate length for different materials for 0.08 GV/m

Structures	Minimum t_{ox} (nm)				Minimum gate length (nm)			
	Si		Ge		Si		Ge	
	SiO_2	HfO_2	SiO_2	HfO_2	SiO_2	HfO_2	SiO_2	HfO_2
Double Gate	9.9065	10.029	8.6959	10.030	4.1281	1.8780	4.7849	2.1735
Pentagonal	9.5186	10.323	10.036	10.324	4.2210	1.8394	4.8920	2.1271
Hexagonal	9.8646	10.279	9.8650	10.280	2.0854	0.8928	2.4174	1.0335
Octagonal	10.024	10.308	10.025	10.309	4.2702	1.8415	4.9498	2.1313
Rectangular	9.8952	10.039	8.8959	10.285	2.7929	1.2325	3.2363	1.4238

6.2.1 The Method for Leakage Current Reduction

The leakage during off state is maximum at the middle of the channel along y-direction as the lateral electric field that creates the depletion is minimum. When it is required to develop a device having high current capability the channel thickness may go high. This may result in insufficient depletion along the central axis of the device. This situation can be aggravated if the work function of the gate material is not sufficiently high. To overcome this problem a layer of dielectric can be placed at the centre of the channel where the electric field is weakest as shown in Fig. 6.4. By placing so the region where the electric field is weakest becomes devoid of any carriers due to the presence of that dielectric material. During the on state adequate amount of current will flow through the rest of the channel region as the channel is heavily doped. The placement of the dielectric layer may increase the threshold voltage. By selecting a dielectric with proper dimension and dielectric constant it is possible to adjust the threshold voltage as per requirement. For drain current modelling of the modified structure the approach adopted in last chapter can be adopted. The segmentation of the modified structure is shown in Fig. 6.5. The equivalent circuit of one segment of the

modified structure is shown in Fig. 6.6. It is a parallel combination of five resistances- two depletion layer resistances ($R_d(x, V_{gs}, V_{ds})$), two non-depletion layer resistances ($R_{nd}(x, V_{gs}, V_{ds})$) and the centre dielectric resistance (R_{di}).

The resistance provided by centre dielectric is given by,

$$R_{di} = \rho \frac{\Delta L}{W t_{di}}$$

Where, ρ is the resistivity of the dielectric

The equivalent circuit reduces to parallel combination of two depletion layer resistances and the centre dielectric resistance when the segment is fully depleted and parallel combination of two non-depletion layer resistances and the centre dielectric resistance when the segment is completely neutral. However all the five resistances appear when the device is partially depleted.

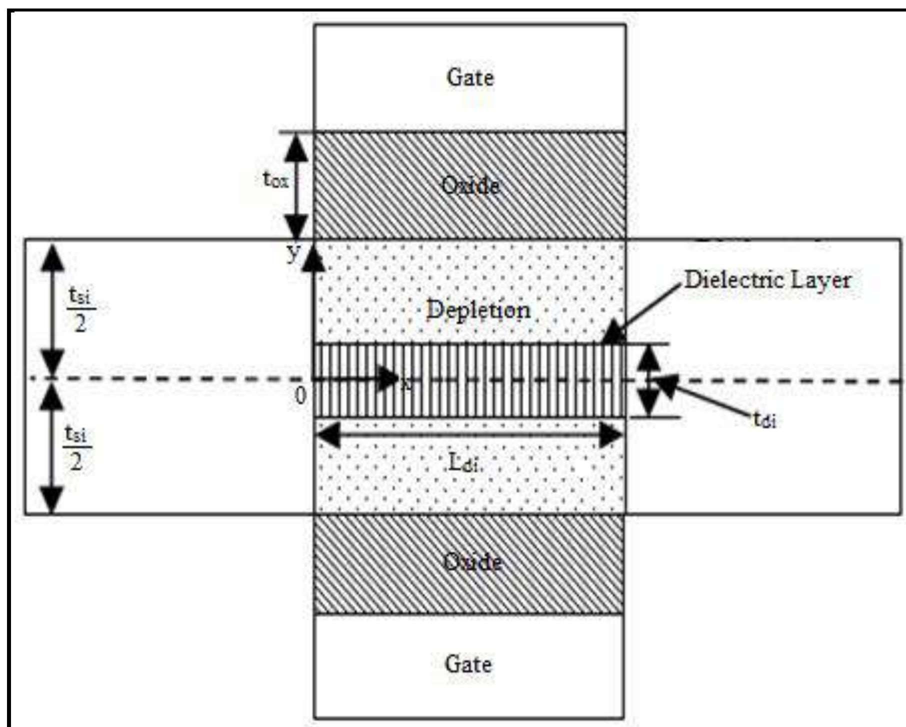

Fig. 6.4: Cross sectional view of a double gate JLT with dielectric at channel centre

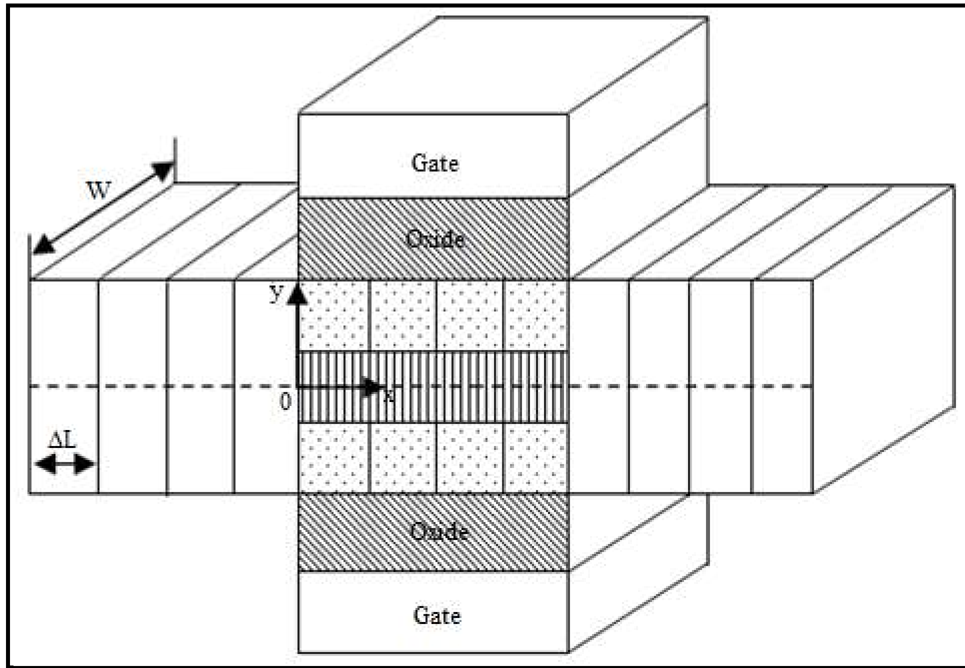

Fig. 6.5: 3-D view of a double gate JLT with dielectric at channel centre showing segmentation

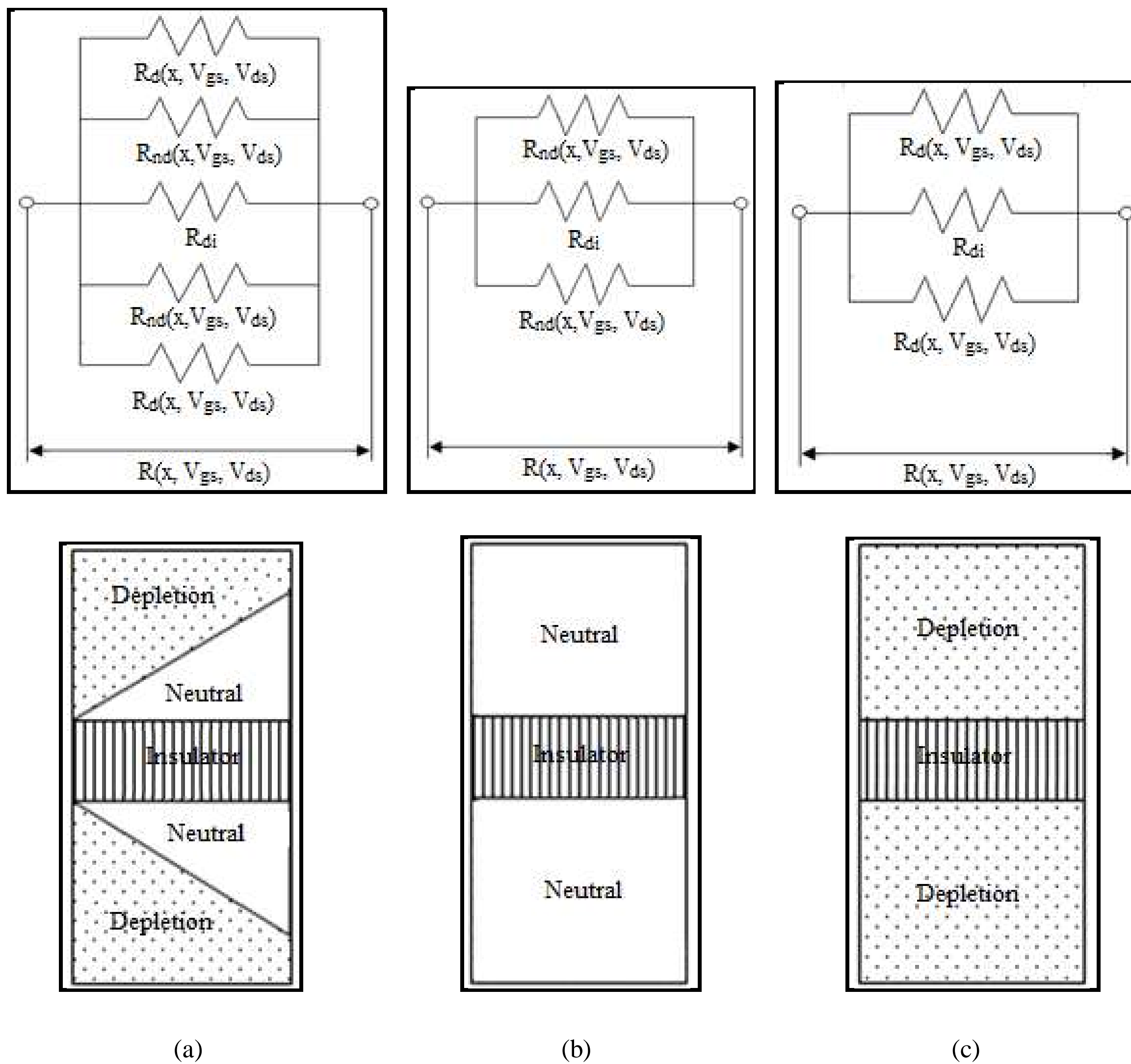

Fig. 6.6: Equivalent circuit of a segment (a) A segment with combination of insulator, depletion and neutral semiconductor region (b) A segment with combination of insulator and neutral semiconductor region (c) A segment with combination of insulator and depletion region

The equivalent resistance of one segment is,

$R^{/}(x, V_{gs},V_{ds})=R_d(x, V_{gs},V_{ds})||R_{nd}(x, V_{gs},V_{ds})\ ||R_{di}\ ||R_{nd}(x, V_{gs},V_{ds})||R_d(x,V_{gs},V_{ds})$ (6.13)

The drain current through one segment for the proposed structure can be obtained by replacing $R(x, V_{gs},V_{ds})$ with $R^{/}(x, V_{gs},V_{ds})$ in equation (5.6) of chapter 5

$$I_d^{/} = \frac{\phi\{(m+1)\Delta L\} - \phi(m\Delta L)}{R^{/}(V_{gs}, V_{ds})} \qquad (6.14)$$

Considering the complete channel the drain current expression can also be written as,

$$I_d^{/} = \frac{\phi(L) - \phi(0)}{\sum_{x=0}^{L} R^{/}(x, V_{gs}, V_{ds})} \qquad (6.15)$$

6.2.2 Results and Discussion and Validation

The model is simulated in MATLAB simulation environment. Result obtained in the MATLAB simulation has been compared with the simulation result obtained from Cogenda VisualTCAD 1.8.2 2D device simulator. Fermi Dirac statistics is used for all the simulations. The transfer characteristics of the modified structure is compared with that of conventional structures.

Fig. 6.7 shows the transfer characteristic of JLT for t_{di}=2nm, 4nm, 6nm. The length of the dielectric is L_{di}=10nm and the dielectric constant is 3.9. The drain current in the subthreshold decreases as the thickness of the dielectric increases as it is able to block more leakage current with higher thickness of the centre dielectric.

Fig. 6.8 shows the transfer characteristic for L_{di}=6nm, 8nm, 10nm. The thickness of the dielectric is t_{di}=2nm and the dielectric constant is 3.9. The drain current decreases with increase in length of the central dielectric as the resistance offered by the dielectric increases with increase in length.

Fig. 6.9 shows the transfer characteristic for ϵ_{di}=3.9, 10, 22. The length and thickness of the dielectric are L_{di}=10nm, t_{di}=2nm. The subthreshold current decreases for higher dielectric constant of the dielectric.

The comparison of current density variation with gate voltage for different dimensions and dielectric constant shows that the proposed structure exhibits better subthreshold behaviour with reduced off-state leakage current. The current reduces with increase in length, thickness and dielectric constant of the dielectric placed at the central axis.

In Fig. 6.10 a comparison of the present structure with conventional structure is done keeping effective channel area same at 100nm^2. From the figure it is clear that the leakage current reduction by placing a dielectric layer at the channel centre is not simply because of effective channel thickness reduction. In all the simulations SiO_2(ϵ_{ox}=3.9) has been taken as the gate dielectric and the work function of the gate material is taken as Φ_M= 5.4eV. In all the figures it is seen that the subthreshold current of the JLT with centre dielectric is less compared to the conventional JLT, while in the on state the drain current density for all the structures of JLT are almost equal. The model is in close agreement with TCAD simulation results. Although the drain current expression shown in equation (6.15), takes the complete channel into account, to reduce computation time expression of equation (6.14) may be used which is fully analytical in nature. The comparison for computation of the two models is shown in table 6.4.

Table 6.4 Comparison of simulation of two drain current models

	Simulation time
TCAD	11 sec
Equation (6.15)	0.915 sec
Equation (6.14)	0.124 sec

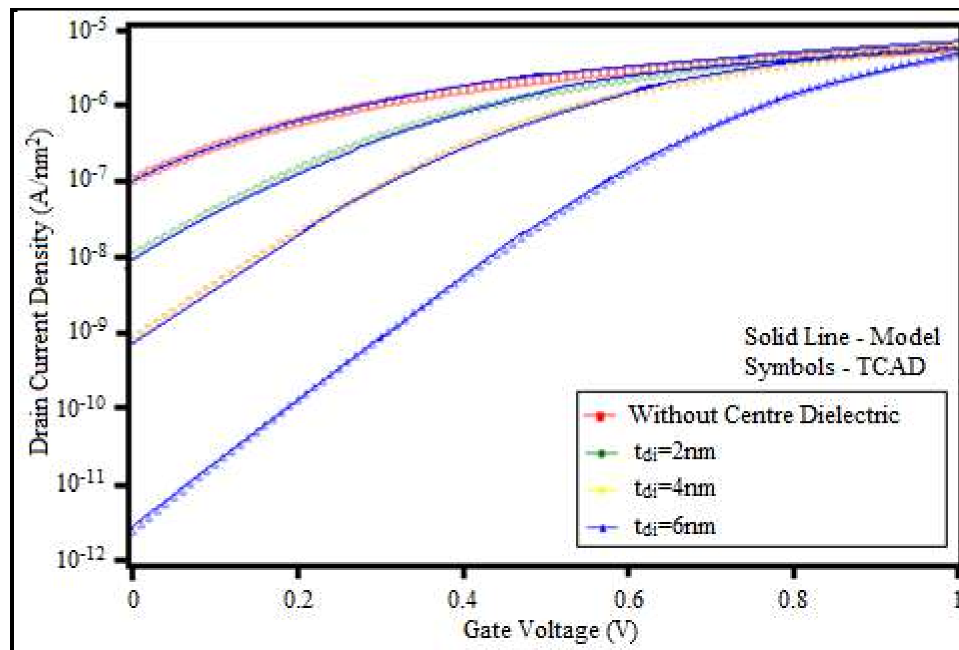

Fig. 6.7: Transfer Characteristic Comparison for different centre dielectric thickness

Average Error = 4.5%

Maximum error =6.9%

Minimum error =0%

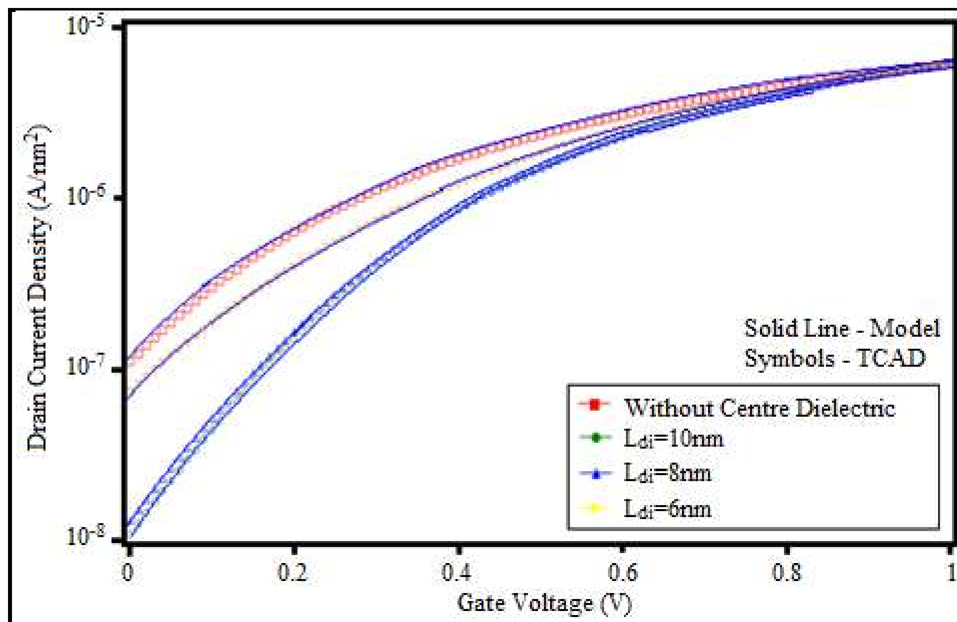

Fig. 6.8: Transfer Characteristic Comparison for different dielectric constant value of centre dielectric

Average Error = 4.2%
Maximum error =6.5%
Minimum error =0%

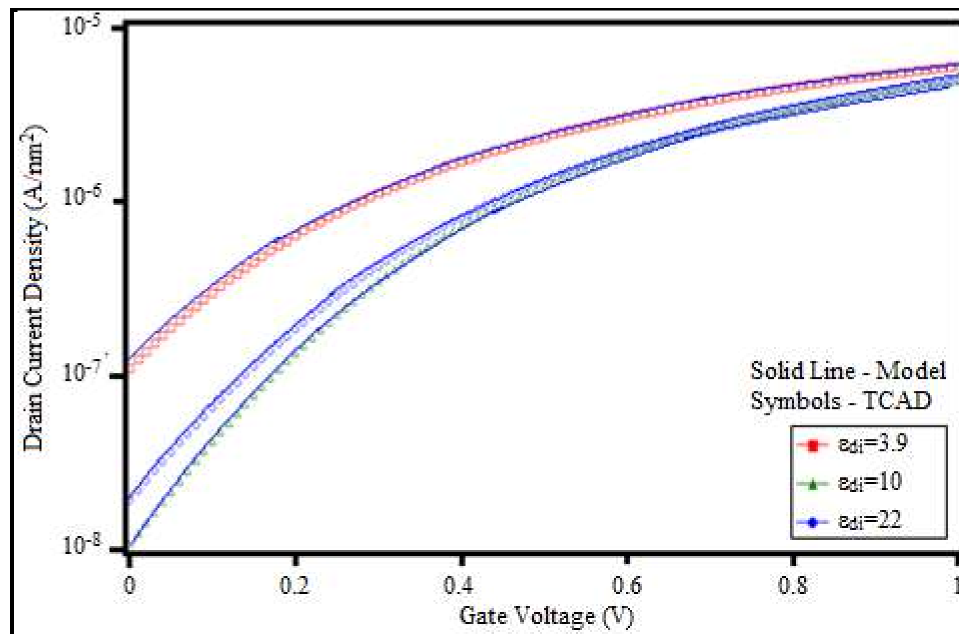

Fig. 6.9: Transfer Characteristic Comparison for different centre dielectric length

Average Error = 2.75%
Maximum error =5.1%
Minimum error =0%

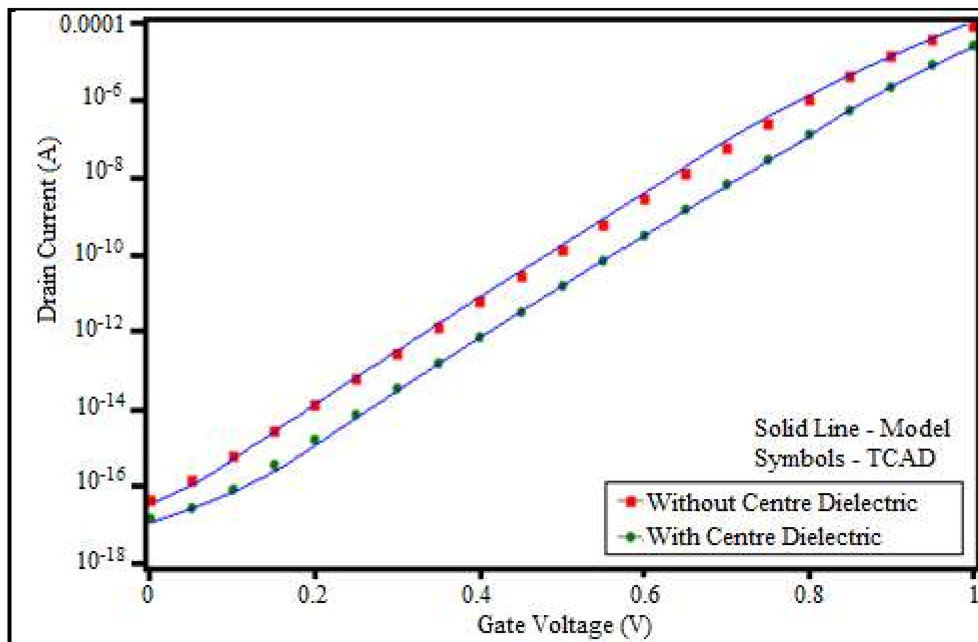

Fig. 6.10: Transfer Characteristic Comparison of conventional JLT and JLT with centre dielectric layer with same effective channel area (200 nm^2)

Average Error = 3.15%
Maximum error =6.3%
Minimum error =0%

6.3 Mobility Enhancement

In this section two techniques are proposed to enhance the carrier mobility of a DG JLT.

1. The first technique uses two gate dielectrics placed diagonally with each other. The dielectrics used are SiO_2 and HfO_2 with dielectric constants 3.9 and 22 respectively. The dielectrics are placed in following two ways.

    a. Symmetrically as shown in Fig. 6.11

    b. Asymmetrically as shown in Fig. 6.12

2. The second technique uses a gradual doping concentration variation in the channel as shown in Fig. 6.13. The doping profile of the channel is shown in Fig. 6.14

6.3.1 Drain Current Model for The Proposed Structures

(a) Structures With Diagonal Dielectric

The effective dielectric constant of the Symmetric structures is,

$$\in_{ox}^{/} = \frac{\in_{ox1}\in_{ox2} L}{(L-x)\in_{ox2} + x\in_{ox1}} \tag{6.16}$$

The depletion width for the structure of Fig. 6.11 can be obtained by replacing $\in_{ox}$ with $\in_{ox}^{/}$ in the depletion width expression obtained in chapter 4 as,

$$W_{ds}^{/} = t_{si} - \sqrt{\frac{4t_{si}\in_{si} t_{ox} qN_d + \in_{ox}^{/} t_{si}^{2} qN_d - 8\in_{ox}^{/}\in_{si}(\phi_{gs}-\phi_0)}{\in_{ox}^{/} qN_d}} \tag{6.17}$$

Replacing W_d with $W_{ds}^{/}$ in resistance expressions of chapter 5 the drain current expression can be obtained for the structure.

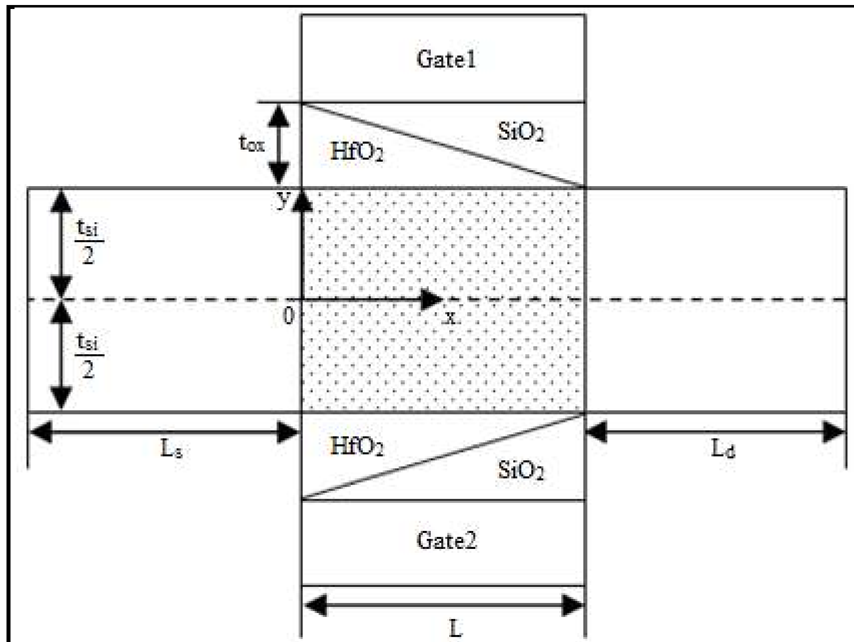

Fig. 6.11: Cross sectional view of a Symmetric DG JLT with two dielectrics diagonally placed

Channel length (L)	20nm
Source-Drain length (L_s=L_d)	5nm
Channel thickness (t_{si})	10nm
Gate oxide thickness (t_{ox})	2nm

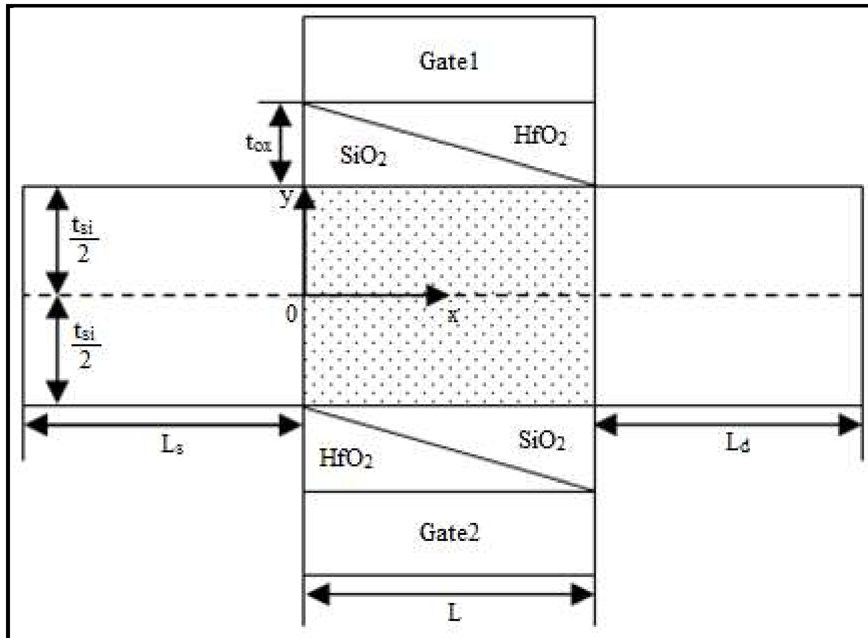

Fig. 6.12: Cross sectional view of a Asymmetric DG JLT with two dielectrics diagonally placed

Channel length (L)	20nm
Source-Drain length (L_s=L_d)	5nm
Channel thickness (t_{si})	10nm
Gate oxide thickness (t_{ox})	2nm

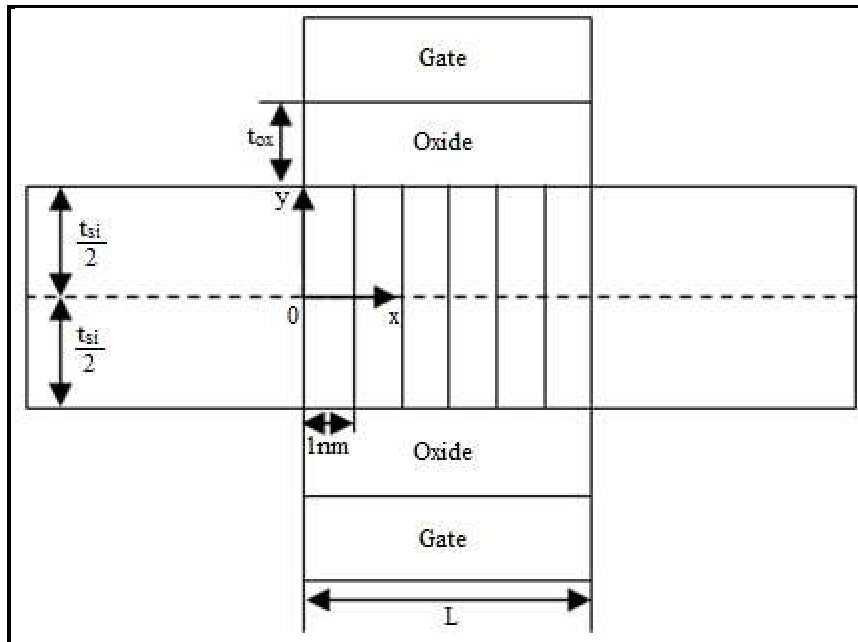

Fig. 6.13: Cross sectional view of a DG JLT with gradual variation of doping concentration in the channel

Channel length (L)	20nm
Source-Drain length (L_s=L_d)	5nm
Channel thickness (t_{si})	10nm
Gate oxide thickness (t_{ox})	2nm

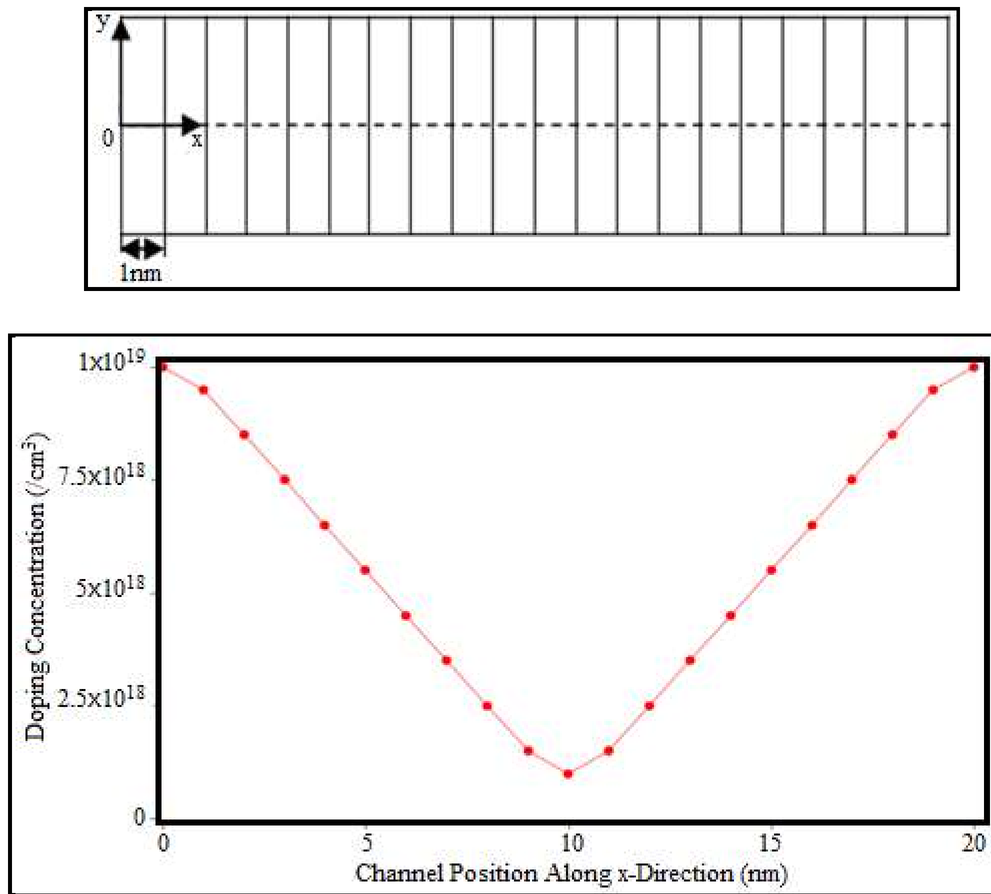

Fig. 6.14: Doping profile of the DG JLT with gradual variation of doping concentration

For the asymmetric structure of Fig. 6.12 the effective dielectric constant for gate1 and gate2 are-

$$\in_{oxg1} = \frac{\in_{ox1}\in_{ox2} L}{(L-x)\in_{ox1} + x\in_{ox2}}$$

$$\in_{oxg2} = \frac{\in_{ox1}\in_{ox2} L}{(L-x)\in_{ox2} + x\in_{ox1}}$$

The depletion width variation due to gate1 and gate2 for the structure of Fig. 6.12 are

$$W_{d1} = \frac{4(\in_{si} t_{ox} qN_d + t_{si}\in_{oxg1} qN_d)}{4\in_{oxg1} qN_d} + \frac{\sqrt{16(\in_{si} t_{ox} qN_d + t_{si}\in_{oxg1} qN_d)^2 - 8\in_{oxg1} qN_d (2\in_{oxg1}\in_{si}(\phi_{gs}-\phi_{01}) - \in_{oxg1} t_{si}^2 qN_d)}}{4\in_{oxg1} qN_d}$$

and

$$W_{d2} = \frac{-4(\in_{si} t_{ox} qN_d - t_{si}\in_{oxg2} qN_d)}{4\in_{oxg2} qN_d} + \frac{\sqrt{16(\in_{si} t_{ox} qN_d - t_{si}\in_{oxg2} qN_d)^2 + 8\in_{oxg2} qN_d (\in_{oxg2} t_{si}^2 qN_d - 2\in_{oxg2}\in_{si}(\phi_{gs}-\phi_{02}))}}{4\in_{oxg2} qN_d}$$

Total depletion width can be written as,

$$W_{da} = W_{d1} + W_{d2} \tag{6.18}$$

The electric field due to the two gates of the asymmetric structure will be different. Consequently, the depletion width for the two halves of the device will start reducing at two different gate voltages, V_{th1} and V_{th2}. The overall threshold voltage of the device will be the minimum of these two values of the gate voltage. Hence the threshold voltage for the proposed asymmetric structure can be written as,

$$V_{th} = \min(V_{th1}, V_{th2})$$

Where,

$$V_{th1} = \phi_{01} + V_{fb} + \frac{\in_{oxg1} t_{si}^{2} q N_d + 4 \in_{si} t_{ox} t_{si} q N_d}{2 \in_{oxg1} \in_{si}} \tag{6.19}$$

$$V_{th2} = \phi_{02} + V_{fb} - \frac{\in_{oxg2} t_{si}^{2} q N_d - 4 \in_{si} t_{ox} t_{si} q N_d}{2 \in_{oxg2} \in_{si}} \tag{6.20}$$

The longitudinal potential at the centre of the channel due to gate1 and gate2 respectively can be given as,

$$\phi_{01}(x) = \left[\frac{(V_{ds} + C_a \lambda_1^{2}) e^{\frac{L+L_d}{\lambda_1}} - \frac{C_a \lambda_1^{2}}{e^{\frac{L_s}{\lambda_1}}}}{(e^{2\frac{L+L_d}{\lambda_1}} - e^{-2\frac{L_s}{\lambda_1}})} e^{\frac{x}{\lambda_1}} \right] -$$

$$\left[\frac{\{(V_{ds} + C_a \lambda_1^{2}) e^{\frac{L+L_d}{\lambda_1}} - \frac{C_a \lambda_1^{2}}{e^{\frac{L_s}{\lambda_1}}}\} e^{-2\frac{L_s}{\lambda_1}} - C_a \lambda_1^{2} (e^{2\frac{L+L_d}{\lambda_1}} - e^{-2\frac{L_s}{\lambda_1}}) e^{\frac{L_s}{\lambda_1}}}{(e^{2\frac{L+L_d}{\lambda_1}} - e^{-2\frac{L_s}{\lambda_1}})} e^{-\frac{x}{\lambda_1}} \right] - C_a \lambda_2^{2} \tag{6.21}$$

$$\phi_{02}(x)=\left[\frac{(V_{ds}+C_b\lambda_2^{\,2})e^{\frac{L+L_d}{\lambda_2}}-\dfrac{C_b\lambda_2^{\,2}}{e^{\frac{L_s}{\lambda_2}}}}{(e^{2\frac{L+L_d}{\lambda_2}}-e^{-2\frac{L_s}{\lambda_2}})}e^{\frac{x}{\lambda_2}}\right]-$$

$$\left[\frac{\{(V_{ds}+C_b\lambda_2^{\,2})e^{\frac{L+L_d}{\lambda_2}}-\dfrac{C_b\lambda_2^{\,2}}{e^{\frac{L_s}{\lambda_2}}}\}e^{-2\frac{L_s}{\lambda_2}}-C_b\lambda_2^{\,2}(e^{2\frac{L+L_d}{\lambda_2}}-e^{-2\frac{L_s}{\lambda_2}})e^{\frac{L_s}{\lambda_2}}}{(e^{2\frac{L+L_d}{\lambda_2}}-e^{-2\frac{L_s}{\lambda_2}})}e^{-\frac{x}{\lambda_2}}\right]-C_b\lambda_2^{\,2}$$

(6.22)

Where,

$$C_a=-\frac{qN_d}{\in_{si}}-\frac{1}{\lambda_1^{\,2}}\phi_{gs}$$

$$C_b=-\frac{qN_d}{\in_{si}}-\frac{1}{\lambda_2^{\,2}}\phi_{gs}$$

Total longitudinal potential at the centre of the channel can be given as,

$$\phi_0^{/}(x)=\phi_{01}(x)-\phi_{02}(x) \tag{6.23}$$

The drain current expressions for the proposed structures can be obtained by replacing the W_d and $\phi_0(x)$ in the drain current expressions of chapter 5 with $W_{da}^{/}$ and $\phi_0^{/}(x)$ obtained from (6.18) and (6.23).

Fig. 6.13 shows a DG JLT with gradual variation of doping in the channel. The doping in the source and drain region is kept constant at $10^{19}/cm^3$ while in the channel it is maximum at the source-channel and drain-channel boundary ($10^{19}/cm^3$) and gradually decreases in the x- direction to a minimum of $10^{18}/cm^3$ at the middle of the channel. Gradual doping variation keeps all the features of a JLT. The doping profile for the structure is shown in Fig. 6.14.

(b) The Structure With Gradual Doping Concentration

The expression for the doping variation with channel position can be given as,

$$N_d(x) = ax^2 + bx + c$$

Where,

$$a = \frac{4(N_{d\max} - N_{d\min})}{L^2}$$

$$b = -\frac{4(N_{d\max} - N_{d\min})}{L}$$

$$c = N_{d\max}$$

$N_{d\max}$ is the maximum doping concentration and $N_{d\min}$ is the minimum doping concentration, L is the channel length.

$$N_d(x) = \frac{4(N_{d\max} - N_{d\min})}{L^2}x^2 - \frac{4(N_{d\max} - N_{d\min})}{L}x + N_{d\max} \tag{6.24}$$

The drain current expression for the structure of Fig. 6.13 can be obtained by replacing N_d with $N_d(x)$ in equation (5.19) of chapter 5.

6.3.2 Mobility Model for The Proposed Structures

(a) Structures With Diagonal Dielectric

Field dependent mobility expression for n-type and p-type semiconductor can be written as [28],

$$\mu_n = -\frac{v_d}{E} = -1.55\times10^3\left[\frac{1}{1+(\frac{E}{6.91\times10^3})^{1.11}}\right]^{0.9} \tag{6.25}$$

$$\mu_n = -\frac{v_d}{E} = -5.75\times10^2\left[\frac{1}{1+(\frac{E}{1.45\times10^4})^{2.637}}\right]^{0.38} \tag{6.26}$$

The longitudinal and lateral electric field for the symmetric two dielectric structure is obtained by taking the negative gradient of potential obtained in chapter 4 as,

$$E_1(x) = -\frac{d\phi(x,y)}{dx} = -\frac{d\phi_0(x)}{dx} + \frac{4\in_{ox}^{/}}{t_{si}(4t_{ox}\in_{si} + t_{si}\in_{ox}^{/})}\frac{d\phi_0(x)}{dx}y^2 \tag{6.27}$$

where,

$$\frac{d\phi_0(x)}{dx} = \frac{1}{\lambda}\left[\begin{array}{c} \dfrac{(V_{ds}+C\lambda^2)e^{\frac{L+L_d}{\lambda}} - \dfrac{C\lambda^2}{e^{\frac{L_s}{\lambda}}}}{(e^{2\frac{L+L_d}{\lambda}} - e^{-2\frac{L_s}{\lambda}})}e^{\frac{x}{\lambda}} + \\ \dfrac{\{(V_{ds}+C\lambda^2)e^{\frac{L+L_d}{\lambda}} - \dfrac{C\lambda^2}{e^{\frac{L_s}{\lambda}}}\}e^{-2\frac{L_s}{\lambda}} - C\lambda^2(e^{2\frac{L+L_d}{\lambda}} - e^{-2\frac{L_s}{\lambda}})e^{\frac{L_s}{\lambda}}}{(e^{2\frac{L+L_d}{\lambda}} - e^{-2\frac{L_s}{\lambda}})}e^{-\frac{x}{\lambda}} \end{array}\right] \tag{6.28}$$

and

$$E_1(y) = -\frac{d\phi(x,y)}{dy} = -\frac{8\in_{ox}^{/}}{t_{si}(4t_{ox}\in_{si} + t_{si}\in_{ox}^{/})}\{\phi_{gs} - \phi_0(x)\}y \tag{6.29}$$

Therefore the mobility variation in x and y direction can be written as,

$$\mu_{n1}(x) = -1.55\times10^3\left[\frac{1}{1+(\frac{E_1(x)}{6.91\times10^3})^{1.11}}\right]^{0.9} \tag{6.30}$$

$$\mu_{n1}(y) = -1.55\times10^3\left[\frac{1}{1+(\frac{E_1(y)}{6.91\times10^3})^{1.11}}\right]^{0.9} \tag{6.31}$$

Hole mobility expressions can also be written proceeding in a similar way.

$$\mu_{p1}(x) = -5.75\times10^2\left[\frac{1}{1+(\frac{E_1(x)}{1.45\times10^4})^{2.637}}\right]^{0.38} \tag{6.32}$$

$$\mu_{p1}(y) = -5.75\times10^2\left[\frac{1}{1+(\frac{E_1(y)}{1.45\times10^4})^{2.637}}\right]^{0.38} \tag{6.33}$$

For the asymmetric structure the electric field due to the two gates are different in magnitude and opposite in direction to each other. Hence the resultant electric field which can be obtained by taking the vector addition of the two electric fields due to the two gates is simply the difference between the two electric fields. The longitudinal and lateral electric field for the asymmetric two dielectric structure is obtained as,

$$E_2(x) = \frac{d\phi_{02}(x)}{dx} - \frac{\phi_{01}(x)}{dx} - \left[\frac{4\in_{ox2}}{t_{si}(4\in_{si} t_{ox} + \in_{ox2} t_{si})}(\frac{\phi_{02}(x)}{dx}) - \frac{4\in_{ox1}}{t_{si}(4\in_{si} t_{ox} + \in_{ox1} t_{si})}(\frac{d\phi_{01}(x)}{dx})\right] y^2 \tag{6.34}$$

Where,

$$\frac{d\phi_{01}(x)}{dx} = \frac{1}{\lambda_1}\left[\frac{(V_{ds} + C_a\lambda_1^2)e^{\frac{L+L_d}{\lambda_1}} - \frac{C_a\lambda_1^2}{e^{\frac{L_s}{\lambda_1}}}}{(e^{2\frac{L+L_d}{\lambda_1}} - e^{-2\frac{L_s}{\lambda_1}})} e^{\frac{x}{\lambda_1}} + \frac{\{(V_{ds} + C_a\lambda_1^2)e^{\frac{L+L_d}{\lambda_1}} - \frac{C_a\lambda_1^2}{e^{\frac{L_s}{\lambda_1}}}\}e^{-2\frac{L_s}{\lambda_1}} - C_a\lambda_1^2(e^{2\frac{L+L_d}{\lambda_1}} - e^{-2\frac{L_s}{\lambda_1}})e^{\frac{L_s}{\lambda_1}}}{(e^{2\frac{L+L_d}{\lambda_1}} - e^{-2\frac{L_s}{\lambda_1}})} e^{-\frac{x}{\lambda_1}}\right] \tag{6.35}$$

and

$$\frac{d\phi_{02}(x)}{dx} = \frac{1}{\lambda_2}\left[\frac{(V_{ds}+C_b\lambda_2^{\,2})e^{\frac{L+L_d}{\lambda_2}}-\frac{C_b\lambda_2^{\,2}}{e^{\frac{L_s}{\lambda_2}}}}{(e^{2\frac{L+L_d}{\lambda_2}}-e^{-2\frac{L_s}{\lambda_2}})}e^{\frac{x}{\lambda_2}} + \frac{\{(V_{ds}+C_b\lambda_2^{\,2})e^{\frac{L+L_d}{\lambda_2}}-\frac{C_b\lambda_2^{\,2}}{e^{\frac{L_s}{\lambda_2}}}\}e^{-2\frac{L_s}{\lambda_2}}-C_b\lambda_2^{\,2}(e^{2\frac{L+L_d}{\lambda_2}}-e^{-2\frac{L_s}{\lambda_2}})e^{\frac{L_s}{\lambda_2}}}{(e^{2\frac{L+L_d}{\lambda_2}}-e^{-2\frac{L_s}{\lambda_2}})}e^{-\frac{x}{\lambda_2}}\right] \tag{6.36}$$

$$E_2(y) = \left[\frac{8\in_{ox2}}{t_{si}(4\in_{si}t_{ox}+\in_{ox2}t_{si})}(\phi_{gs}-\phi_{02}(x))-\frac{8\in_{ox1}}{t_{si}(4\in_{si}t_{ox}+\in_{ox1}t_{si})}(\phi_{gs}-\phi_{01}(x))\right]y \tag{6.37}$$

Therefore the electron mobility variation in x and y direction can be written as,

$$\mu_{n2}(x) = -1.55\times10^{3}\left[\frac{1}{1+(\frac{E_2(x)}{6.91\times10^{3}})^{1.11}}\right]^{0.9} \tag{6.38}$$

$$\mu_{n2}(y) = -1.55\times10^{3}\left[\frac{1}{1+(\frac{E_2(y)}{6.91\times10^{3}})^{1.11}}\right]^{0.9} \tag{6.39}$$

Hole mobility expressions can also be written in a similar way.

$$\mu_{p2}(x) = -5.75\times10^{2}\left[\frac{1}{1+(\frac{E_2(x)}{1.45\times10^{2}})^{2.637}}\right]^{0.38} \quad (6.40)$$

$$\mu_{p2}(y) = -5.75\times10^{2}\left[\frac{1}{1+(\frac{E_2(y)}{1.45\times10^{4}})^{2.637}}\right]^{0.38} \quad (6.41)$$

(b) The Structure With Gradual Doping Concentration

Doping dependent expression for mobility can be given as [28],

$$\mu_n = 88T_n^{-0.57} + \frac{1250T_n^{-2.33}}{1+\left[\frac{N_d}{1.26\times10^{17}T_n^{2.4}}\right]0.88T_n^{-0.146}} \quad (6.42)$$

$$\mu_p = 54.3T_n^{-0.57} + \frac{407T_n^{-2.33}}{1+\left[\frac{N_d}{2.35\times10^{17}T_n^{2.4}}\right]0.88T_n^{-0.146}} \quad (6.43)$$

Where,

$T_n = \frac{T}{300}$, T is temperature in Kelvin. Considering T as the room temperature (300K) mobility expression can be written as,

$$\mu_n = 88 + \frac{1250}{1+\left[\frac{N_d}{1.26\times10^{17}}\right]0.88} \quad (6.44)$$

$$\mu_p = 54.3 + \frac{407}{1+\left[\frac{N_d}{2.35\times10^{17}}\right]0.88} \quad (6.45)$$

Substituting $N_d(x)$ from (6.24) in (6.44) and (6.45) the mobility expressions for the structure with gradual doping variation can be obtained as,

$$\mu_{n3} = 88 + \frac{1250}{1 + \left[\frac{N_d(x)}{1.26 \times 10^{17}}\right]0.88} \tag{6.46}$$

$$\mu_{p3} = 54.3 + \frac{407}{1 + \left[\frac{N_d(x)}{2.35 \times 10^{17}}\right]0.88} \tag{6.47}$$

6.3.3 Results, Discussion and Validation

The models for the proposed structures simulated in MATLAB simulation environment. Result obtained in the MATLAB simulation has been compared with the simulation result obtained from Cogenda VisualTCAD 1.8.2 2D device simulator. Fermi-Dirac statistics is used throughout all the simulations.

Fig. 6.15-6.20 shows the comparison of electron and hole mobility variation and electric field variation with channel position along x and y directions in the subthreshold region ($V_{gs} < V_{th}$). In Fig. 6.15 longitudinal electric field variation with channel position along x direction is shown. In Fig. 6.16 transverse electric field variation with channel position along y direction is shown. In Fig. 6.17 electron mobility variation with channel position along x direction is shown. In Fig. 6.18 hole mobility variation with channel position along x direction is shown. In Fig. 6.19 electron mobility variation with channel position along y direction is shown. In Fig. 6.20 hole mobility variation with channel position along y direction is shown.

Fig. 6.21-6.26 shows the comparison of electron and hole mobility variation and electric field variation with channel position along x and y directions in the on state ($V_{gs} > V_{th}$). In Fig. 6.21 longitudinal electric field variation with channel position along x direction is shown. In Fig. 6.22 transverse electric field variation with channel position along y direction is shown. In Fig. 6.23 electron mobility variation with channel position along x

direction is shown. In Fig. 6.24 hole mobility variation with channel position along x direction is shown. In Fig. 6.25 electron mobility variation with channel position along y direction is shown. In Fig. 6.26 hole mobility variation with channel position along y direction is shown.

In all the cases the channel length is taken as L=20nm, source and drain lengths are taken as L_s=L_d=5nm, the gate dielectric thickness is taken as, t_{ox}=2nm, the Si layer thickness is taken as, t_{si}=10nm, the drain to source voltage is taken as, V_{ds}=0.001V and the work function of the gate material is taken as, Φ_M=5.4eV. A lower value of the applied drain voltage is taken to reduce the applied electric field below the Silicon breakdown field ($3x10^5$V/cm). From the figures it is clear that the mobility in the subthreshold region is maximum for the conventional JLT and minimum for the JLT with gradual doping concentration variation in the channel. On the other hand in the on state, carrier mobility is minimum for conventional JLT and maximum for gradually doped JLT. The carrier mobility for the JLT with gradual doping concentration has a maximum value at the middle. The doping concentration at the middle of the channel is minimum resulting a high mobility at the middle.

A comparison of transfer characteristics for the structures is also shown in Fig. 6.27 and Fig. 6.28. In Fig. 6.27 the JLT with gradual channel doping concentration variation uses SiO_2 as the gate dielectric while in Fig. 6.28 comparison for the same structure with HfO_2 as the gate dielectric is also shown. From the figures it is seen that the proposed structures also shows lower leakage current compared to the conventional one. According to Fig. 6.27 the JLT with two dielectric placed diagonally has a better subthreshold characteristics with lower off state leakage current. But Fig. 6.28 reveals the fact that gradual doping concentration variation in the channel reduces the leakage current to a minimum among the structures. The better result shown by the two dielectric JLT in Fig. 6.27 is only because of the presence of a high K dielectric and not because of it structural changes.

In all the plots the conventional DG JLT is denoted as Struct 1, the JLT with symmetric diagonal dielectric is denoted as Struct 2, the JLT with asymmetric diagonal

dielectric is denoted as Struct 3 and the JLT with gradual doping concentration in channel with SiO_2 as the gate dielectric is denoted as Struct 4.

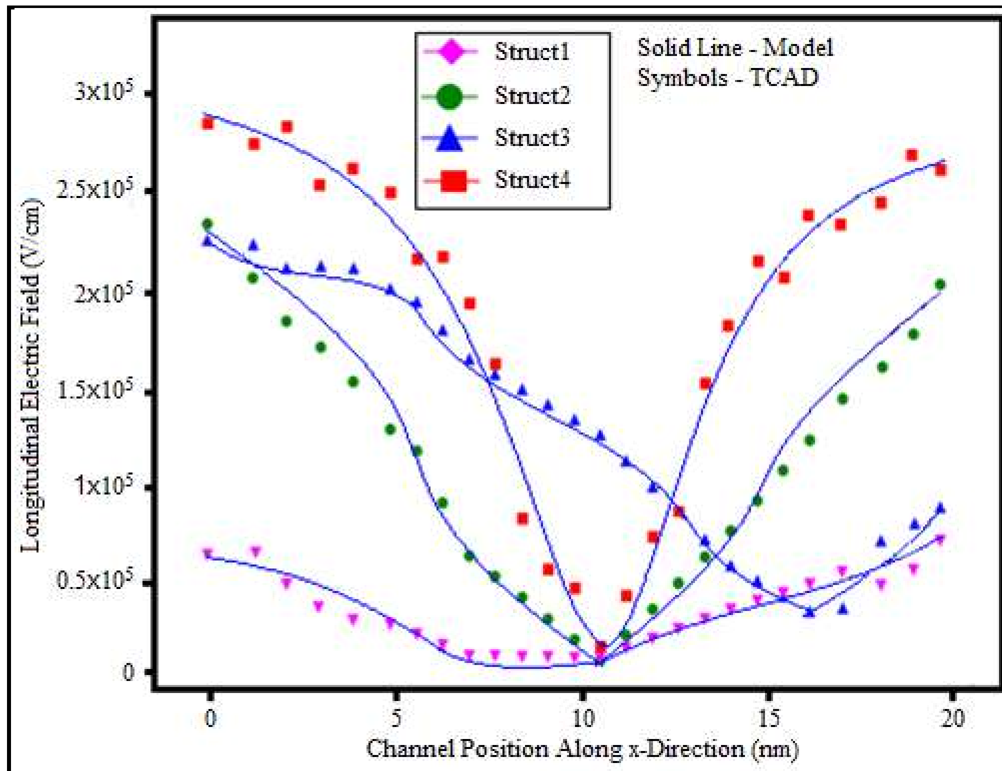

Fig. 6.15: Longitudinal electric field variation with channel position along x direction (Subthreshold)

Average error = 5.1%
Maximum error =8.3%
Minimum error =0%

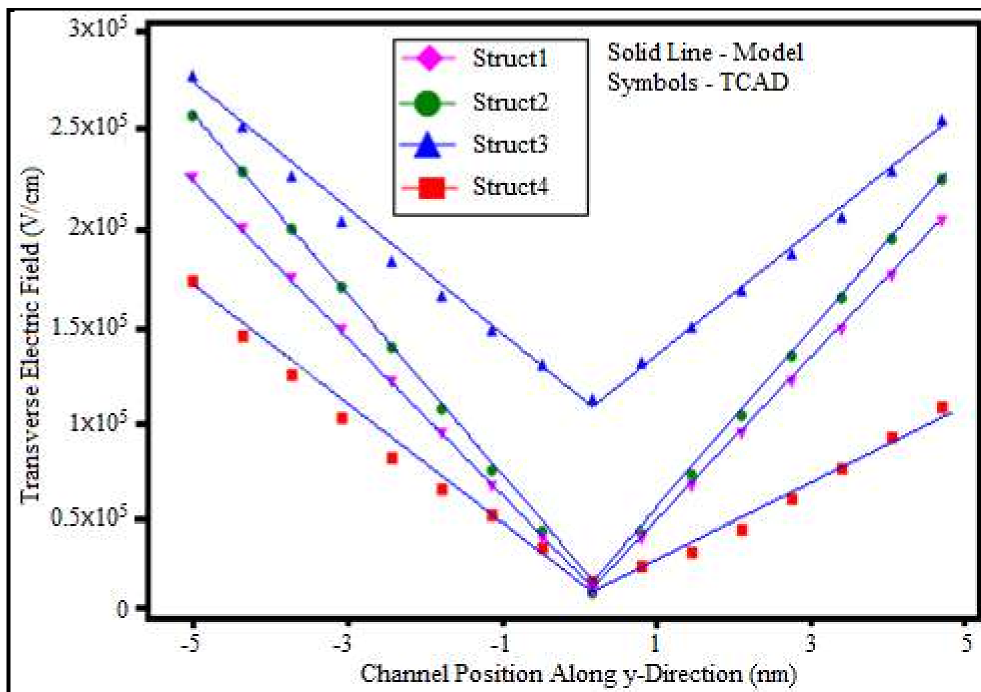

Fig. 6.16: Transverse electric field variation with channel position along y direction (Subthreshold)

Average error = 3.1%
Maximum error =7.6%
Minimum error =0%

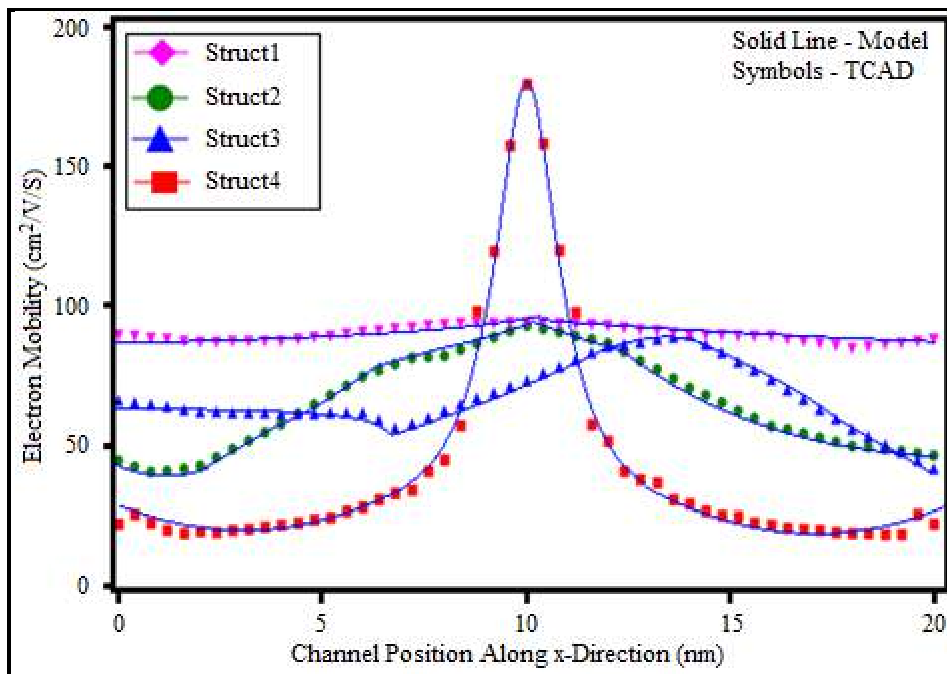

Fig. 6.17: Electron mobility variation with channel position along x direction (Subthreshold)

Average error = 3.2%
Maximum error =7.5%
Minimum error =0%

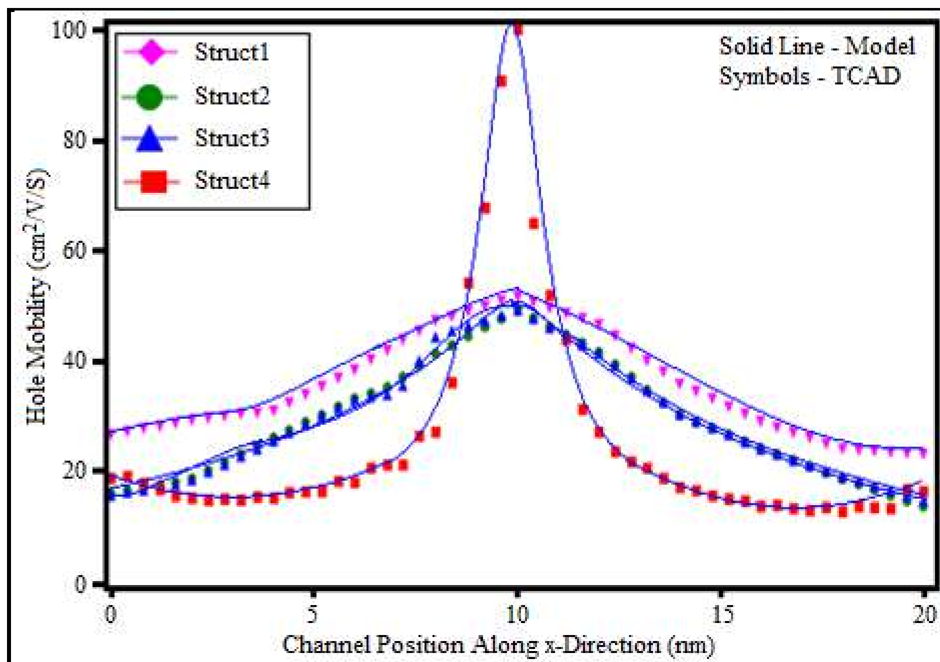

Fig. 6.18: Hole mobility variation with channel position along x direction (Subthreshold)

Average error = 3.1%
Maximum error =8.7%
Minimum error =0%

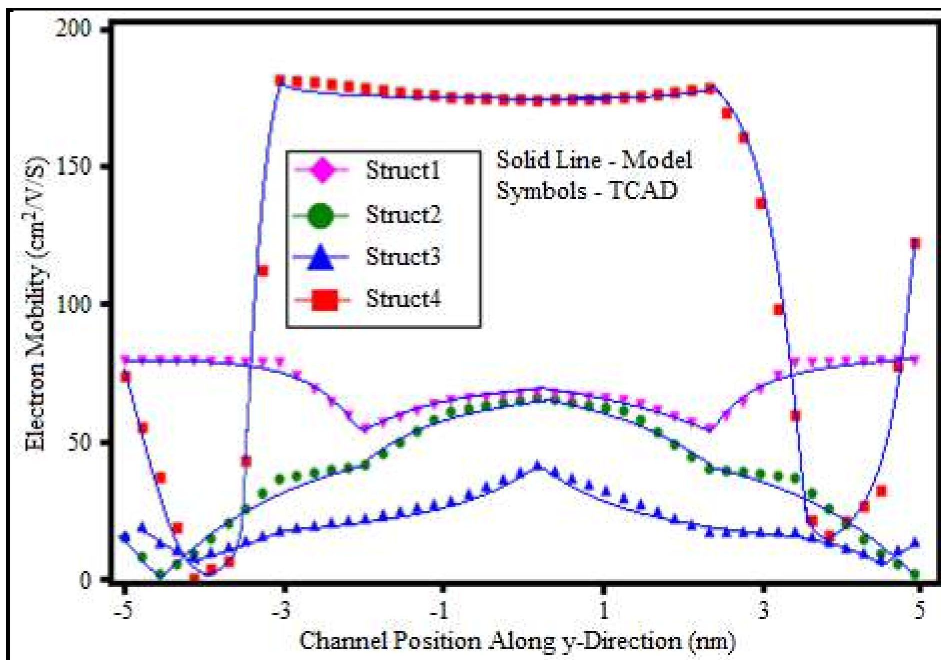

Fig. 6.19: Electron mobility variation with channel position along y direction (Subthreshold)

Average error = 2.9%
Maximum error =8.3%
Minimum error =0%

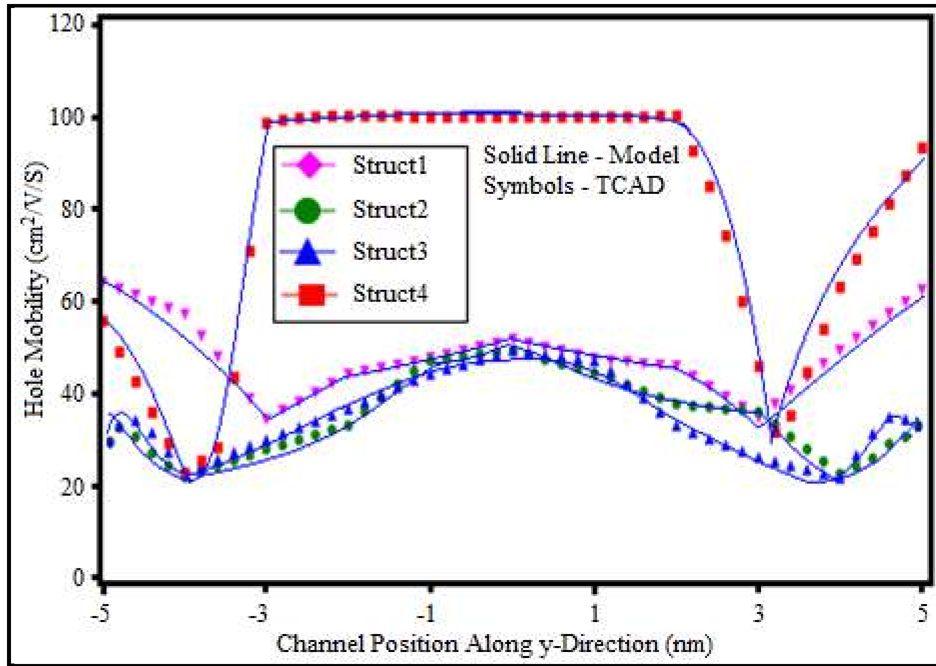

Fig. 6.20: Hole mobility variation with channel position along y direction (Subthreshold)

Average error = 2.7%
Maximum error =7.4%
Minimum error =0%

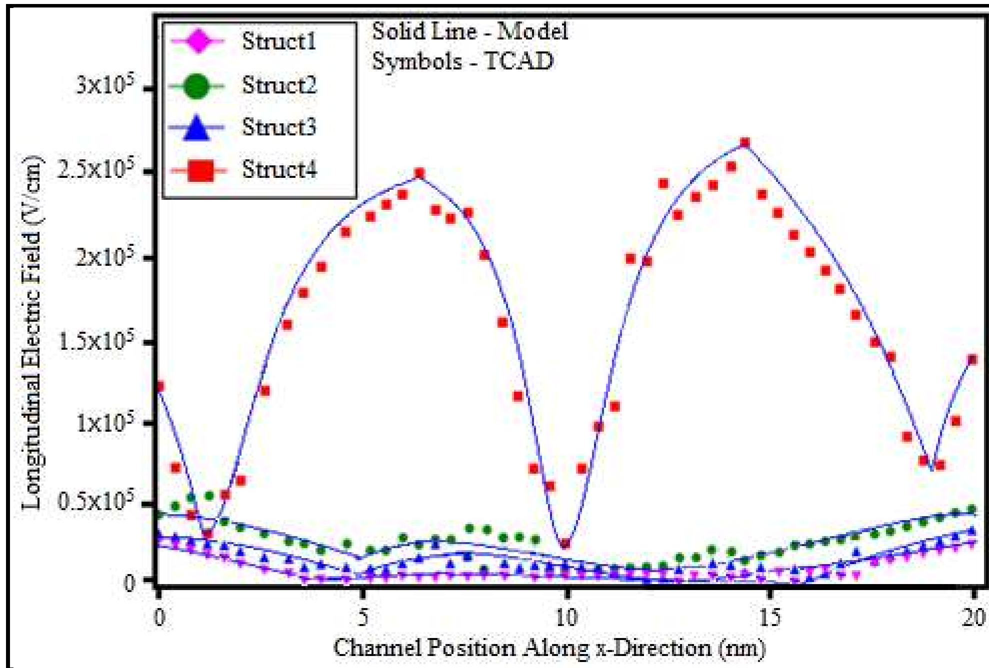

Fig. 6.21: Longitudinal electric field variation with channel position along x direction (On state)

Average error = 3.3%
Maximum error =5.6%
Minimum error =0%

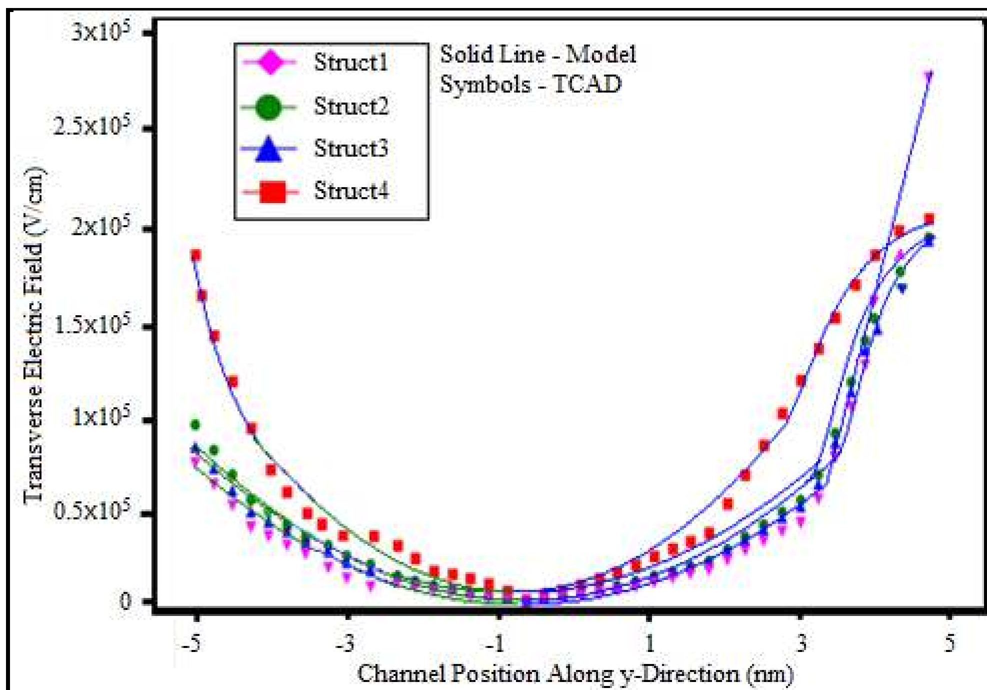

Fig. 6.22: Transverse electric field variation with channel position along y direction (On state)

Average error = 3.7%
Maximum error =8.2%
Minimum error =0%

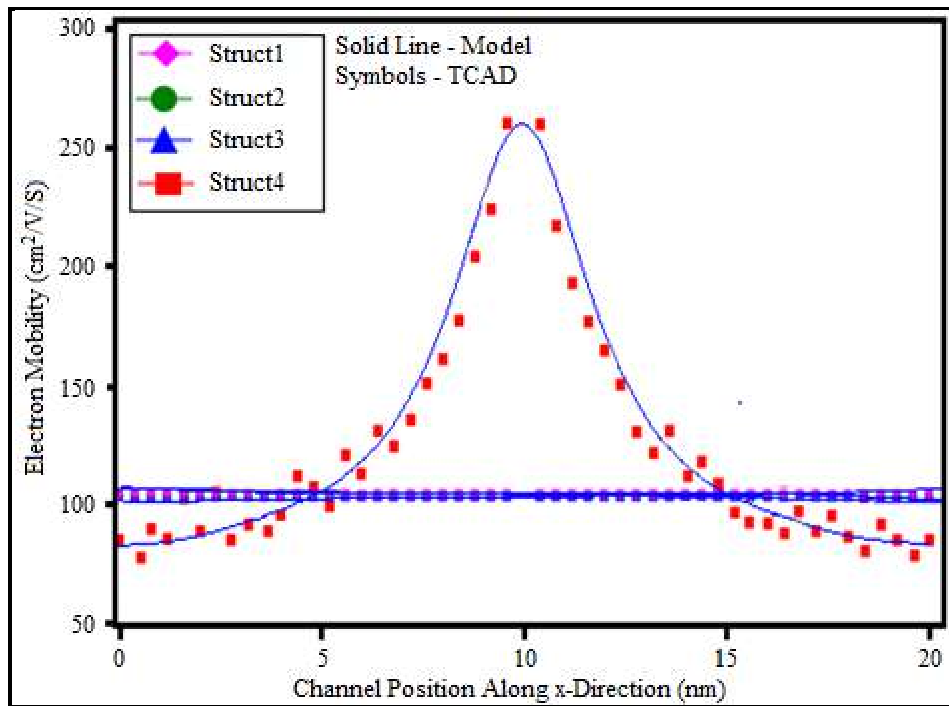

Fig. 6.23: Electron mobility variation with channel position along x direction (On state)

Average error = 3.3%
Maximum error =8.2%
Minimum error =0%

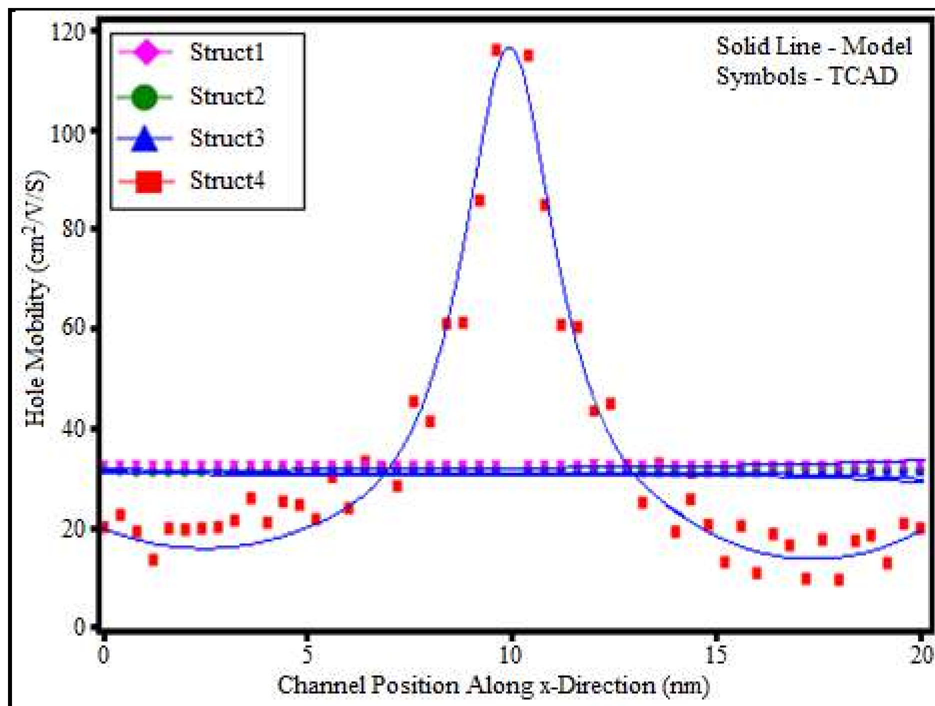

Fig. 6.24: Hole mobility variation with channel position along x direction (On state)

Average error = 4.6%
Maximum error =9.2%
Minimum error =0%

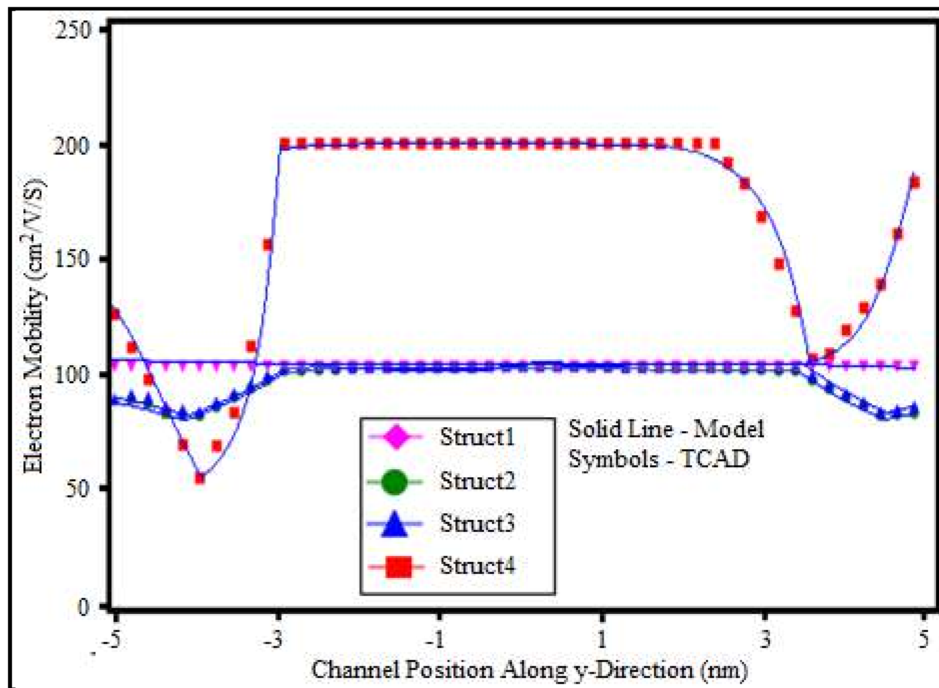

Fig. 6.25: Electron mobility variation with channel position along y direction (On state)

Average error = 4.3%
Maximum error =7.7%
Minimum error =0%

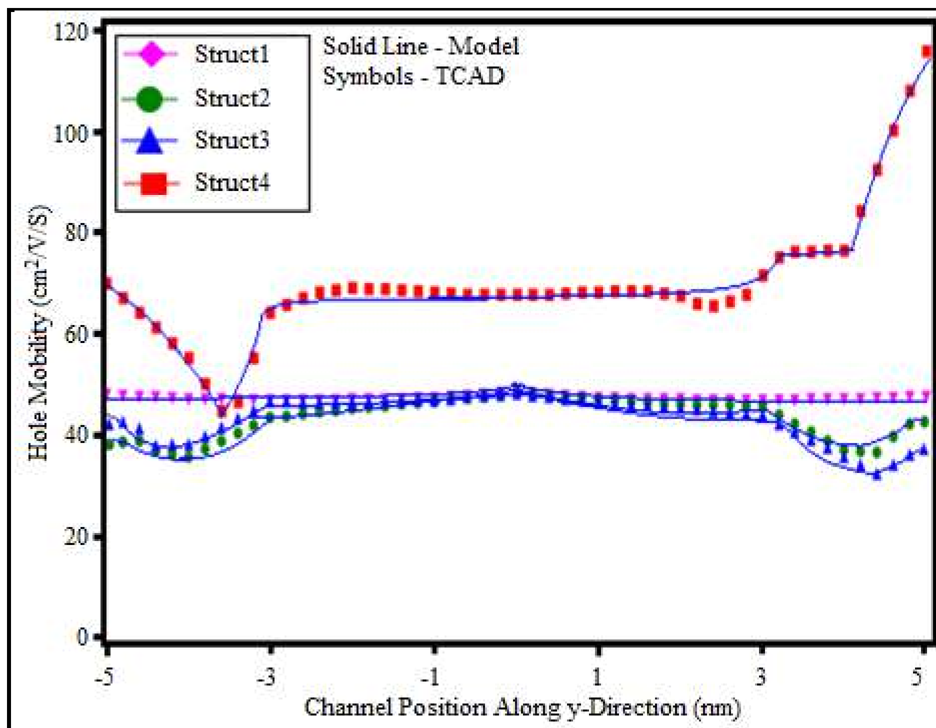

Fig. 6.26: Hole mobility variation with channel position along y direction (On state)

Average error = 3.1%
Maximum error =8.6%
Minimum error =0%

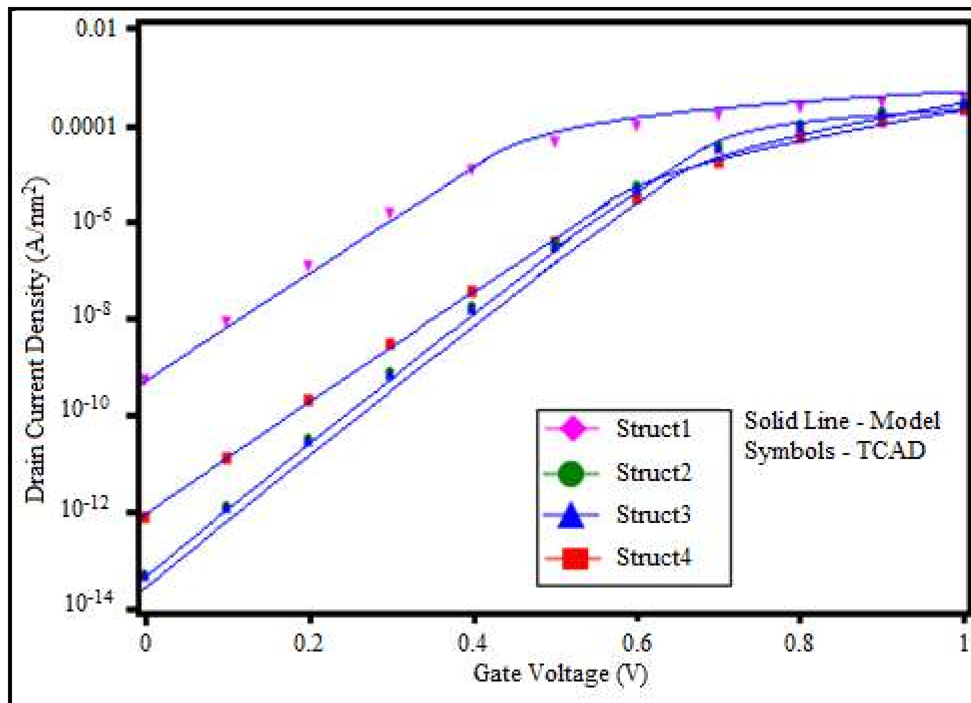

Fig. 6.27: Transfer Characteristics Comparison with SiO_2 as the dielectric for gradual channel doping variation

Average error = 3.4%
Maximum error =5.8%
Minimum error =0%

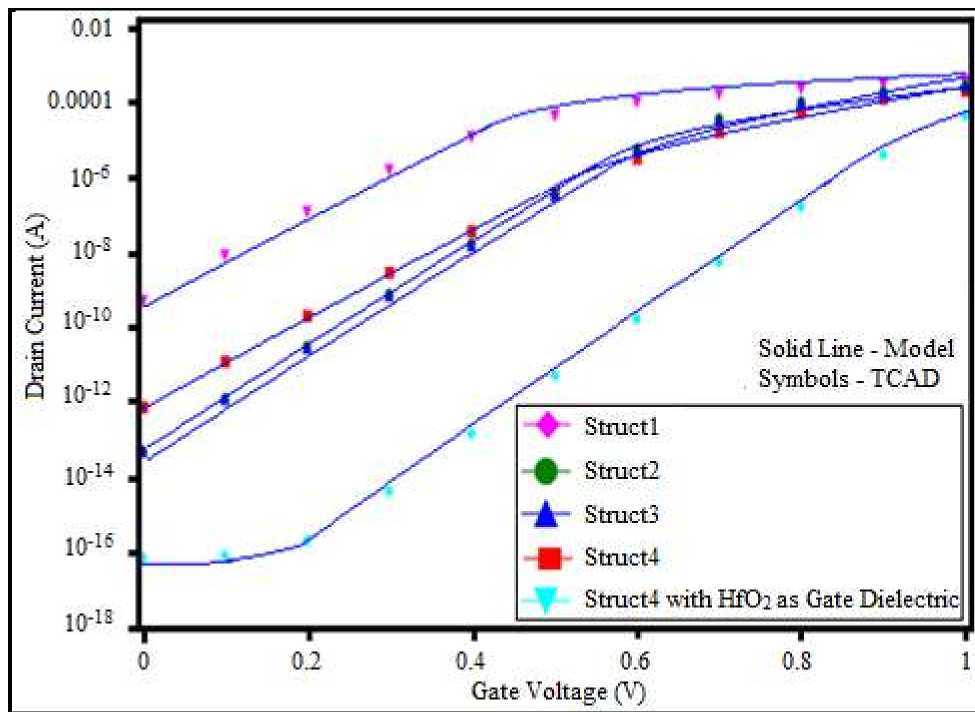

Fig. 6.28: Transfer Characteristic comparison with HfO_2 as the dielectric for Gradual channel doping variation

Average error = 2.1%
Maximum error =5.8%
Minimum error =0%

6.4 Implementation of The Proposal for Leakage Current Reduction and Mobility Enhancement in CMOS Inverter Circuit

The basic circuit diagram of a CMOS inverter using JLT is shown in Fig. 6.29.

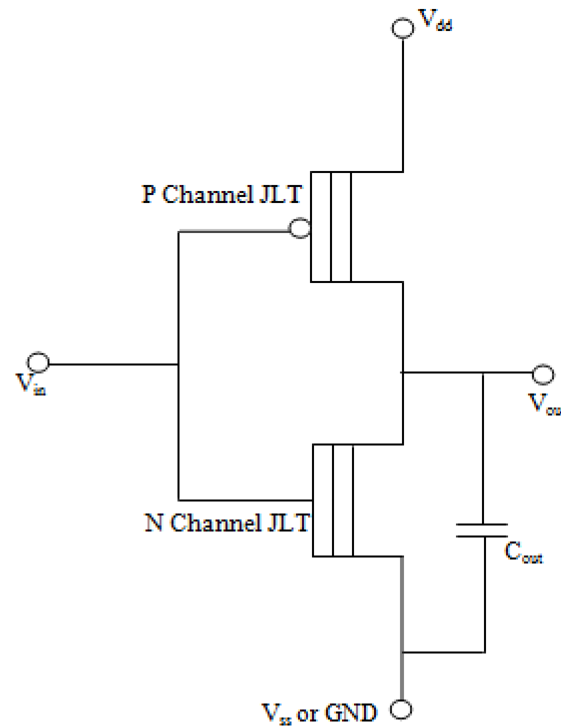

Fig. 6.29: CMOS Inverter Using JLT

6.4.1 Conventional JLT

$$R_d n(x, V_{gs}, V_{ds}) = \frac{1}{q\mu_p p_n}\frac{\Delta L}{WW_d}$$

$$R_d p(x, V_{gs}, V_{ds}) = \frac{1}{q\mu_n n_p}\frac{\Delta L}{WW_d}$$

$$R_{nd} n(x, V_{gs}, V_{ds}) = \frac{1}{q\mu_n n_n}\frac{\Delta L}{W(t_{si} - W_d)}$$

$$R_{nd}\,p(x,V_{gs},V_{ds}) = \frac{1}{q\mu_p p_p}\frac{\Delta L}{W(t_{si}-W_d)}$$

Since the substrate is heavily doped, the approximate carrier density of the non-depleted region of n-channel JLT is given as,

$$n_n = \frac{N_d}{2} + \sqrt{\frac{N_d^{\,2}}{4} + n_i^{\,2}}$$

The carrier density of the depleted region of n-channel JLT is given as,

$$p_n = \frac{n_i^{\,2}}{\dfrac{N_d}{2} + \sqrt{\dfrac{N_d^{\,2}}{4} + n_i^{\,2}}}$$

the approximate carrier density of the non-depleted region of p-channel JLT is given as,

$$p_p = \frac{N_a}{2} + \sqrt{\frac{N_a^{\,2}}{4} + n_i^{\,2}}$$

The carrier density of the depleted region of p-channel JLT is given as,

$$n_p = \frac{n_i^{\,2}}{\dfrac{N_a}{2} + \sqrt{\dfrac{N_a^{\,2}}{4} + n_i^{\,2}}}$$

Where, n_i is intrinsic carrier concentration

$$\phi_0(0)=\left[\frac{V_{ds}(e^{\frac{L+L_d}{\lambda}}-e^{\frac{L+L_d-2L_s}{\lambda}})+(-\frac{qN_d}{\in_{si}}-\frac{1}{\lambda^2}\phi_{gs})\lambda^2(e^{\frac{L+L_d}{\lambda}}-e^{-\frac{L_s}{\lambda}}-e^{\frac{L+L_d-2L_s}{\lambda}}+e^{\frac{2(L+L_d)-L_s}{\lambda}}-e^{2\frac{L+L_d}{\lambda}}+e^{-2\frac{L_s}{\lambda}})}{(e^{2\frac{L+L_d}{\lambda}}-e^{-2\frac{L_s}{\lambda}})}\right]$$

$$=V_{ds}\frac{(e^{\frac{L+L_d}{\lambda}}-e^{\frac{L+L_d-2L_s}{\lambda}})}{(e^{2\frac{L+L_d}{\lambda}}-e^{-2\frac{L_s}{\lambda}})}-\phi_{gs}\frac{(e^{\frac{L+L_d}{\lambda}}-e^{-\frac{L_s}{\lambda}}-e^{\frac{L+L_d-2L_s}{\lambda}}+e^{\frac{2(L+L_d)-L_s}{\lambda}}-e^{2\frac{L+L_d}{\lambda}}+e^{-2\frac{L_s}{\lambda}})}{(e^{2\frac{L+L_d}{\lambda}}-e^{-2\frac{L_s}{\lambda}})}$$

$$-\frac{qN_d}{\in_{si}}\lambda^2\frac{(e^{\frac{L+L_d}{\lambda}}-e^{-\frac{L_s}{\lambda}}-e^{\frac{L+L_d-2L_s}{\lambda}}+e^{\frac{2(L+L_d)-L_s}{\lambda}}-e^{2\frac{L+L_d}{\lambda}}+e^{-2\frac{L_s}{\lambda}})}{(e^{2\frac{L+L_d}{\lambda}}-e^{-2\frac{L_s}{\lambda}})}$$

$$\phi_0(0)=AV_{ds}-B\phi_{gs}-C_n$$

$$\phi_0(\Delta L)=$$

$$V_{ds}\frac{(e^{\frac{L+L_d+\Delta L}{\lambda}}-e^{\frac{L+L_d-2L_s-\Delta L}{\lambda}})}{(e^{2\frac{L+L_d}{\lambda}}-e^{-2\frac{L_s}{\lambda}})}-\phi_{gs}\frac{(e^{\frac{L+L_d+\Delta L}{\lambda}}-e^{\frac{-L_s+\Delta L}{\lambda}}-e^{\frac{L+L_d-2L_s-\Delta L}{\lambda}}+e^{\frac{2(L+L_d)-L_s-\Delta L}{\lambda}}-e^{2\frac{L+L_d}{\lambda}}+e^{-2\frac{L_s}{\lambda}})}{(e^{2\frac{L+L_d}{\lambda}}-e^{-2\frac{L_s}{\lambda}})}$$

$$-\frac{qN_d}{\in_{si}}\lambda^2\frac{(e^{\frac{L+L_d+\Delta L}{\lambda}}-e^{-\frac{L_s+\Delta L}{\lambda}}-e^{\frac{L+L_d-2L_s-\Delta L}{\lambda}}+e^{\frac{2(L+L_d)-L_s-\Delta L}{\lambda}}-e^{2\frac{L+L_d}{\lambda}}+e^{-2\frac{L_s}{\lambda}})}{(e^{2\frac{L+L_d}{\lambda}}-e^{-2\frac{L_s}{\lambda}})}$$

$$\phi_0(\Delta L)=A^{/}V_{ds}-B^{/}\phi_{gs}-C_n^{/}$$

For p-channel JLT

$$\phi_0(0)=AV_{ds}-B\phi_{gs}-C_p$$

and

$$\phi_0(\Delta L)=A^{/}V_{ds}-B^{/}\phi_{gs}-C_p^{/}$$

Where,

$$C_p = -\frac{qN_a}{\in_{si}}\lambda^2 \frac{(e^{\frac{L+L_d+\Delta L}{\lambda}} - e^{-\frac{L_s+\Delta L}{\lambda}} - e^{\frac{L+L_d-2L_s-\Delta L}{\lambda}} + e^{\frac{2(L+L_d)-L_s-\Delta L}{\lambda}} - e^{2\frac{L+L_d}{\lambda}} + e^{-2\frac{L_s}{\lambda}})}{(e^{2\frac{L+L_d}{\lambda}} - e^{-2\frac{L_s}{\lambda}})}$$

$$C_p^{/} = -\frac{qN_a}{\in_{si}}\lambda^2 \frac{(e^{\frac{L+L_d+\Delta L}{\lambda}} - e^{-\frac{L_s+\Delta L}{\lambda}} - e^{\frac{L+L_d-2L_s-\Delta L}{\lambda}} + e^{\frac{2(L+L_d)-L_s-\Delta L}{\lambda}} - e^{2\frac{L+L_d}{\lambda}} + e^{-2\frac{L_s}{\lambda}})}{(e^{2\frac{L+L_d}{\lambda}} - e^{-2\frac{L_s}{\lambda}})}$$

Voltage Transfer Characteristics

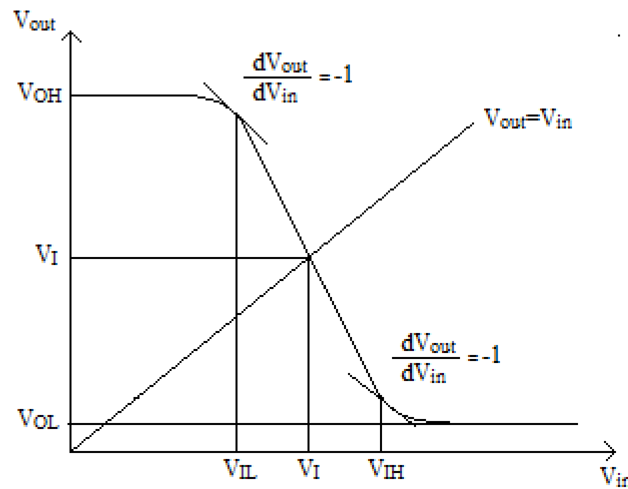

Fig. 6.30: Voltage Transfer Characteristics of Inverter [29]

Input Low:

To find input low the p-channel JLT is considered to be non-saturated and n-channel JLT is considered to be saturated [29].

$I_{dpnonsat} = I_{dnsat}$

At Saturation,

$$\phi_{gsn} = V_{gsn} - V_{fbn} = 0 \tag{6.49}$$

or,

$$I_{dnsat} = I_{dpnonsat}$$

$$\frac{\phi(\Delta L)-\phi(0)}{Rn(V_{gs},V_{ds})} = \frac{\phi(\Delta L)-\phi(0)}{Rp(V_{gs},V_{ds})}$$

$$Rp(V_{gs},V_{ds}) = R_d\, p(V_{gs},V_{ds}) = \frac{\Delta L}{q\mu_n n_p W t_{si}}$$

$$Rn(V_{gs},V_{ds}) = R_{nd} n(V_{gs},V_{ds}) = \frac{\Delta L}{q\mu_n n_n W t_{si}}$$

$$[(A^{/}-A)V_{dsp} - (B^{/}-B)\phi_{gsp} - (C_p^{/}-C_p)]n_p = [(A^{/}-A)V_{dsn} - (C_n^{/}-C_n)]n_n$$

$$[(A^{/}-A)(V_{dd}-V_{out}) - (B^{/}-B)(V_{dd}-V_{in}-V_{fbp}) - (C_p^{/}-C_p)]n_p$$
$$= [(A^{/}-A)(V_{out}) - (C_n^{/}-C_n)]n_n \tag{6.50}$$

$$I_{dn}(V_{out}) = I_{dp}(V_{in},V_{out})$$

$$\frac{dV_{out}}{dV_{in}} = \frac{\dfrac{\partial I_{dp}}{\partial V_{in}}}{\dfrac{dI_{dn}}{dV_{out}} - \dfrac{\partial I_{dp}}{\partial V_{out}}} = -1$$

$$(B^{/}-B) = -(A^{/}-A)\frac{(n_n+n_p)}{n_p}$$

or, (6.51)

$$\frac{(A^{/}-A)(n_n+2n_p)V_{dd} - (A^{/}-A)(n_n+n_p)V_{in} - (A^{/}-A)(n_n+n_p)V_{fbp} - \{(C_p^{/}-C_p)n_p - (C_n^{/}-C_n)n_n\}}{(A^{/}-A)(n_n+n_p)}$$

$$= V_{out}$$

$$V_{in} = (V_{dd} - V_{fbp}) = V_{IL}$$

Input High:

$$I_{dnnonsat} = I_{dpsat}$$

$$\phi_{gsp} = V_{gsp} - V_{fbp} = 0 \tag{6.52}$$

$$\frac{\phi(\Delta L) - \phi(O)}{R_d(V_{gs}, V_{ds})} = \frac{\phi(\Delta L) - \phi(O)}{R_{nd}\,p(V_{gs}, V_{ds})}$$

$$\{(A^{/} - A)V_{dsp} - (C_p^{/} - C_p)\}p_p = \{(A^{/} - A)V_{dsn} - (B^{/} - B)\phi_{gsn} - (C_n^{/} - C_n)\}p_n$$

$$\begin{aligned}&\{(A^{/} - A)(V_{dd} - V_{out}) - (C_p^{/} - C_p)\}p_p \\ &= \{(A^{/} - A)(V_{out}) - (B^{/} - B)(V_{in} - V_{fbn}) - (C_n^{/} - C_n)\}p_n\end{aligned} \tag{6.53}$$

$$I_{dp}(V_{out}) = I_{dn}(V_{in}, V_{out})$$

$$\frac{dV_{out}}{dV_{in}} = \frac{\dfrac{\partial I_{dn}}{\partial V_{in}}}{\dfrac{dI_{dp}}{dV_{out}} - \dfrac{\partial I_{dn}}{\partial V_{out}}} = -1$$

$$-(A^{/} - A)\frac{p_p}{p_n} = (B^{/} - B)$$

$$\frac{(A^{/} - A)p_p V_{dd} - (A^{/} - A)p_p(V_{in} - V_{fbn}) - \{(C_p^{/} - C_p)p_p - (C_n^{/} - C_n)p_n)}{(A^{/} - A)(p_n + p_p)}$$

$$= V_{out}$$

$$V_{in} = V_{fbn} = V_{IH}$$

Output Low:

$$I_{dnsat} = I_{dpnonsat}$$

$$V_{in} = V_{dd}$$

$$\begin{aligned}&[(A^{/} - A)(V_{dd} - V_{out}) - (B^{/} - B)(V_{dd} - V_{in} - V_{fbp}) - (C_p^{/} - C_p)]n_p \\ &= [(A^{/} - A)(V_{out}) - (C_n^{/} - C_n)]n_n\end{aligned}$$

$$V_{out} = \frac{(A^{/} - A)n_p V_{dd} + (B^{/} - B)n_p V_{fbp} - (C_p^{/} - C_p)n_p + (C_n^{/} - C_n)n_n}{(A^{/} - A)(n_n + n_p)} = V_{OL}$$

Output High:

$$I_{dnnonsat} = I_{dpsat}$$

$$V_{in} = 0$$

$$V_{out} = \frac{(A^{/} - A)p_p V_{dd} - (B^{/} - B)p_n V_{fbn} - (C_p^{/} - C_p)p_p + (C_n^{/} - C_n)p_n}{(A^{/} - A)(p_n + p_p)} = V_{OH}$$

Inverter Threshold Voltage

$$\frac{\phi(\Delta L) - \phi(O)}{R_{nd} n(V_{gs}, V_{ds})} = \frac{\phi(\Delta L) - \phi(O)}{R_{nd} p(V_{gs}, V_{ds})}$$

$$\phi_{gsp} = \phi_{gsn} = 0$$

$$V_{dsp} = V_{dd} - V_I$$

$$V_{dsn} = V_I$$

$$\frac{(A^{/} - A)V_{dsn} - (B^{/} - B)\phi_{gsn} - (C_p^{/} - C_p)}{\dfrac{\Delta L}{2q\mu_n n_n W t_{si}}} = \frac{(A^{/} - A)V_{dsp} - (B^{/} - B)\phi_{gsp} - (C_n^{/} - C_n)}{\dfrac{\Delta L}{2q\mu_p p_p W t_{si}}}$$

$$\mu_n n_n \{(A^{/} - A)V_I - (C_n^{/} - C_n)\} = \mu_p p_p \{(A^{/} - A)(V_{dd} - V_I) - (C_p^{/} - C_p)\}$$

$$V_I = \frac{\mu_p p_p (A^{/} - A)V_{dd} + \{\mu_n n_n (C_n^{/} - C_n) - \mu_p p_p (C_p^{/} - C_p)\}}{(\mu_n n_n + \mu_p p_p)(A^{/} - A)}$$

Noise Margin:

Noise margin for logic 1 voltages

$$V_{NMH} = V_{OH} - V_{IH} = \frac{(A^{/} - A)p_p V_{dd} - (B^{/} - B)p_n V_{fbn} - (A^{/} - A)(p_n + p_p)V_{fbn} - (C_p^{/} - C_p)p_p + (C_n^{/} - C_n)p_n}{(A^{/} - A)(p_n + p_p)}$$

Noise margin for logic 0 voltages

$$V_{NML} = V_{IL} - V_{OL} = \frac{(A' - A)n_n V_{dd} - (B' - B)n_p V_{fbp} - (A' - A)(n_n + n_p)V_{fbp} + (C_p' - C_p)n_p - (C_n' - C_n)n_n}{(A' - A)(n_n + n_p)}$$

Fall Time

$$t_{HL} = C_{out} \int_{V_1}^{V_0} \frac{dV_{out}}{I_{dn}}$$

$V_o = 0.1V_{OH}$ and $V_1 = 0.9V_{OH}$

$$I_{dn} = \frac{q\mu_n n_n W t_{si}[(A' - A)V_{out} - (C_n' - C_n)]}{\Delta L}$$

$$t_{HL} = C_{out} \int_{V_1}^{V_0} \frac{dV_{out}}{\frac{q\mu_n n_n W t_{si}[(A' - A)V_{out} - (C_n' - C_n)]}{\Delta L}}$$

$$t_{HL} = \frac{\Delta L C_{out}}{q\mu_n n_n W t_{si}(A' - A)}\left[\ln\{V_o - \frac{(C_n' - C_n)}{(A' - A)}\} - \ln\{V_1 - \frac{(C_n' - C_n)}{(A' - A)}\}\right]$$

Rise Time

$$t_{LH} = C_{out} \int_{V_0}^{V_1} \frac{dV_{out}}{I_{dp}}$$

$V_o = 0.1V_{OH}$ and $V_1 = 0.9V_{OH}$

$$I_{dp} = \frac{q\mu_p p_p W t_{si}[\{(A' - A)(V_{dd} - V_{out}) - (C_p' - C_p)\}]}{\Delta L}$$

$$t_{LH} = C_{out} \int_{V_0}^{V_1} \frac{dV_{out}}{\frac{q\mu_p p_p W t_{si}[\{(A' - A)(V_{dd} - V_{out}) - (C_p' - C_p)\}]}{\Delta L}}$$

$$t_{LH} = \frac{\Delta L C_{out}}{q\mu_p p_p W t_{si}(A' - A)}\left[\ln\{V_{dd} - V_1 - \frac{(C_p' - C_p)}{(A' - A)}\} - \ln\{V_{dd} - V_0 - \frac{(C_p' - C_p)}{(A' - A)}\}\right]$$

Propagation Delay

$$t_{PHL}=\frac{\Delta LC_{out}}{q\mu_n n_n W t_{si}(A^{/}-A)}\left[\ln\{V_I-\frac{(C_n^{/}-C_n)}{(A^{/}-A)}\}-\ln\{V_{OH}-\frac{(C_n^{/}-C_n)}{(A^{/}-A)}\}\right]$$

$$t_{PLH}=\frac{\Delta LC_{out}}{q\mu_p p_p W t_{si}(A^{/}-A)}\left[\ln\{V_{dd}-V_{OH}-\frac{(C_p^{/}-C_p)}{(A^{/}-A)}\}-\ln\{V_{dd}-V_I-\frac{(C_p^{/}-C_p)}{(A^{/}-A)}\}\right]$$

Propagation delay is given as,

$$t_P=\frac{t_{PHL}+t_{PLH}}{2}$$

Power Loss

$$P_d=V_{out}I_{ds}$$

6.4.2 JLT with A Dielectric Layer at Centre

$$R_d n(x,V_{gs},V_{ds})=\frac{1}{q\mu_p p_n}\frac{\Delta L}{WW_d}$$

$$R_d p(x,V_{gs},V_{ds})=\frac{1}{q\mu_n n_p}\frac{\Delta L}{WW_d}$$

$$R_{nd} n(x,V_{gs},V_{ds})=\frac{1}{q\mu_n n_n}\frac{\Delta L}{W(t_{si}-t_{di}-W_d)}$$

$$R_{nd} p(x,V_{gs},V_{ds})=\frac{1}{q\mu_p p_p}\frac{\Delta L}{W(t_{si}-t_{di}-W_d)}$$

$$\phi_0(0)=\left[\frac{V_{ds}(e^{\frac{L+L_d}{\lambda}}-e^{\frac{L+L_d-2L_s}{\lambda}})+(-\frac{qN_d}{\in_{si}}-\frac{1}{\lambda^2}\phi_{gs})\lambda^2(e^{\frac{L+L_d}{\lambda}}-e^{-\frac{L_s}{\lambda}}-e^{\frac{L+L_d-2L_s}{\lambda}}+e^{\frac{2(L+L_d)-L_s}{\lambda}}-e^{2\frac{L+L_d}{\lambda}}+e^{-2\frac{L_s}{\lambda}})}{(e^{2\frac{L+L_d}{\lambda}}-e^{-2\frac{L_s}{\lambda}})}\right]$$

$$=V_{ds}\frac{(e^{\frac{L+L_d}{\lambda}}-e^{\frac{L+L_d-2L_s}{\lambda}})}{(e^{2\frac{L+L_d}{\lambda}}-e^{-2\frac{L_s}{\lambda}})}-\phi_{gs}\frac{(e^{\frac{L+L_d}{\lambda}}-e^{-\frac{L_s}{\lambda}}-e^{\frac{L+L_d-2L_s}{\lambda}}+e^{\frac{2(L+L_d)-L_s}{\lambda}}-e^{2\frac{L+L_d}{\lambda}}+e^{-2\frac{L_s}{\lambda}})}{(e^{2\frac{L+L_d}{\lambda}}-e^{-2\frac{L_s}{\lambda}})}-\frac{qN_d}{\in_{si}}\frac{1}{(e^{2\frac{L+L_d}{\lambda}}-e^{-2\frac{L_s}{\lambda}})}$$

$$\phi_0(0)=AV_{ds}-B\phi_{gs}-C_n$$

$$\phi_0(\Delta L)=$$

$$V_{ds}\frac{(e^{\frac{L+L_d+\Delta L}{\lambda}}-e^{\frac{L+L_d-2L_s-\Delta L}{\lambda}})}{(e^{2\frac{L+L_d}{\lambda}}-e^{-2\frac{L_s}{\lambda}})}-\phi_{gs}\frac{(e^{\frac{L+L_d+\Delta L}{\lambda}}-e^{-\frac{L_s+\Delta L}{\lambda}}-e^{\frac{L+L_d-2L_s-\Delta L}{\lambda}}+e^{\frac{2(L+L_d)-L_s-\Delta L}{\lambda}}-e^{2\frac{L+L_d}{\lambda}}+e^{-2\frac{L_s}{\lambda}})}{(e^{2\frac{L+L_d}{\lambda}}-e^{-2\frac{L_s}{\lambda}})}$$

$$-\frac{qN_d}{\in_{si}}\frac{1}{(e^{2\frac{L+L_d}{\lambda}}-e^{-2\frac{L_s}{\lambda}})}$$

$$\phi_0(\Delta L)=A^{/}V_{ds}-B^{/}\phi_{gs}-C_n^{/}$$

For p-channel JLT

$$\phi_0(0)=AV_{ds}-B\phi_{gs}-C_p$$

and

$$\phi_0(\Delta L)=A^{/}V_{ds}-B^{/}\phi_{gs}-C_p^{/}$$

Where,

$$C_p=-\frac{qN_a}{\in_{si}}\lambda^2\frac{(e^{\frac{L+L_d+\Delta L}{\lambda}}-e^{-\frac{L_s+\Delta L}{\lambda}}-e^{\frac{L+L_d-2L_s-\Delta L}{\lambda}}+e^{\frac{2(L+L_d)-L_s-\Delta L}{\lambda}}-e^{2\frac{L+L_d}{\lambda}}+e^{-2\frac{L_s}{\lambda}})}{(e^{2\frac{L+L_d}{\lambda}}-e^{-2\frac{L_s}{\lambda}})}$$

$$C_p^{/}=-\frac{qN_a}{\in_{si}}\lambda^2\frac{(e^{\frac{L+L_d+\Delta L}{\lambda}}-e^{-\frac{L_s+\Delta L}{\lambda}}-e^{\frac{L+L_d-2L_s-\Delta L}{\lambda}}+e^{\frac{2(L+L_d)-L_s-\Delta L}{\lambda}}-e^{2\frac{L+L_d}{\lambda}}+e^{-2\frac{L_s}{\lambda}})}{(e^{2\frac{L+L_d}{\lambda}}-e^{-2\frac{L_s}{\lambda}})}$$

Input Low:

$I_{dpnonsat} = I_{dnsat}$

At Saturation,

$$\phi_{gsn} = V_{gsn} - V_{fbn} = 0 \tag{6.54}$$

or,

$$I_{dnsat} = I_{dpnonsat}$$

$$\frac{\phi(\Delta L) - \phi(0)}{Rn(V_{gs}, V_{ds})} = \frac{\phi(\Delta L) - \phi(0)}{Rp(V_{gs}, V_{ds})}$$

$$Rn(V_{gs}, V_{ds}) = R_{nd} n(V_{gs}, V_{ds}) \,||\, R_{di} \,||\, R_{nd} n(V_{gs}, V_{ds}) = \frac{\rho \Delta L}{q\mu_n n_n W \rho(t_{si} - t_{di}) + Wt_{di}}$$

$$Rp(V_{gs}, V_{ds}) = R_d\, p(V_{gs}, V_{ds}) \,||\, R_{di} \,||\, R_d\, p(V_{gs}, V_{ds}) = \frac{\rho \Delta L}{q\mu_n n_p W \rho(t_{si} - t_{di}) + Wt_{di}}$$

$$\{(A^{/} - A)V_{dsp} - (B^{/} - B)\phi_{gsp} - (C_p^{/} - C_p)\}\{q\mu_n n_p W \rho(t_{si} - t_{di}) + Wt_{di}\}$$
$$= \{(A^{/} - A)V_{dsn} - (B^{/} - B)\phi_{gsn} - (C_n^{/} - C_n)\}\{q\mu_n n_n W \rho(t_{si} - t_{di}) + Wt_{di}\}$$

$$\{(A^{/} - A)(V_{dd} - V_{out}) - (B^{/} - B)(V_{dd} - V_{in} - V_{fbp}) - (C_p^{/} - C_p)\}\{q\mu_n n_p W \rho(t_{si} - t_{di}) + Wt_{di}\}$$
$$= \{(A^{/} - A)(V_{out}) - (B^{/} - B)(V_{in} - V_{fbn}) - (C_n^{/} - C_n)\}\{\{q\mu_n n_n W \rho(t_{si} - t_{di}) + Wt_{di}\}\} \tag{6.55}$$

$$\frac{dV_{out}}{dV_{in}} = \frac{\dfrac{\partial I_{dp}}{\partial V_{in}}}{\dfrac{dI_{dn}}{dV_{out}} - \dfrac{\partial I_{dp}}{\partial V_{out}}} = -1$$

or,

$$(B^{/}-B)=-(A^{/}-A)\frac{\{q\mu_n n_n W\rho(t_{si}-t_{di})+Wt_{di}\}+\{q\mu_n n_p W\rho(t_{si}-t_{di})+Wt_{di}\}}{\{q\mu_n n_p W\rho(t_{si}-t_{di})+Wt_{di}\}}$$

$$\frac{(A^{/}-A)V_{dd}(\{q\mu_n n_n W\rho(t_{si}-t_{di})+3Wt_{di}+2\{q\mu_n n_p W\rho(t_{si}-t_{di})}{(A^{/}-A)\{q\mu_n n_n W\rho(t_{si}-t_{di})+2Wt_{di}+q\mu_n n_p W\rho(t_{si}-t_{di})\}}$$
$$-\frac{(A^{/}-A)\{q\mu_n n_n W\rho(t_{si}-t_{di})+2Wt_{di}+q\mu_n n_p W\rho(t_{si}-t_{di})\}(V_{in}+V_{fbp})}{(A^{/}-A)\{q\mu_n n_n W\rho(t_{si}-t_{di})+2Wt_{di}+q\mu_n n_p W\rho(t_{si}-t_{di})\}}$$
$$-\frac{\{(C_p^{/}-C_p)\{q\mu_n n_p W\rho(t_{si}-t_{di})+Wt_{di}\}-(C_n^{/}-C_n)\{q\mu_n n_n W\rho(t_{si}-t_{di})+Wt_{di}\}\}}{(A^{/}-A)\{q\mu_n n_n W\rho(t_{si}-t_{di})+2Wt_{di}+q\mu_n n_p W\rho(t_{si}-t_{di})\}}$$
$$=V_{out}$$

$$V_{in}=(V_{dd}-V_{fbp})=V_{IL}$$

Input High:

$$I_{dnnonsat}=I_{dpsat}$$

$$\phi_{gsp}=V_{gsp}-V_{fbp}=0 \tag{6.56}$$

$$\frac{\phi(\Delta L)-\phi(\mathrm{O})}{Rn(V_{gs},V_{ds})}=\frac{\phi(\Delta L)-\phi(\mathrm{O})}{Rp(V_{gs},V_{ds})}$$

$$Rn(V_{gs},V_{ds})=R_d n(V_{gs},V_{ds})\,||\,R_{di}\,||\,R_d n(V_{gs},V_{ds})=\frac{\rho\Delta L}{q\mu_p p_n W\rho(t_{si}-t_{di})+Wt_{di}}$$

$$Rp(V_{gs},V_{ds})=R_{nd}\,p(V_{gs},V_{ds})\,||\,R_{di}\,||\,R_{nd}\,p(V_{gs},V_{ds})=\frac{\rho\Delta L}{q\mu_p p_p W\rho(t_{si}-t_{di})+Wt_{di}}$$

$$\{(A^{/}-A)V_{dsp}-(B^{/}-B)\phi_{gsp}-(C_p^{/}-C_p)\}\{q\mu_p p_p W\rho(t_{si}-t_{di})+Wt_{di}\}$$
$$=\{(A^{/}-A)V_{dsn}-(B^{/}-B)\phi_{gsn}-(C_n^{/}-C_n)\}\{q\mu_p p_n W\rho(t_{si}-t_{di})+Wt_{di}\}$$

$$\{(A^{/}-A)(V_{dd}-V_{out})-(B^{/}-B)(V_{dd}-V_{in}-V_{fbp})-(C_p^{/}-C_p)\}\{q\mu_p p_p W\rho(t_{si}-t_{di})+Wt_{di}\}$$
$$=\{(A^{/}-A)(V_{out})-(B^{/}-B)(V_{in}-V_{fbn})-(C_n^{/}-C_n)\}\{q\mu_p p_n W\rho(t_{si}-t_{di})+Wt_{di}\} \tag{6.57}$$

$$\frac{dV_{out}}{dV_{in}}=\frac{\dfrac{\partial I_{dn}}{\partial V_{in}}}{\dfrac{dI_{dp}}{dV_{out}}-\dfrac{\partial I_{dn}}{\partial V_{out}}}=-1$$

$$-(A^{/}-A)\frac{\{q\mu_p p_p W\rho(t_{si}-t_{di})+Wt_{di}\}}{\{q\mu_p p_n W\rho(t_{si}-t_{di})+Wt_{di}\}}=(B^{/}-B)$$

$$\frac{(A^{/}-A)\{q\mu_p p_p W\rho(t_{si}-t_{di})+Wt_{di}\}V_{dd}-(A^{/}-A)\{q\mu_p p_p W\rho(t_{si}-t_{di})+Wt_{di}\}(V_{in}-V_{fbn})}{(A^{/}-A)\{q\mu_p p_n W\rho(t_{si}-t_{di})+2Wt_{di}+q\mu_p p_p W\rho(t_{si}-t_{di})\}}$$
$$-\frac{[(C_p^{/}-C_p)\{q\mu_p p_p W\rho(t_{si}-t_{di})+Wt_{di}\}-(C_n^{/}-C_n)\{q\mu_p p_n W\rho(t_{si}-t_{di})+Wt_{di}\}]}{(A^{/}-A)\{q\mu_p p_n W\rho(t_{si}-t_{di})+2Wt_{di}+q\mu_p p_p W\rho(t_{si}-t_{di})\}}$$
$$=V_{out}$$

$$V_{in}=V_{fbn}=V_{IH}$$

Output Low:

$$V_{out}=\frac{(A^{/}-A)\{q\mu_n n_p W\rho(t_{si}-t_{di})+Wt_{di}\}V_{dd}}{(A^{/}-A)\{qW\rho(t_{si}-t_{di})(\mu_n n_n+\mu_n n_p)+2Wt_{di}\}}+\frac{(B^{/}-B)\{q\mu_n n_p W\rho(t_{si}-t_{di})+Wt_{di}\}V_{fbp}}{(A^{/}-A)\{qW\rho(t_{si}-t_{di})(\mu_n n_n+\mu_n n_p)+2Wt_{di}\}}$$
$$-\frac{(C_p^{/}-C_p)\{q\mu_n n_p W\rho(t_{si}-t_{di})+Wt_{di}\}-(C_n^{/}-C_n)\{q\mu_n n_n W\rho(t_{si}-t_{di})+Wt_{di}\}}{(A^{/}-A)\{qW\rho(t_{si}-t_{di})(\mu_n n_n+\mu_n n_p)+2Wt_{di}\}}=V_{OL}$$

Output High:

$$V_{out}=\frac{(A^{/}-A)\{q\mu_p p_p W\rho(t_{si}-t_{di})+Wt_{di}\}V_{dd}}{(A^{/}-A)\{q\mu_p(p_n+p_p)W\rho(t_{si}-t_{di})+2Wt_{di}\}}-\frac{(B^{/}-B)\{q\mu_p p_n W\rho(t_{si}-t_{di})+Wt_{di}\}V_{fbn}}{(A^{/}-A)\{q\mu_p(p_n+p_p)W\rho(t_{si}-t_{di})+2Wt_{di}\}}$$
$$\frac{-(C_p^{/}-C_p)\{q\mu_p p_p W\rho(t_{si}-t_{di})+Wt_{di}\}+(C_n^{/}-C_n)\{q\mu_p p_n W\rho(t_{si}-t_{di})+Wt_{di}\}}{(A^{/}-A)\{q\mu_p(p_n+p_p)W\rho(t_{si}-t_{di})+2Wt_{di}\}}=V_{OH}$$

Inverter Threshold Voltage

$$\frac{\phi(\Delta L)-\phi(0)}{Rn(V_{gs},V_{ds})}=\frac{\phi(\Delta L)-\phi(0)}{Rp(V_{gs},V_{ds})}$$

$$Rn(V_{gs},V_{ds})=R_{nd}n(V_{gs},V_{ds})\,||\,R_{di}\,||\,R_{nd}n(V_{gs},V_{ds})=\frac{\rho\Delta L}{q\mu_n n_n W\rho(t_{si}-t_{di})+Wt_{di}}$$

$$Rp(V_{gs},V_{ds})=R_{nd}p(V_{gs},V_{ds})\,||\,R_{di}\,||\,R_{nd}p(V_{gs},V_{ds})=\frac{\rho\Delta L}{q\mu_p p_p W\rho(t_{si}-t_{di})+Wt_{di}}$$

$$\phi_{gsp}=\phi_{gsn}=0$$

$$V_{dsp}=V_{dd}-V_I$$

$$V_{dsn}=V_I$$

$$\{(A^/-A)V_{dsn}-(B^/-B)\phi_{gsn}-(C_n^/-C_n)\}\{q\mu_n n_n W\rho(t_{si}-t_{di})+Wt_{di}\}$$
$$=\{(A^/-A)V_{dsp}-(B^/-B)\phi_{gsp}-(C_p^/-C_p)\}\{q\mu_p p_p W\rho(t_{si}-t_{di})+Wt_{di}\}$$

$$V_I=\frac{\{q\mu_p p_p W\rho(t_{si}-t_{di})+Wt_{di}\}(A^/-A)V_{dd}+qW\rho(t_{si}-t_{di})\{\mu_n n_n(C_n^/-C_n)-\mu_p p_p(C_p^/-C_p)\}}{(A^/-A)\{qW\rho(t_{si}-t_{di})(\mu_n n_n+\mu_p p_p)+2Wt_{di}\}}$$

Noise Margin:

Noise margin for logic 1 voltages

$$V_{NMH}=V_{OH}-V_{IH}=\frac{(A^/-A)\{q\mu_p p_p W\rho(t_{si}-t_{di})+Wt_{di}\}V_{dd}}{(A^/-A)\{q\mu_p(p_n+p_p)W\rho(t_{si}-t_{di})+2Wt_{di}\}}$$
$$-\frac{[(B^/-B)\{q\mu_p p_n W\rho(t_{si}-t_{di})+Wt_{di}\}+(A^/-A)\{q\mu_p(p_n+p_p)W\rho(t_{si}-t_{di})+2Wt_{di}\}]V_{fbn}}{(A^/-A)\{q\mu_p(p_n+p_p)W\rho(t_{si}-t_{di})+2Wt_{di}\}}$$
$$\frac{-(C_p^/-C_p)\{q\mu_p p_p W\rho(t_{si}-t_{di})+Wt_{di}\}+(C_n^/-C_n)\{q\mu_p p_n W\rho(t_{si}-t_{di})+Wt_{di}\}}{(A^/-A)\{q\mu_p(p_n+p_p)W\rho(t_{si}-t_{di})+2Wt_{di}\}}$$

Noise margin for logic 0 voltages

$$V_{NML} = V_{IL} - V_{OL} = \frac{(A^{/} - A)\{q\mu_n n_n W\rho(t_{si} - t_{di}) + Wt_{di}\}V_{dd}}{(A^{/} - A)\{qW\rho(t_{si} - t_{di})(\mu_n n_n + \mu_n n_p) + 2Wt_{di}\}}$$

$$+ \frac{[(A^{/} - A)\{qW\rho(t_{si} - t_{di})(\mu_n n_n + \mu_n n_p) + 2Wt_{di}\} - (B^{/} - B)\{q\mu_n n_p W\rho(t_{si} - t_{di}) + Wt_{di}\}]V_{fbp}}{(A^{/} - A)\{qW\rho(t_{si} - t_{di})(\mu_n n_n + \mu_n n_p) + 2Wt_{di}\}}$$

$$+ \frac{(C_p^{/} - C_p)\{q\mu_n n_p W\rho(t_{si} - t_{di}) + Wt_{di}\} - (C_n^{/} - C_n)\{q\mu_n n_n W\rho(t_{si} - t_{di}) + Wt_{di}\}}{(A^{/} - A)\{qW\rho(t_{si} - t_{di})(\mu_n n_n + \mu_n n_p) + 2Wt_{di}\}}$$

Fall Time:

$$t_{HL} = C_{out} \int_{V_1}^{V_0} \frac{dV_{out}}{I_{dn}}$$

$V_o = 0.1V_{OH}$ and $V_1 = 0.9V_{OH}$

$$I_{dn} = \frac{\{q\mu_n n_n W\rho(t_{si} - t_{di}) + Wt_{di}\}[(A^{/} - A)V_{out} - (C_n^{/} - C_n)]}{\rho\Delta L}$$

$$t_{HL} = C_{out} \int_{V_1}^{V_0} \frac{dV_{out}}{\frac{\{q\mu_n n_n W\rho(t_{si} - t_{di}) + Wt_{di}\}[(A^{/} - A)V_{out} - (C_n^{/} - C_n)]}{\rho\Delta L}}$$

$$t_{HL} = \frac{\Delta L\rho C_{out}}{\{q\mu_n n_n W\rho(t_{si} - t_{di}) + Wt_{di}\}(A^{/} - A)}\left[\ln\{V_o - \frac{(C_n^{/} - C_n)}{(A^{/} - A)}\} - \ln\{V_1 - \frac{(C_n^{/} - C_n)}{(A^{/} - A)}\}\right]$$

Rise Time:

$$t_{LH} = C_{out} \int_{V_0}^{V_1} \frac{dV_{out}}{I_{dp}}$$

$V_o = 0.1V_{OH}$ and $V_1 = 0.9V_{OH}$

$$I_{dp} = \frac{\{q\mu_p p_p W\rho(t_{si} - t_{di}) + Wt_{di}\}[\{(A' - A)(V_{dd} - V_{out}) - (C_p' - C_p)\}]}{\rho\Delta L}$$

$$t_{LH} = C_{out}\int_{V_0}^{V_1} \frac{dV_{out}}{\frac{\{q\mu_p p_p W\rho(t_{si} - t_{di}) + Wt_{di}\}[\{(A' - A)(V_{dd} - V_{out}) - (C_p' - C_p)\}]}{\rho\Delta L}}$$

$$t_{LH} = \frac{\Delta L\rho C_{out}}{\{q\mu_p p_p W\rho(t_{si} - t_{di}) + Wt_{di}\}(A' - A)}\left[\ln\{V_{dd} - V_1 - \frac{(C_p' - C_p)}{(A' - A)}\} - \ln\{V_{dd} - V_0 - \frac{(C_p' - C_p)}{(A' - A)}\}\right]$$

Propagation Delay

$$t_{PHL} = \frac{\Delta L\rho C_{out}}{\{q\mu_n n_n W\rho(t_{si} - t_{di}) + Wt_{di}\}(A' - A)}\left[\ln\{V_I - \frac{(C_n' - C_n)}{(A' - A)}\} - \ln\{V_{OH} - \frac{(C_n' - C_n)}{(A' - A)}\}\right]$$

$$t_{PLH} = \frac{\Delta L\rho C_{out}}{\{q\mu_p p_p W\rho(t_{si} - t_{di}) + Wt_{di}\}(A' - A)}\left[\ln\{V_{dd} - V_{OH} - \frac{(C_p' - C_p)}{(A' - A)}\} - \ln\{V_{dd} - V_I - \frac{(C_p' - C_p)}{(A' - A)}\}\right]$$

Propagation delay is given as,

$$t_P = \frac{t_{PHL} + t_{PLH}}{2}$$

Power Loss

$$P_d = V_{out} I_{ds}$$

6.4.3 JLT with Diagonal Dielectric (Symmetric)

$$R_d n(x, V_{gs}, V_{ds}) = \frac{1}{q\mu_p p_n}\frac{\Delta L}{WW_d}$$

$$R_d p(x, V_{gs}, V_{ds}) = \frac{1}{q\mu_n n_p}\frac{\Delta L}{WW_d}$$

$$R_{nd}n(x,V_{gs},V_{ds})=\frac{1}{q\mu_n n_n}\frac{\Delta L}{W(t_{si}-W_d)}$$

$$R_{nd}\,p(x,V_{gs},V_{ds})=\frac{1}{q\mu_p p_p}\frac{\Delta L}{W(t_{si}-W_d)}$$

$$\phi_0(0)=\left[\frac{V_{ds}(e^{\frac{L+L_d}{\lambda_1}}-e^{\frac{L+L_d-2L_s}{\lambda_1}})+(-\frac{qN_d}{\in_{si}}-\frac{1}{\lambda_1^{2}}\phi_{gs})\lambda_1^{2}(e^{\frac{L+L_d}{\lambda_1}}-e^{-\frac{L_s}{\lambda_1}}-e^{\frac{L+L_d-2L_s}{\lambda_1}}+e^{\frac{2(L+L_d)-L_s}{\lambda_1}}-e^{2\frac{L+L_d}{\lambda_1}}+e^{-2\frac{L_s}{\lambda_1}})}{(e^{2\frac{L+L_d}{\lambda_1}}-e^{-2\frac{L_s}{\lambda_1}})}\right]$$

$$=V_{ds}\frac{(e^{\frac{L+L_d}{\lambda_1}}-e^{\frac{L+L_d-2L_s}{\lambda_1}})}{(e^{2\frac{L+L_d}{\lambda_1}}-e^{-2\frac{L_s}{\lambda_1}})}-\phi_{gs}\frac{(e^{\frac{L+L_d}{\lambda_1}}-e^{-\frac{L_s}{\lambda_1}}-e^{\frac{L+L_d-2L_s}{\lambda_1}}+e^{\frac{2(L+L_d)-L_s}{\lambda_1}}-e^{2\frac{L+L_d}{\lambda_1}}+e^{-2\frac{L_s}{\lambda_1}})}{(e^{2\frac{L+L_d}{\lambda_1}}-e^{-2\frac{L_s}{\lambda_1}})}$$

$$-\frac{qN_d}{\in_{si}}\lambda_1^{2}\frac{(e^{\frac{L+L_d}{\lambda_1}}-e^{-\frac{L_s}{\lambda_1}}-e^{\frac{L+L_d-2L_s}{\lambda_1}}+e^{\frac{2(L+L_d)-L_s}{\lambda_1}}-e^{2\frac{L+L_d}{\lambda_1}}+e^{-2\frac{L_s}{\lambda_1}})}{(e^{2\frac{L+L_d}{\lambda_1}}-e^{-2\frac{L_s}{\lambda_1}})}$$

Where,

$$\lambda_1=\sqrt{\frac{t_{si}(4\in_{si}t_{ox}+\in_{ox}^{/}t_{si})}{8\in_{ox}^{/}}}$$

$$\phi_0(0)=A_1V_{ds}-B_1\phi_{gs}-C_{1n}$$

$$\phi_0(\Delta L)=$$

$$V_{ds}\frac{(e^{\frac{L+L_d+\Delta L}{\lambda_1}}-e^{\frac{L+L_d-2L_s-\Delta L}{\lambda_1}})}{(e^{2\frac{L+L_d}{\lambda_1}}-e^{-2\frac{L_s}{\lambda_1}})}-\phi_{gs}\frac{(e^{\frac{L+L_d+\Delta L}{\lambda_1}}-e^{-\frac{L_s+\Delta L}{\lambda_1}}-e^{\frac{L+L_d-2L_s-\Delta L}{\lambda_1}}+e^{\frac{2(L+L_d)-L_s-\Delta L}{\lambda_1}}-e^{2\frac{L+L_d}{\lambda_1}}+e^{-2\frac{L_s}{\lambda_1}})}{(e^{2\frac{L+L_d}{\lambda_1}}-e^{-2\frac{L_s}{\lambda_1}})}$$

$$-\frac{qN_d}{\in_{si}}\lambda_1^{2}\frac{(e^{\frac{L+L_d+\Delta L}{\lambda_1}}-e^{-\frac{L_s+\Delta L}{\lambda_1}}-e^{\frac{L+L_d-2L_s-\Delta L}{\lambda_1}}+e^{\frac{2(L+L_d)-L_s-\Delta L}{\lambda_1}}-e^{2\frac{L+L_d}{\lambda_1}}+e^{-2\frac{L_s}{\lambda_1}})}{(e^{2\frac{L+L_d}{\lambda_1}}-e^{-2\frac{L_s}{\lambda_1}})}$$

$$\phi_0(\Delta L)=A_1^{/}V_{ds}-B_1^{/}\phi_{gs}-C_{1n}^{/}$$

For p-channel JLT

$$\phi_0(0) = A_1 V_{ds} - B_1 \phi_{gs} - C_{1p}$$

$$\phi_0(\Delta L) = A_1^{/} V_{ds} - B_1^{/} \phi_{gs} - C_{1p}^{/}$$

Where,

$$C_{1p} = -\frac{qN_a}{\in_{si}} \lambda_1^2 \frac{(e^{\frac{L+L_d}{\lambda_1}} - e^{-\frac{L_s}{\lambda_1}} - e^{\frac{L+L_d-2L_s}{\lambda_1}} + e^{\frac{2(L+L_d)-L_s}{\lambda_1}} - e^{2\frac{L+L_d}{\lambda_1}} + e^{-2\frac{L_s}{\lambda_1}})}{(e^{2\frac{L+L_d}{\lambda_1}} - e^{-2\frac{L_s}{\lambda_1}})}$$

$$C_{1p}^{/} = -\frac{qN_a}{\in_{si}} \lambda_1^2 \frac{(e^{\frac{L+L_d+\Delta L}{\lambda_1}} - e^{-\frac{L_s+\Delta L}{\lambda_1}} - e^{\frac{L+L_d-2L_s-\Delta L}{\lambda_1}} + e^{\frac{2(L+L_d)-L_s-\Delta L}{\lambda_1}} - e^{2\frac{L+L_d}{\lambda_1}} + e^{-2\frac{L_s}{\lambda_1}})}{(e^{2\frac{L+L_d}{\lambda_1}} - e^{-2\frac{L_s}{\lambda_1}})}$$

Input Low:

$I_{dpnonsat} = I_{dnsat}$

At Saturation,

$$\phi_{gsn} = V_{gsn} - V_{fbn} = 0 \tag{6.58}$$

or,

$$I_{dnsat} = I_{dpnonsat}$$

$$\frac{\phi(\Delta L) - \phi(0)}{Rn(V_{gs}, V_{ds})} = \frac{\phi(\Delta L) - \phi(0)}{Rp(V_{gs}, V_{ds})}$$

$$Rp(V_{gs}, V_{ds}) = R_d\, p(V_{gs}, V_{ds}) = \frac{\Delta L}{q\mu_n n_p W t_{si}}$$

$$Rn(V_{gs},V_{ds}) = R_{nd}n(V_{gs},V_{ds}) = \frac{\Delta L}{q\mu_n n_n W t_{si}}$$

$$[(A_1^/ - A_1)V_{dsp} - (B_1^/ - B_1)\phi_{gsp} - (C_{1p}^/ - C_{1p})]n_p = [(A_1^/ - A_1)V_{dsn} - (B_1^/ - B_1)\phi_{gsn} - (C_{1n}^/ - C_{1n})]n_n$$

$$[(A_1^/ - A_1)(V_{dd} - V_{out}) - (B_1^/ - B_1)(V_{dd} - V_{in} - V_{fbp}) - (C_{1p}^/ - C_{1p})]n_p$$
$$= [(A_1^/ - A_1)(V_{out}) - (B_1^/ - B_1)(V_{in} - V_{fbn}) - (C_{1n}^/ - C_{1n})]n_n \quad (6.59)$$

$$\frac{dV_{out}}{dV_{in}} = \frac{\dfrac{\partial I_{dp}}{\partial V_{in}}}{\dfrac{dI_{dn}}{dV_{out}} - \dfrac{\partial I_{dp}}{\partial V_{out}}} = -1$$

or, $(B_1^/ - B_1) = -(A_1^/ - A_1)\dfrac{(n_n + n_p)}{n_p}$

$$\frac{(A_1^/ - A_1)(n_n + 2n_p)V_{dd} - (A_1^/ - A_1)(n_n + n_p)V_{in} - (A_1^/ - A_1)(n_n + n_p)V_{fbp} - \{(C_{1p}^/ - C_p)n_p - (C_{1n}^/ - C_{1n})n_n\}}{(A_1^/ - A_1)(n_n + n_p)}$$
$$= V_{out}$$
$$V_{in} = (V_{dd} - V_{fbp}) = V_{IL}$$

Input High:

$$I_{dnnonsat} = I_{dpsat}$$

$$\phi_{gsp} = V_{gsp} - V_{fbp} = 0 \quad (6.60)$$

$$\frac{\phi(\Delta L) - \phi(0)}{R_d(V_{gs},V_{ds})} = \frac{\phi(\Delta L) - \phi(0)}{R_{nd}\,p(V_{gs},V_{ds})}$$

$$\{(A_1^/ - A_1)V_{dsp} - (B_1^/ - B_1)\phi_{gsp} - (C_{1p}^/ - C_{1p})\}p_p = \{(A_1^/ - A_1)V_{dsn} - (B_1^/ - B_1)\phi_{gsn} - (C_{1n}^/ - C_{1n})\}p_n$$

$$\{(A_1^{/}-A_1)(V_{dd}-V_{out})-(B_1^{/}-B_1)(V_{dd}-V_{in}-V_{fbp})-(C_{1p}^{/}-C_{1p})\}p_p$$
$$=\{(A_1^{/}-A_1)(V_{out})-(B_1^{/}-B_1)(V_{in}-V_{fbn})-(C_{1n}^{/}-C_{1n})\}p_n \tag{6.61}$$

$$\frac{dV_{out}}{dV_{in}}=\frac{\dfrac{\partial I_{dn}}{\partial V_{in}}}{\dfrac{dI_{dp}}{dV_{out}}-\dfrac{\partial I_{dn}}{\partial V_{out}}}=-1$$

$$-(A_1^{/}-A_1)\frac{p_p}{p_n}=(B_1^{/}-B_1)$$

$$\frac{(A_1^{/}-A_1)p_pV_{dd}-(A_1^{/}-A_1)p_p(V_{in}-V_{fbn})-\{(C_{1p}^{/}-C_{1p})p_p-(C_{1n}^{/}-C_{1n})p_n)}{(A_1^{/}-A_1)(p_n+p_p)}$$
$$=V_{out}$$

$$V_{in}=V_{fbn}=V_{IH}$$

Output Low:

$$V_{out}=\frac{(A_1^{/}-A_1)n_pV_{dd}+(B_1^{/}-B_1)n_pV_{fbp}-(C_{1p}^{/}-C_{1p})n_p+(C_{1n}^{/}-C_{1n})n_n}{(A_1^{/}-A_1)(n_n+n_p)}=V_{OL}$$

Output High:

$$V_{out}=\frac{(A_1^{/}-A_1)p_pV_{dd}-(B_1^{/}-B_1)p_nV_{fbn}-(C_{1p}^{/}-C_{1p})p_p+(C_{1n}^{/}-C_{1n})p_n}{(A_1^{/}-A_1)(p_n+p_p)}=V_{OH}$$

Inverter Threshold Voltage

$$\frac{\phi(\Delta L)-\phi(0)}{R_{nd}n(V_{gs},V_{ds})}=\frac{\phi(\Delta L)-\phi(0)}{R_{nd}p(V_{gs},V_{ds})}$$

$$\phi_{gsp}=\phi_{gsn}=0$$

$$V_{dsp} = V_{dd} - V_I$$

$$V_{dsn} = V_I$$

$$\frac{(A_1^{/} - A_1)V_{dsn} - (B_1^{/} - B_1)\phi_{gsn} - (C_{1p}^{/} - C_{1p})}{\dfrac{\Delta L}{2q\mu_n n_n W t_{si}}} = \frac{(A_1^{/} - A_1)V_{dsp} - (B_1^{/} - B_1)\phi_{gsp} - (C_{1n}^{/} - C_{1n})}{\dfrac{\Delta L}{2q\mu_p p_p W t_{si}}}$$

$$\mu_n n_n\{(A_1^{/} - A_1)V_I - (C_{1n}^{/} - C_{1n})\} = \mu_p p_p\{(A_1^{/} - A_1)(V_{dd} - V_I) - (C_{1p}^{/} - C_{1p})\}$$

$$V_I = \frac{\mu_p p_p (A_1^{/} - A_1)V_{dd} + \{\mu_n n_n (C_{1n}^{/} - C_{1n}) - \mu_p p_p (C_{1p}^{/} - C_{1p})\}}{(\mu_n n_n + \mu_p p_p)(A_1^{/} - A_1)}$$

Noise Margin:

Noise margin for logic 1 voltages

$$V_{NMH} = V_{OH} - V_{IH} = \frac{(A_1^{/} - A_1)p_p V_{dd} - (B_1^{/} - B_1)p_n V_{fbn} - (C_{1p}^{/} - C_{1p})p_p + (C_{1n}^{/} - C_{1n})p_n}{(A_1^{/} - A_1)(p_n + p_p)} - V_{fbn}$$

Noise margin for logic 0 voltages

$$V_{NML} = V_{IL} - V_{OL} = \frac{(A_1^{/} - A_1)n_n V_{dd} - \{(A_1^{/} - A_1)(n_n + n_p) + (B_1^{/} - B_1)n_p\}V_{fbp} + (C_{1p}^{/} - C_{1p})n_p - (C_{1n}^{/} - C_{1n})n_n}{(A_1^{/} - A_1)(n_n + n_p)}$$

Fall Time:

$$t_{HL} = C_{out}\int_{V_1}^{V_0} \frac{dV_{out}}{I_{dn}}$$

$V_o = 0.1V_{OH}$ and $V_1 = 0.9V_{OH}$

$$I_{dn} = \frac{q\mu_n n_n W t_{si}[(A_1^/ - A_1)V_{out} - (C_{1n}^/ - C_{1n})]}{\Delta L}$$

$$t_{HL} = C_{out}\int_{V_1}^{V_0} \frac{dV_{out}}{\frac{q\mu_n n_n W t_{si}[(A_1^/ - A_1)V_{out} - (C_{1n}^/ - C_{1n})]}{\Delta L}}$$

$$t_{HL} = \frac{\Delta L C_{out}}{q\mu_n n_n W t_{si}(A_1^/ - A_1)}\left[\ln\{V_o - \frac{(C_{1n}^/ - C_{1n})}{(A_1^/ - A_1)}\} - \ln\{V_1 - \frac{(C_{1n}^/ - C_{1n})}{(A_1^/ - A_1)}\}\right]$$

Rise Time:

$$t_{LH} = C_{out}\int_{V_0}^{V_1} \frac{dV_{out}}{I_{dp}}$$

$V_o = 0.1V_{OH}$ and $V_1 = 0.9V_{OH}$

$$I_{dp} = \frac{q\mu_p p_p W t_{si}[\{(A_1^/ - A_1)(V_{dd} - V_{out}) - (C_{1p}^/ - C_{1p})\}]}{\Delta L}$$

$$t_{LH} = C_{out}\int_{V_0}^{V_1} \frac{dV_{out}}{\frac{q\mu_p p_p W t_{si}[\{(A_1^/ - A_1)(V_{dd} - V_{out}) - (C_{1p}^/ - C_{1p})\}]}{\Delta L}}$$

$$t_{LH} = \frac{\Delta L C_{out}}{q\mu_p p_p W t_{si}(A_1^/ - A_1)}\left[\ln\{V_{dd} - V_1 - \frac{(C_{1p}^/ - C_{1p})}{(A_1^/ - A_1)}\} - \ln\{V_{dd} - V_0 - \frac{(C_{1p}^/ - C_{1p})}{(A_1^/ - A_1)}\}\right]$$

Propagation Delay

$$t_{PHL} = \frac{\Delta L C_{out}}{q\mu_n n_n W t_{si}(A_1^/ - A_1)}\left[\ln\{V_I - \frac{(C_{1n}^/ - C_{1n})}{(A_1^/ - A_1)}\} - \ln\{V_{OH} - \frac{(C_{1n}^/ - C_{1n})}{(A_1^/ - A_1)}\}\right]$$

$$t_{PLH} = \frac{\Delta L C_{out}}{q\mu_p p_p W t_{si}(A_1^{/} - A_1)}\left[\ln\{V_{dd} - V_{OH} - \frac{(C_{1p}^{/} - C_{1p})}{(A_1^{/} - A_1)}\} - \ln\{V_{dd} - V_I - \frac{(C_{1p}^{/} - C_{1p})}{(A_1^{/} - A_1)}\}\right]$$

Propagation delay is given as,

$$t_P = \frac{t_{PHL} + t_{PLH}}{2}$$

Power Loss

$$P_d = V_{out} I_{ds}$$

6.4.4 JLT with Diagonal Dielectric (Asymmetric)

$$R_d n(x, V_{gs}, V_{ds}) = \frac{1}{q\mu_p p_n}\frac{\Delta L}{WW_d}$$

$$R_d p(x, V_{gs}, V_{ds}) = \frac{1}{q\mu_n n_p}\frac{\Delta L}{WW_d}$$

$$R_{nd} n(x, V_{gs}, V_{ds}) = \frac{1}{q\mu_n n_n}\frac{\Delta L}{W(t_{si} - W_d)}$$

$$R_{nd} p(x, V_{gs}, V_{ds}) = \frac{1}{q\mu_p p_p}\frac{\Delta L}{W(t_{si} - W_d)}$$

$$\phi_{01}(0)=\left[\frac{V_{ds}(e^{\frac{L+L_d}{\lambda_1}}-e^{\frac{L+L_d-2L_s}{\lambda_1}})+(-\frac{qN_d}{\epsilon_{si}}-\frac{1}{\lambda_1^2}\phi_{gs})\lambda_1^2(e^{\frac{L+L_d}{\lambda_1}}-e^{-\frac{L_s}{\lambda_1}}-e^{\frac{L+L_d-2L_s}{\lambda_1}}+e^{\frac{2(L+L_d)-L_s}{\lambda_1}}-e^{2\frac{L+L_d}{\lambda_1}}+e^{-2\frac{L_s}{\lambda_1}})}{(e^{2\frac{L+L_d}{\lambda_1}}-e^{-2\frac{L_s}{\lambda_1}})}\right]$$

$$=V_{ds}\frac{(e^{\frac{L+L_d}{\lambda_1}}-e^{\frac{L+L_d-2L_s}{\lambda_1}})}{(e^{2\frac{L+L_d}{\lambda_1}}-e^{-2\frac{L_s}{\lambda_1}})}-\phi_{gs}\frac{(e^{\frac{L+L_d}{\lambda_1}}-e^{-\frac{L_s}{\lambda_1}}-e^{\frac{L+L_d-2L_s}{\lambda_1}}+e^{\frac{2(L+L_d)-L_s}{\lambda_1}}-e^{2\frac{L+L_d}{\lambda_1}}+e^{-2\frac{L_s}{\lambda_1}})}{(e^{2\frac{L+L_d}{\lambda_1}}-e^{-2\frac{L_s}{\lambda_1}})}$$

$$-\frac{qN_d}{\epsilon_{si}}\lambda_1^2\frac{(e^{\frac{L+L_d}{\lambda_1}}-e^{-\frac{L_s}{\lambda_1}}-e^{\frac{L+L_d-2L_s}{\lambda_1}}+e^{\frac{2(L+L_d)-L_s}{\lambda_1}}-e^{2\frac{L+L_d}{\lambda_1}}+e^{-2\frac{L_s}{\lambda_1}})}{(e^{2\frac{L+L_d}{\lambda_1}}-e^{-2\frac{L_s}{\lambda_1}})}$$

$$\phi_{02}(0)=\left[\frac{V_{ds}(e^{\frac{L+L_d}{\lambda_2}}-e^{\frac{L+L_d-2L_s}{\lambda_2}})+(-\frac{qN_d}{\epsilon_{si}}-\frac{1}{\lambda_2^2}\phi_{gs})\lambda_2^2(e^{\frac{L+L_d}{\lambda_2}}-e^{-\frac{L_s}{\lambda_2}}-e^{\frac{L+L_d-2L_s}{\lambda_2}}+e^{\frac{2(L+L_d)-L_s}{\lambda_2}}-e^{2\frac{L+L_d}{\lambda_2}}+e^{-2\frac{L_s}{\lambda_2}})}{(e^{2\frac{L+L_d}{\lambda_2}}-e^{-2\frac{L_s}{\lambda_2}})}\right]$$

$$=V_{ds}\frac{(e^{\frac{L+L_d}{\lambda_2}}-e^{\frac{L+L_d-2L_s}{\lambda_2}})}{(e^{2\frac{L+L_d}{\lambda_2}}-e^{-2\frac{L_s}{\lambda_2}})}-\phi_{gs}\frac{(e^{\frac{L+L_d}{\lambda_2}}-e^{-\frac{L_s}{\lambda_2}}-e^{\frac{L+L_d-2L_s}{\lambda_2}}+e^{\frac{2(L+L_d)-L_s}{\lambda_2}}-e^{2\frac{L+L_d}{\lambda_2}}+e^{-2\frac{L_s}{\lambda_2}})}{(e^{2\frac{L+L_d}{\lambda_2}}-e^{-2\frac{L_s}{\lambda_2}})}$$

$$-\frac{qN_d}{\epsilon_{si}}\lambda_2^2\frac{(e^{\frac{L+L_d}{\lambda_2}}-e^{-\frac{L_s}{\lambda_2}}-e^{\frac{L+L_d-2L_s}{\lambda_2}}+e^{\frac{2(L+L_d)-L_s}{\lambda_2}}-e^{2\frac{L+L_d}{\lambda_2}}+e^{-2\frac{L_s}{\lambda_2}})}{(e^{2\frac{L+L_d}{\lambda_2}}-e^{-2\frac{L_s}{\lambda_2}})}$$

Where,

$$\lambda_1=\sqrt{\frac{t_{si}(4\in_{si}t_{ox}+\in_{oxg1}t_{si})}{8\in_{oxg1}}}$$

$$\lambda_2=\sqrt{\frac{t_{si}(4\in_{si}t_{ox}+\in_{oxg2}t_{si})}{8\in_{oxg2}}}$$

$$\phi_{01}(0)=A_1V_{ds}-B_1\phi_{gs}-C_{1n}$$

$$\phi_{02}(0) = A_2 V_{ds} - B_2 \phi_{gs} - C_{2n}$$

$$\phi_0^{/}(0) = \phi_{01}(0) - \phi_{02}(0) = (A_1 - A_2)V_{ds} - (B_1 - B_2)\phi_{gs} - (C_{1n} - C_{2n})$$

$$\phi_{01}(\Delta L) =$$

$$V_{ds}\frac{(e^{\frac{L+L_d+\Delta L}{\lambda_1}} - e^{\frac{L+L_d-2L_s-\Delta L}{\lambda_1}})}{(e^{2\frac{L+L_d}{\lambda_1}} - e^{-2\frac{L_s}{\lambda_1}})} - \phi_{gs}\frac{(e^{\frac{L+L_d+\Delta L}{\lambda_1}} - e^{-\frac{L_s+\Delta L}{\lambda_1}} - e^{\frac{L+L_d-2L_s-\Delta L}{\lambda_1}} + e^{\frac{2(L+L_d)-L_s-\Delta L}{\lambda_1}} - e^{2\frac{L+L_d}{\lambda_1}} + e^{-2\frac{L_s}{\lambda_1}})}{(e^{2\frac{L+L_d}{\lambda_1}} - e^{-2\frac{L_s}{\lambda_1}})}$$

$$-\frac{qN_d}{\in_{si}}\lambda_1^2\frac{(e^{\frac{L+L_d+\Delta L}{\lambda_1}} - e^{-\frac{L_s+\Delta L}{\lambda_1}} - e^{\frac{L+L_d-2L_s-\Delta L}{\lambda_1}} + e^{\frac{2(L+L_d)-L_s-\Delta L}{\lambda_1}} - e^{2\frac{L+L_d}{\lambda_1}} + e^{-2\frac{L_s}{\lambda_1}})}{(e^{2\frac{L+L_d}{\lambda_1}} - e^{-2\frac{L_s}{\lambda_1}})}$$

$$\phi_{02}(\Delta L) =$$

$$V_{ds}\frac{(e^{\frac{L+L_d+\Delta L}{\lambda_2}} - e^{\frac{L+L_d-2L_s-\Delta L}{\lambda_2}})}{(e^{2\frac{L+L_d}{\lambda_2}} - e^{-2\frac{L_s}{\lambda_2}})} - \phi_{gs}\frac{(e^{\frac{L+L_d+\Delta L}{\lambda_2}} - e^{-\frac{L_s+\Delta L}{\lambda_2}} - e^{\frac{L+L_d-2L_s-\Delta L}{\lambda_2}} + e^{\frac{2(L+L_d)-L_s-\Delta L}{\lambda_2}} - e^{2\frac{L+L_d}{\lambda_2}} + e^{-2\frac{L_s}{\lambda_2}})}{(e^{2\frac{L+L_d}{\lambda_2}} - e^{-2\frac{L_s}{\lambda_2}})}$$

$$-\frac{qN_d}{\in_{si}}\lambda_2^2\frac{(e^{\frac{L+L_d+\Delta L}{\lambda_2}} - e^{-\frac{L_s+\Delta L}{\lambda_2}} - e^{\frac{L+L_d-2L_s-\Delta L}{\lambda_2}} + e^{\frac{2(L+L_d)-L_s-\Delta L}{\lambda_2}} - e^{2\frac{L+L_d}{\lambda_2}} + e^{-2\frac{L_s}{\lambda_2}})}{(e^{2\frac{L+L_d}{\lambda_2}} - e^{-2\frac{L_s}{\lambda_2}})}$$

$$\phi_{01}(\Delta L) = A_1^{/}V_{ds} - B_1^{/}\phi_{gs} - C_{1n}^{/}$$

$$\phi_{02}(\Delta L) = A_2^{/}V_{ds} - B_2^{/}\phi_{gs} - C_{2n}^{/}$$

$$\phi_0^{/}(\Delta L) = \phi_{01}(\Delta L) - \phi_{02}(\Delta L) = (A_1^{/} - A_2^{/})V_{ds} - (B_1^{/} - B_2^{/})\phi_{gs} - (C_{1n}^{/} - C_{2n}^{/})$$

For p-channel JLT

$$\phi_0^{/}(0) = \phi_{01}(0) - \phi_{02}(0) = (A_1 - A_2)V_{ds} - (B_1 - B_2)\phi_{gs} - (C_{1p} - C_{2p})$$

and

$$\phi_0^{/}(\Delta L)=\phi_{01}(\Delta L)-\phi_{02}(\Delta L)=(A_1^{/}-A_2^{/})V_{ds}-(B_1^{/}-B_2^{/})\phi_{gs}-(C_{1p}^{/}-C_{2p}^{/})$$

Where,

$$C_{1p}=-\frac{qN_a}{\in_{si}}\lambda_1^2\frac{(e^{\frac{L+L_d}{\lambda_1}}-e^{-\frac{L_s}{\lambda_1}}-e^{\frac{L+L_d-2L_s}{\lambda_1}}+e^{\frac{2(L+L_d)-L_s}{\lambda_1}}-e^{2\frac{L+L_d}{\lambda_1}}+e^{-2\frac{L_s}{\lambda_1}})}{(e^{2\frac{L+L_d}{\lambda_1}}-e^{-2\frac{L_s}{\lambda_1}})}$$

$$C_{2p}=-\frac{qN_a}{\in_{si}}\lambda_2^2\frac{(e^{\frac{L+L_d}{\lambda_2}}-e^{-\frac{L_s}{\lambda_2}}-e^{\frac{L+L_d-2L_s}{\lambda_2}}+e^{\frac{2(L+L_d)-L_s}{\lambda_2}}-e^{2\frac{L+L_d}{\lambda_2}}+e^{-2\frac{L_s}{\lambda_2}})}{(e^{2\frac{L+L_d}{\lambda_2}}-e^{-2\frac{L_s}{\lambda_2}})}$$

$$C_{1p}^{/}=-\frac{qN_a}{\in_{si}}\lambda_1^2\frac{(e^{\frac{L+L_d+\Delta L}{\lambda_1}}-e^{-\frac{L_s+\Delta L}{\lambda_1}}-e^{\frac{L+L_d-2L_s-\Delta L}{\lambda_1}}+e^{\frac{2(L+L_d)-L_s-\Delta L}{\lambda_1}}-e^{2\frac{L+L_d}{\lambda_1}}+e^{-2\frac{L_s}{\lambda_1}})}{(e^{2\frac{L+L_d}{\lambda_1}}-e^{-2\frac{L_s}{\lambda_1}})}$$

$$C_{2p}^{/}=-\frac{qN_a}{\in_{si}}\lambda_2^2\frac{(e^{\frac{L+L_d+\Delta L}{\lambda_2}}-e^{-\frac{L_s+\Delta L}{\lambda_2}}-e^{\frac{L+L_d-2L_s-\Delta L}{\lambda_2}}+e^{\frac{2(L+L_d)-L_s-\Delta L}{\lambda_2}}-e^{2\frac{L+L_d}{\lambda_2}}+e^{-2\frac{L_s}{\lambda_2}})}{(e^{2\frac{L+L_d}{\lambda_2}}-e^{-2\frac{L_s}{\lambda_2}})}$$

Input Low:

$I_{dpnonsat}= I_{dnsat}$

At Saturation,

$$\phi_{gsn}=V_{gsn}-V_{fbn}=0 \tag{6.62}$$

or,

$$I_{dnsat}=I_{dpnonsat}$$

$$\frac{\phi^{/}(\Delta L)-\phi^{/}(0)}{Rn(V_{gs},V_{ds})}=\frac{\phi^{/}(\Delta L)-\phi^{/}(0)}{Rp(V_{gs},V_{ds})}$$

$$Rp(V_{gs},V_{ds})=R_{d}\,p(V_{gs},V_{ds})=\frac{\Delta L}{q\mu_{n}n_{p}Wt_{si}}$$

$$Rn(V_{gs},V_{ds})=R_{nd}n(V_{gs},V_{ds})=\frac{\Delta L}{q\mu_{n}n_{n}Wt_{si}}$$

$$[(A_{3}^{/}-A_{3})V_{dsp}-(B_{3}^{/}-B_{3})\phi_{gsp}-(C_{3p}^{/}-C_{3p})]n_{p}$$
$$=[(A_{3}^{/}-A_{3})V_{dsn}-(B_{3}^{/}-B_{3})\phi_{gsn}-(C_{3n}^{/}-C_{3n})]n_{n}$$

$$A_{3}=(A_{1}-A_{2})$$

$$B_{3}=(B_{1}-B_{2})$$

$$C_{3p}=(C_{1p}-C_{2p})$$

$$C_{3n}=(C_{1n}-C_{2n})$$

$$A_{3}^{/}=(A_{1}^{/}-A_{2}^{/})$$

$$B_{3}^{/}=(B_{1}^{/}-B_{2}^{/})$$

$$C_{3p}^{/}=(C_{1p}^{/}-C_{2p}^{/})$$

$$C_{3n}^{/}=(C_{1n}^{/}-C_{2n}^{/})$$

$$[(A_{3}^{/}-A_{3})(V_{dd}-V_{out})-(B_{3}^{/}-B_{3})(V_{dd}-V_{in}-V_{fbp})-(C_{3p}^{/}-C_{3p})]n_{p}$$
$$=[(A_{3}^{/}-A_{3})(V_{out})-(B_{3}^{/}-B_{3})(V_{in}-V_{fbn})-(C_{3n}^{/}-C_{3n})]n_{n} \quad (6.63)$$

$$\frac{dV_{out}}{dV_{in}} = \frac{\frac{\partial I_{dp}}{\partial V_{in}}}{\frac{dI_{dn}}{dV_{out}} - \frac{\partial I_{dp}}{\partial V_{out}}} = -1$$

$$(B_3^{/} - B_3) = -(A_3^{/} - A_3)\frac{(n_n + n_p)}{n_p}$$

$$\frac{(A_3^{/} - A_3)(n_n + 2n_p)V_{dd} - (A_3^{/} - A_3)(n_n + n_p)V_{in} - (A_3^{/} - A_3)(n_n + n_p)V_{fbp} - \{(C_{3p}^{/} - C_{3p})n_p - (C_{3n}^{/} - C_{3n})n_n\}}{(A_3^{/} - A_3)(n_n + n_p)}$$

$$= V_{out}$$

$$V_{in} = (V_{dd} - V_{fbp}) = V_{IL}$$

Input High:

$$I_{dnnonsat} = I_{dpsat}$$

$$\phi_{gsp} = V_{gsp} - V_{fbp} = 0 \tag{6.64}$$

$$\frac{\phi(\Delta L) - \phi(O)}{R_d(V_{gs}, V_{ds})} = \frac{\phi(\Delta L) - \phi(O)}{R_{nd}\,p(V_{gs}, V_{ds})}$$

$$[(A_3^{/} - A_3)V_{dsp} - (B_3^{/} - B_3)\phi_{gsp} - (C_{3p}^{/} - C_{3p})]p_p$$
$$= [(A_3^{/} - A_3)V_{dsn} - (B_3^{/} - B_3)\phi_{gsn} - (C_{3n}^{/} - C_{3n})]p_n$$

$$[(A_3^{/} - A_3)(V_{dd} - V_{out}) - (B_3^{/} - B_3)(V_{dd} - V_{in} - V_{fbp}) - (C_{3p}^{/} - C_{3p})]p_p$$
$$= [(A_3^{/} - A_3)(V_{out}) - (B_3^{/} - B_3)(V_{in} - V_{fbn}) - (C_{3n}^{/} - C_{3n})]p_n \tag{6.65}$$

$$\frac{dV_{out}}{dV_{in}} = \frac{\frac{\partial I_{dn}}{\partial V_{in}}}{\frac{dI_{dp}}{dV_{out}} - \frac{\partial I_{dn}}{\partial V_{out}}} = -1$$

$$-(A_3^{/}-A_3)\frac{p_p}{p_n}=(B_3^{/}-B_3)$$

$$\frac{(A_3^{/}-A_3)p_pV_{dd}-(A_3^{/}-A_3)p_p(V_{in}-V_{fbn})-\{(C_{3p}^{/}-C_{3p})p_p-(C_{3n}^{/}-C_{3n})p_n)}{(A_3^{/}-A_3)(p_n+p_p)}$$

$$=V_{out}$$

$$V_{in}=V_{fbn}=V_{IH}$$

Output Low:

$$V_{out}=\frac{(A_3^{/}-A_3)n_pV_{dd}+(B_3^{/}-B_3)n_pV_{fbp}-(C_{3p}^{/}-C_{3p})n_p+(C_{3n}^{/}-C_{3n})n_n}{(A_3^{/}-A_3)(n_n+n_p)}=V_{OL}$$

Output High:

$$V_{out}=\frac{(A_3^{/}-A_3)p_pV_{dd}-(B_3^{/}-B_3)p_nV_{fbn}-(C_{3p}^{/}-C_{3p})p_p+(C_{3n}^{/}-C_{3n})p_n}{(A_3^{/}-A_3)(p_n+p_p)}=V_{OH}$$

Inverter Threshold Voltage

$$\frac{\phi(\Delta L)-\phi(O)}{R_{nd}n(V_{gs},V_{ds})}=\frac{\phi(\Delta L)-\phi(O)}{R_{nd}p(V_{gs},V_{ds})}$$

$$\phi_{gsp}=\phi_{gsn}=0$$

$$V_{dsp}=V_{dd}-V_I$$

$$V_{dsn}=V_I$$

$$\frac{(A_3^{/}-A_3)V_{dsn}-(B_3^{/}-B_3)\phi_{gsn}-(C_{3p}^{/}-C_{3p})}{\dfrac{\Delta L}{2q\mu_n n_n W t_{si}}}$$
$$=\frac{(A_3^{/}-A_3)V_{dsp}-(B_3^{/}-B_3)\phi_{gsp}-(C_{3n}^{/}-C_{3n})}{\dfrac{\Delta L}{2q\mu_p p_p W t_{si}}}$$

$$\mu_n n[(A_3^{/}-A_3)V_I-(C_{3n}^{/}-C_{3n})]=\mu_p p[(A_3^{/}-A_3)(V_{dd}-V_I)-(C_{3p}^{/}-C_{3p})]$$

$$V_I=\frac{\mu_p p_p(A^{/}-A)V_{dd}+[\mu_n n_n\{(C_{1n}^{/}-C_{2n}^{/})-(C_{1n}-C_{2n})\}-\mu_p p_p\{(C_{1p}^{/}-C_{2p}^{/})-(C_{1p}-C_{2p})\}]}{(\mu_n n_n+\mu_p p_p)(A^{/}-A)}$$

Noise Margin:

Noise margin for logic 1 voltages

$$V_{NMH}=V_{OH}-V_{IH}=\frac{(A_3^{/}-A_3)p_pV_{dd}-(B_3^{/}-B_3)p_nV_{fbn}-(C_{3p}^{/}-C_{3p})p_p+(C_{3n}^{/}-C_{3n})p_n}{(A_3^{/}-A_3)(p_n+p_p)}-V_{fbn}$$

Noise margin for logic 0 voltages

$$V_{NML}=V_{IL}-V_{OL}=\frac{(A_3^{/}-A_3)n_nV_{dd}-\{(A_3^{/}-A_3)(n_n+n_p)+(B_3^{/}-B_3)n_p\}V_{fbp}+(C_{3p}^{/}-C_{3p})n_p-(C_{3n}^{/}-C_{3n})n_n}{(A_3^{/}-A_3)(n_n+n_p)}$$

Fall Time:

$$t_{HL}=C_{out}\int_{V_1}^{V_0}\frac{dV_{out}}{I_{dn}}$$

$V_o=0.1V_{OH}$ and $V_1=0.9V_{OH}$

$$I_{dn}=\frac{q\mu_n n_n W t_{si}[(A_3^{/}-A_3)V_{out}-(C_{3n}^{/}-C_{3n})]}{\Delta L}$$

$$t_{HL} = C_{out} \int_{V_1}^{V_0} \frac{dV_{out}}{\frac{q\mu_n n_n W t_{si} [(A_3^{/} - A_3)V_{out} - (C_{3n}^{/} - C_{3n})]}{\Delta L}}$$

$$t_{HL} = \frac{\Delta L C_{out}}{q\mu_n n_n W t_{si} (A_3^{/} - A_3)} \left[\ln\{V_o - \frac{(C_{3n}^{/} - C_{3n})}{(A_3^{/} - A_3)}\} - \ln\{V_1 - \frac{(C_{3n}^{/} - C_{3n})}{(A_3^{/} - A_3)}\} \right]$$

Rise Time:

$$t_{LH} = C_{out} \int_{V_0}^{V_1} \frac{dV_{out}}{I_{dp}}$$

$V_o = 0.1V_{OH}$ and $V_1 = 0.9V_{OH}$

$$I_{dp} = \frac{q\mu_p p_p W t_{si} [\{(A_3^{/} - A_3)(V_{dd} - V_{out}) - (C_{3p}^{/} - C_{3p})\}]}{\Delta L}$$

$$t_{LH} = C_{out} \int_{V_0}^{V_1} \frac{dV_{out}}{\frac{q\mu_p p_p W t_{si} [\{(A_3^{/} - A_3)(V_{dd} - V_{out}) - (C_{3p}^{/} - C_{3p})\}]}{\Delta L}}$$

$$t_{LH} = \frac{\Delta L C_{out}}{q\mu_p p_p W t_{si} (A_3^{/} - A_3)} \left[\ln\{V_{dd} - V_1 - \frac{(C_{3p}^{/} - C_{3p})}{(A_3^{/} - A_3)}\} - \ln\{V_{dd} - V_0 - \frac{(C_{3p}^{/} - C_{3p})}{(A_3^{/} - A_3)}\} \right]$$

Propagation Delay

$$t_{PHL} = \frac{\Delta L C_{out}}{q\mu_n n_n W t_{si} (A_3^{/} - A_3)} \left[\ln\{V_I - \frac{(C_{3n}^{/} - C_{3n})}{(A_3^{/} - A_3)}\} - \ln\{V_{OH} - \frac{(C_{3n}^{/} - C_{3n})}{(A_3^{/} - A_3)}\} \right]$$

$$t_{PLH} = \frac{\Delta L C_{out}}{q\mu_p p_p W t_{si} (A_3^{/} - A_3)} \left[\ln\{V_{dd} - V_{OH} - \frac{(C_{3p}^{/} - C_{3p})}{(A_3^{/} - A_3)}\} - \ln\{V_{dd} - V_I - \frac{(C_{3p}^{/} - C_{3p})}{(A_3^{/} - A_3)}\} \right]$$

Propagation delay is given as,

$$t_P = \frac{t_{PHL} + t_{PLH}}{2}$$

Power Loss

$$P_d = V_{out} I_{ds}$$

6.4.5 JLT with Varying Doping Concentration

$$R_d n(x, V_{gs}, V_{ds}) = \frac{1}{q\mu_p p_n} \frac{\Delta L}{W W_d}$$

$$R_d p(x, V_{gs}, V_{ds}) = \frac{1}{q\mu_n n_p} \frac{\Delta L}{W W_d}$$

$$R_{nd} n(x, V_{gs}, V_{ds}) = \frac{1}{q\mu_n n_n} \frac{\Delta L}{W(t_{si} - W_d)}$$

$$R_{nd} p(x, V_{gs}, V_{ds}) = \frac{1}{q\mu_p p_p} \frac{\Delta L}{W(t_{si} - W_d)}$$

$$n_n = \frac{N_d(x)}{2} + \sqrt{\frac{N_d{}^2(x)}{4} + n_i{}^2}$$

$$p_n = \frac{n_i^2}{\frac{N_d(x)}{2} + \sqrt{\frac{N_d(x)^2}{4} + n_i^2}}$$

$$p_p = \frac{N_a(x)}{2} + \sqrt{\frac{N_a{}^2(x)}{4} + n_i{}^2}$$

$$n_p = \frac{n_i^2}{\frac{N_a(x)}{2} + \sqrt{\frac{N_a(x)^2}{4} + n_i^2}}$$

$$\phi_0(0)=$$

$$\left[\frac{V_{ds}(e^{\frac{L+L_d}{\lambda}}-e^{\frac{L+L_d-2L_s}{\lambda}})+(-\frac{qN_d(0)}{\in_{si}}-\frac{1}{\lambda^2}\phi_{gs})\lambda^2(e^{\frac{L+L_d}{\lambda}}-e^{-\frac{L_s}{\lambda}}-e^{\frac{L+L_d-2L_s}{\lambda}}+e^{\frac{2(L+L_d)-L_s}{\lambda}}-e^{2\frac{L+L_d}{\lambda}}+e^{-2\frac{L_s}{\lambda}})}{(e^{2\frac{L+L_d}{\lambda}}-e^{-2\frac{L_s}{\lambda}})}\right]$$

$$=V_{ds}\frac{(e^{\frac{L+L_d}{\lambda}}-e^{\frac{L+L_d-2L_s}{\lambda}})}{(e^{2\frac{L+L_d}{\lambda}}-e^{-2\frac{L_s}{\lambda}})}-\phi_{gs}\frac{(e^{\frac{L+L_d}{\lambda}}-e^{-\frac{L_s}{\lambda}}-e^{\frac{L+L_d-2L_s}{\lambda}}+e^{\frac{2(L+L_d)-L_s}{\lambda}}-e^{2\frac{L+L_d}{\lambda}}+e^{-2\frac{L_s}{\lambda}})}{(e^{2\frac{L+L_d}{\lambda}}-e^{-2\frac{L_s}{\lambda}})}$$

$$-\frac{qN_d(0)}{\in_{si}}\lambda^2\frac{(e^{\frac{L+L_d}{\lambda}}-e^{-\frac{L_s}{\lambda}}-e^{\frac{L+L_d-2L_s}{\lambda}}+e^{\frac{2(L+L_d)-L_s}{\lambda}}-e^{2\frac{L+L_d}{\lambda}}+e^{-2\frac{L_s}{\lambda}})}{(e^{2\frac{L+L_d}{\lambda}}-e^{-2\frac{L_s}{\lambda}})}$$

$$\phi_0(0)=AV_{ds}-B\phi_{gs}-C_{4n}$$

$$\phi_0(\Delta L)=$$

$$V_{ds}\frac{(e^{\frac{L+L_d+\Delta L}{\lambda}}-e^{\frac{L+L_d-2L_s-\Delta L}{\lambda}})}{(e^{2\frac{L+L_d}{\lambda}}-e^{-2\frac{L_s}{\lambda}})}-\phi_{gs}\frac{(e^{\frac{L+L_d+\Delta L}{\lambda}}-e^{-\frac{L_s+\Delta L}{\lambda}}-e^{\frac{L+L_d-2L_s-\Delta L}{\lambda}}+e^{\frac{2(L+L_d)-L_s-\Delta L}{\lambda}}-e^{2\frac{L+L_d}{\lambda}}+e^{-2\frac{L_s}{\lambda}})}{(e^{2\frac{L+L_d}{\lambda}}-e^{-2\frac{L_s}{\lambda}})}$$

$$-\frac{qN_d(\Delta L)}{\in_{si}}\lambda^2\frac{(e^{\frac{L+L_d+\Delta L}{\lambda}}-e^{-\frac{L_s+\Delta L}{\lambda}}-e^{\frac{L+L_d-2L_s-\Delta L}{\lambda}}+e^{\frac{2(L+L_d)-L_s-\Delta L}{\lambda}}-e^{2\frac{L+L_d}{\lambda}}+e^{-2\frac{L_s}{\lambda}})}{(e^{2\frac{L+L_d}{\lambda}}-e^{-2\frac{L_s}{\lambda}})}$$

$$\phi_0(\Delta L)=A^{/}V_{ds}-B^{/}\phi_{gs}-C_{4n}^{/}$$

For p-channel JLT

$$\phi_0(0)=AV_{ds}-B\phi_{gs}-C_{4p}$$

and

$$\phi_0(\Delta L)=A^{/}V_{ds}-B^{/}\phi_{gs}-C_{4p}^{/}$$

Where,

$$C_{4p} = -\frac{qN_a(0)}{\in_{si}}\lambda^2 \frac{(e^{\frac{L+L_d+\Delta L}{\lambda}} - e^{-\frac{L_s+\Delta L}{\lambda}} - e^{\frac{L+L_d-2L_s-\Delta L}{\lambda}} + e^{\frac{2(L+L_d)-L_s-\Delta L}{\lambda}} - e^{2\frac{L+L_d}{\lambda}} + e^{-2\frac{L_s}{\lambda}})}{(e^{2\frac{L+L_d}{\lambda}} - e^{-2\frac{L_s}{\lambda}})}$$

$$C_{4p}^{/} = -\frac{qN_a(\Delta L)}{\in_{si}}\lambda^2 \frac{(e^{\frac{L+L_d+\Delta L}{\lambda}} - e^{-\frac{L_s+\Delta L}{\lambda}} - e^{\frac{L+L_d-2L_s-\Delta L}{\lambda}} + e^{\frac{2(L+L_d)-L_s-\Delta L}{\lambda}} - e^{2\frac{L+L_d}{\lambda}} + e^{-2\frac{L_s}{\lambda}})}{(e^{2\frac{L+L_d}{\lambda}} - e^{-2\frac{L_s}{\lambda}})}$$

Voltage Transfer Characteristics

Input Low:

$I_{dpnonsat} = I_{dnsat}$

At Saturation,

$$\phi_{gsn} = V_{gsn} - V_{fbn} = 0 \tag{6.66}$$

or,

$$I_{dnsat} = I_{dpnonsat}$$

$$\frac{\phi(\Delta L) - \phi(0)}{Rn(V_{gs}, V_{ds})} = \frac{\phi(\Delta L) - \phi(0)}{Rp(V_{gs}, V_{ds})}$$

$$Rp(V_{gs}, V_{ds}) = R_d p(V_{gs}, V_{ds}) = \frac{\Delta L}{q\mu_n n_p W t_{si}}$$

$$Rn(V_{gs}, V_{ds}) = R_{nd} n(V_{gs}, V_{ds}) = \frac{\Delta L}{q\mu_n n_n W t_{si}}$$

$$[(A^{/} - A)V_{dsp} - (B^{/} - B)\phi_{gsp} - (C_{4p}^{/} - C_{4p})]n_p = [(A^{/} - A)V_{dsn} - (B^{/} - B)\phi_{gsn} - (C_{4n}^{/} - C_{4n})]n_n$$

$$\begin{aligned}&[(A^{/} - A)(V_{dd} - V_{out}) - (B^{/} - B)(V_{dd} - V_{in} - V_{fbp}) - (C_{4p}^{/} - C_{4p})]n_p \\ &= [(A^{/} - A)(V_{out}) - (B^{/} - B)(V_{in} - V_{fbn}) - (C_{4n}^{/} - C_{4n})]n_n\end{aligned} \tag{6.67}$$

$$\frac{dV_{out}}{dV_{in}} = \frac{\frac{\partial I_{dp}}{\partial V_{in}}}{\frac{dI_{dn}}{dV_{out}} - \frac{\partial I_{dp}}{\partial V_{out}}} = -1$$

$$(B^{/} - B) = -(A^{/} - A)\frac{(n_n + n_p)}{n_p}$$

$$\frac{(A^{/} - A)(n_n + 2n_p)V_{dd} - (A^{/} - A)(n_n + n_p)V_{in} - (A^{/} - A)(n_n + n_p)V_{fbp} - \{(C_{4p}^{/} - C_{4p})n_p - (C_{4n}^{/} - C_{4n})n_n\}}{(A^{/} - A)(n_n + n_p)}$$

$$= V_{out}$$

$$V_{in} = (V_{dd} - V_{fbp}) = V_{IL}$$

Input High:

$$I_{dnnonsat} = I_{dpsat}$$

$$\phi_{gsp} = V_{gsp} - V_{fbp} = 0 \quad (6.68)$$

$$\frac{\phi(\Delta L) - \phi(0)}{R_d(V_{gs}, V_{ds})} = \frac{\phi(\Delta L) - \phi(0)}{R_{nd}\, p(V_{gs}, V_{ds})}$$

$$\{(A^{/} - A)V_{dsp} - (B^{/} - B)\phi_{gsp} - (C_{4p}^{/} - C_{4p})\}p_p = \{(A^{/} - A)V_{dsn} - (B^{/} - B)\phi_{gsn} - (C_{4n}^{/} - C_{4n})\}p_n$$

$$\{(A^{/} - A)(V_{dd} - V_{out}) - (B^{/} - B)(V_{dd} - V_{in} - V_{fbp}) - (C_{4p}^{/} - C_{4p})\}p_p$$
$$= \{(A^{/} - A)(V_{out}) - (B^{/} - B)(V_{in} - V_{fbn}) - (C_{4n}^{/} - C_{4n})\}p_n \quad (6.69)$$

$$\frac{dV_{out}}{dV_{in}} = \frac{\frac{\partial I_{dn}}{\partial V_{in}}}{\frac{dI_{dp}}{dV_{out}} - \frac{\partial I_{dn}}{\partial V_{out}}} = -1$$

$$-(A^{/}-A)\frac{p_p}{p_n}=(B^{/}-B)$$

$$\frac{(A^{/}-A)p_pV_{dd}-(A^{/}-A)p_p(V_{in}-V_{fbn})-\{(C^{/}_{4p}-C_{4p})p_p-(C^{/}_{4n}-C_{4n})p_n)}{(A^{/}-A)(p_n+p_p)}$$

$$=V_{out}$$

$$V_{in}=V_{fbn}=V_{IH}$$

Output Low:

$$V_{out}=\frac{(A^{/}-A)n_pV_{dd}+(B^{/}-B)n_pV_{fbp}-(C^{/}_{4p}-C_{4p})n_p+(C^{/}_{4n}-C_{4n})n_n}{(A^{/}-A)(n_n+n_p)}=V_{OL}$$

Output High:

$$V_{out}=\frac{(A^{/}-A)p_pV_{dd}-(B^{/}-B)p_nV_{fbn}-(C^{/}_{4p}-C_{4p})p_p+(C^{/}_{4n}-C_{4n})p_n}{(A^{/}-A)(p_n+p_p)}=V_{OH}$$

Inverter Threshold Voltage

$$\frac{\phi(\Delta L)-\phi(O)}{R_{nd}n(V_{gs},V_{ds})}=\frac{\phi(\Delta L)-\phi(O)}{R_{nd}p(V_{gs},V_{ds})}$$

$$\phi_{gsp}=\phi_{gsn}=0$$

$$V_{dsp}=V_{dd}-V_I$$

$$V_{dsn}=V_I$$

$$\frac{\dfrac{(A^{/}-A)V_{dsn}-(B^{/}-B)\phi_{gsn}-(C_{4n}^{/}-C_{4n})}{\Delta L}}{2q\mu_n n_n W t_{si}}$$

$$=\frac{\dfrac{(A^{/}-A)V_{dsp}-(B^{/}-B)\phi_{gsp}-(C_{4p}^{/}-C_{4p})}{\Delta L}}{2q\mu_p p_p W t_{si}}$$

$$\mu_n n_n\{(A^{/}-A)V_I-(C_{4n}^{/}-C_{4n})\}=\mu_p p_p\{(A^{/}-A)(V_{dd}-V_I)-(C_{4p}^{/}-C_{4p})\}$$

$$V_I=\frac{\mu_p p_p(A^{/}-A)V_{dd}+\mu_n n_n(C_{4n}^{/}-C_{4n})-\mu_p p_p(C_{4p}^{/}-C_{4p})}{(\mu_n n_n+\mu_p p_p)(A^{/}-A)}$$

Noise Margin:

Noise margin for logic 1 voltages

$$V_{NMH}=V_{OH}-V_{IH}=\frac{(A^{/}-A)p_pV_{dd}-(B^{/}-B)p_nV_{fbn}-(C_{4p}^{/}-C_{4p})p_p+(C_{4n}^{/}-C_{4n})p_n}{(A^{/}-A)(p_n+p_p)}-V_{fbn}$$

$$V_{NML}=V_{IL}-V_{OL}=\frac{(A^{/}-A)n_nV_{dd}-\{(A^{/}-A)(n_n+n_p)+(B^{/}-B)n_p\}V_{fbp}+(C_{4p}^{/}-C_{4p})n_p-(C_{4n}^{/}-C_{4n})n_n}{(A^{/}-A)(n_n+n_p)}$$

Noise margin for logic 0 voltages

Fall Time:

$$t_{HL}=C_{out}\int_{V_1}^{V_0}\frac{dV_{out}}{I_{dn}}$$

$V_o=0.1V_{OH}$ and $V_1=0.9V_{OH}$

$$I_{dn}=\frac{q\mu_n n_n W t_{si}[(A^{/}-A)V_{out}-(C_{4n}^{/}-C_{4n})]}{\Delta L}$$

$$t_{HL} = C_{out} \int_{V_1}^{V_0} \frac{dV_{out}}{\frac{q\mu_n n_n W t_{si}[(A^{/} - A)V_{out} - (C_{4n}^{/} - C_{4n})]}{\Delta L}}$$

$$t_{HL} = \frac{\Delta L C_{out}}{q\mu_n n_n W t_{si}(A^{/} - A)} \left[\ln\{V_o - \frac{(C_{4n}^{/} - C_{4n})}{(A^{/} - A)}\} - \ln\{V_1 - \frac{(C_{4n}^{/} - C_{4n})}{(A^{/} - A)}\} \right]$$

Rise Time:

$$t_{LH} = C_{out} \int_{V_0}^{V_1} \frac{dV_{out}}{I_{dp}}$$

$V_o = 0.1V_{OH}$ and $V_1 = 0.9V_{OH}$

$$I_{dp} = \frac{q\mu_p p_p W t_{si}[\{(A^{/} - A)(V_{dd} - V_{out}) - (C_{4p}^{/} - C_{4p})\}]}{\Delta L}$$

$$t_{LH} = C_{out} \int_{V_0}^{V_1} \frac{dV_{out}}{\frac{q\mu_p p_p W t_{si}[\{(A^{/} - A)(V_{dd} - V_{out}) - (C_{4p}^{/} - C_{4p})\}]}{\Delta L}}$$

$$t_{LH} = \frac{\Delta L C_{out}}{q\mu_p p_p W t_{si}(A^{/} - A)} \left[\ln\{V_{dd} - V_1 - \frac{(C_{4p}^{/} - C_{4p})}{(A^{/} - A)}\} - \ln\{V_{dd} - V_0 - \frac{(C_{4p}^{/} - C_{4p})}{(A^{/} - A)}\} \right]$$

Propagation Delay

$$t_{PHL} = \frac{\Delta L C_{out}}{q\mu_n n_n W t_{si}(A^{/} - A)} \left[\ln\{V_I - \frac{(C_{4n}^{/} - C_{4n})}{(A^{/} - A)}\} - \ln\{V_{OH} - \frac{(C_{4n}^{/} - C_{4n})}{(A^{/} - A)}\} \right]$$

$$t_{PLH} = \frac{\Delta L C_{out}}{q\mu_p p_p W t_{si}(A^{/} - A)} \left[\ln\{V_{dd} - V_{OH} - \frac{(C_{4p}^{/} - C_{4p})}{(A^{/} - A)}\} - \ln\{V_{dd} - V_I - \frac{(C_{4p}^{/} - C_{4p})}{(A^{/} - A)}\} \right]$$

Propagation delay is given as,

$$t_P = \frac{t_{PHL} + t_{PLH}}{2}$$

Power Loss

$$P_d = V_{out} I_{ds}$$

6.4.6 Results

The comparison of voltage transfer characteristics for V_{dd}=2V, 1.5V and 1V is shown in Fig. 6.31, Fig. 6.32 and Fig. 6.33. The comparison of output current variation with input voltage for V_{dd}=2V, 1.5V and 1V is shown in Fig. 6.34, Fig. 6.35 and Fig. 6.36. The comparison of transient response for V_{dd}=2V, 1.5V and 1V is shown in Fig. 6.37, Fig. 6.38 and Fig. 6.39. The comparison of switching power loss for V_{dd}=2V, 1.5V and 1V is shown in Fig. 6.40, Fig. 6.41 and Fig. 6.42. Table 6.5 shows the noise margin for different structures at V_{dd}=2V, 1.5V and 1V. Table 6.6 shows the rise time and fall time for different structures at V_{dd}=2V, 1.5V and 1V. Table 6.7 shows the propagation delay for different structures at V_{dd}=2V, 1.5V and 1V.

In all the plots inverter using the conventional DG JLT is denoted as Struct 1, the JLT with symmetric diagonal dielectric is denoted as Struct 2, the JLT with asymmetric diagonal dielectric is denoted as Struct 3, the JLT with gradual doping concentration in channel with SiO_2 as the gate dielectric is denoted as Struct 4 and the JLT with centre dielectric layer is denoted as Struct 5.

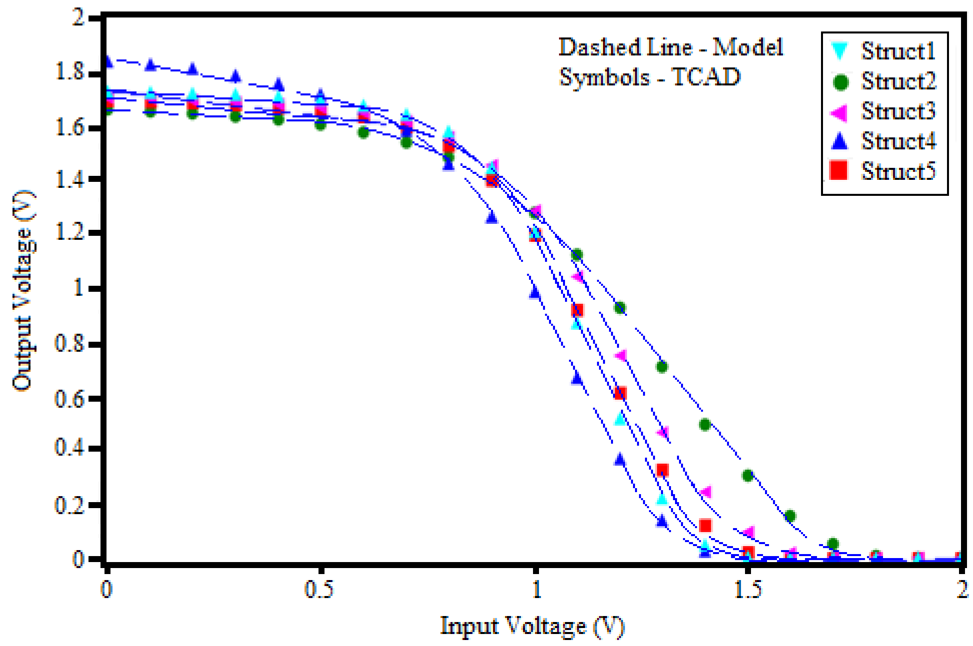

Fig. 6.31: Voltage Transfer Characteristics for V_{dd}=2V

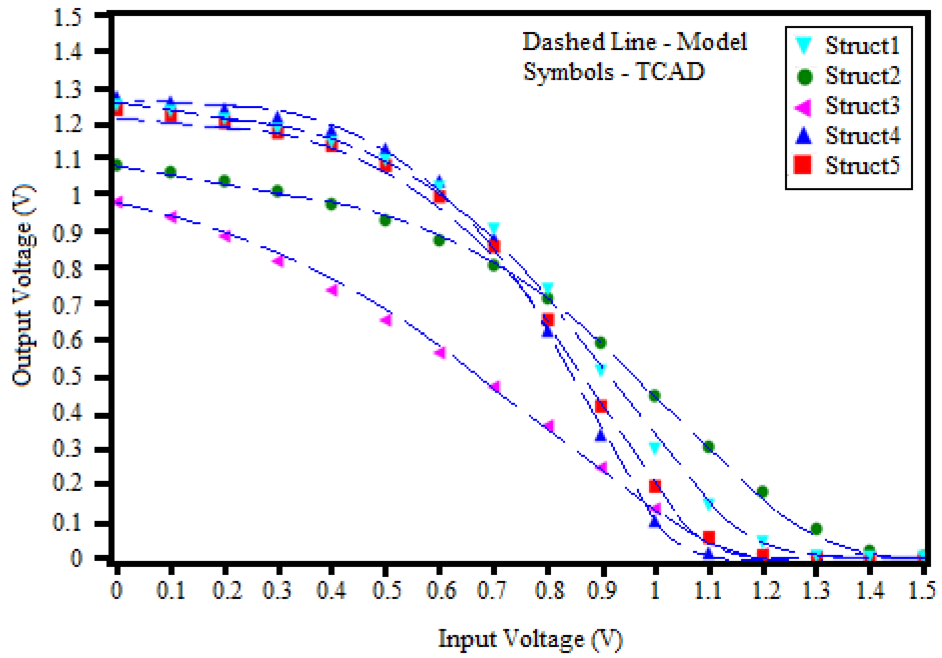

Fig. 6.32: Voltage Transfer Characteristics for V_{dd}=1.5V

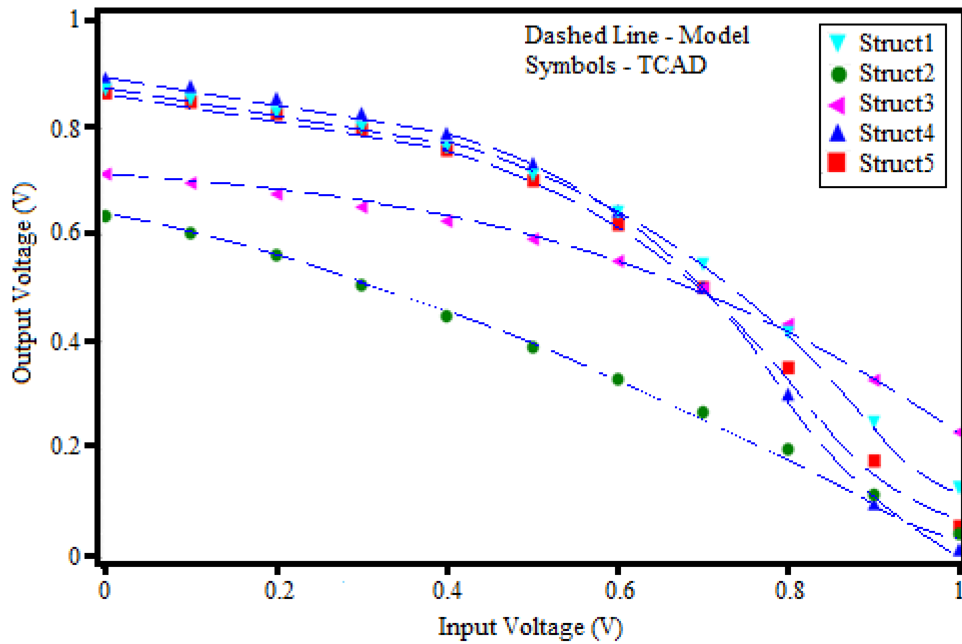

Fig. 6.33: Voltage Transfer Characteristics for V_{dd}=1V

Table 6.5 : Noise Margin of CMOS inverter of different structures of JLT

Structure	V_{dd}=2V				V_{dd}=1.5V				V_{dd}=1V			
	NM_H (V)		NM_L (V)		NM_H (V)		NM_L (V)		NM_H (V)		NM_L (V)	
	Model	TCAD	Model	TCAD	Model	TCAD	Model	TCAD	Model	TCAD	Model	TCAD
Struct1	0.559	0.550	0.172	0.170	0.432	0.428	0.142	0.143	0.227	0.228	0.092	0.090
Struct2	0.530	0.526	0.465	0.470	0.412	0.409	0.125	0.129	0.211	0.213	0.078	0.077
Struct3	0.293	0.300	0.370	0.390	0.062	0.063	0.094	0.093	0.015	0.012	0.032	0.031
Struct4	0.710	0.680	0.523	0.510	0.581	0.580	0.496	0.492	0.562	0.557	0.456	0.452
Struct5	0.671	0.668	0.436	0.430	0.491	0.487	0.413	0.410	0.425	0.421	0.398	0.391

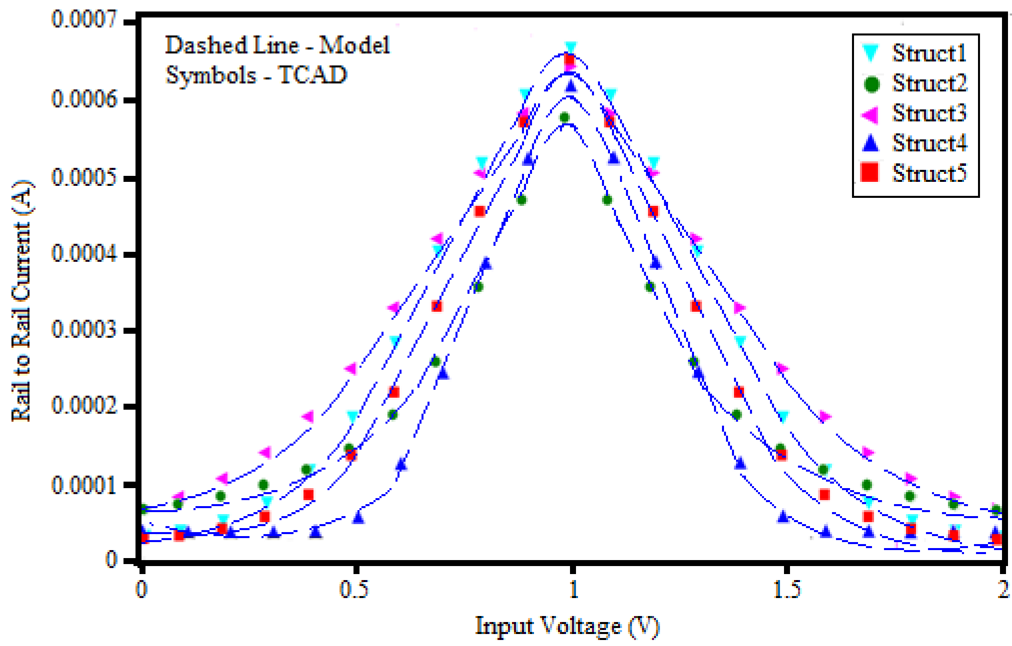

Fig. 6.34: Rail to Rail Current Variation with Input Voltage for V_{dd}=2V

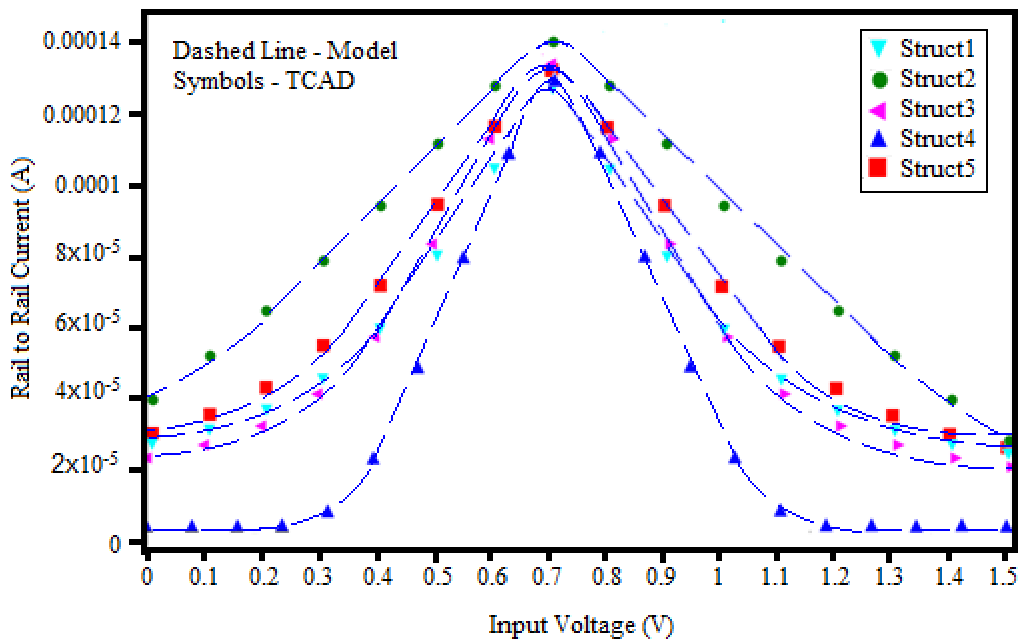

Fig. 6.35: Rail to Rail Current Variation with Input Voltage for V_{dd}=1.5V

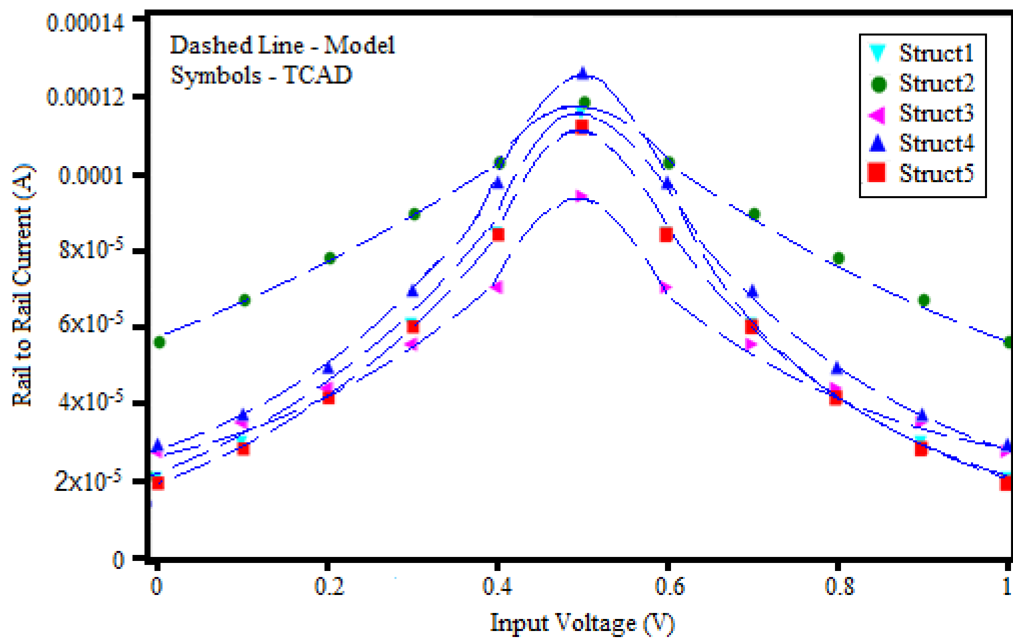

Fig. 6.36: Rail to Rail Current Variation with Input Voltage for V_{dd}=1V

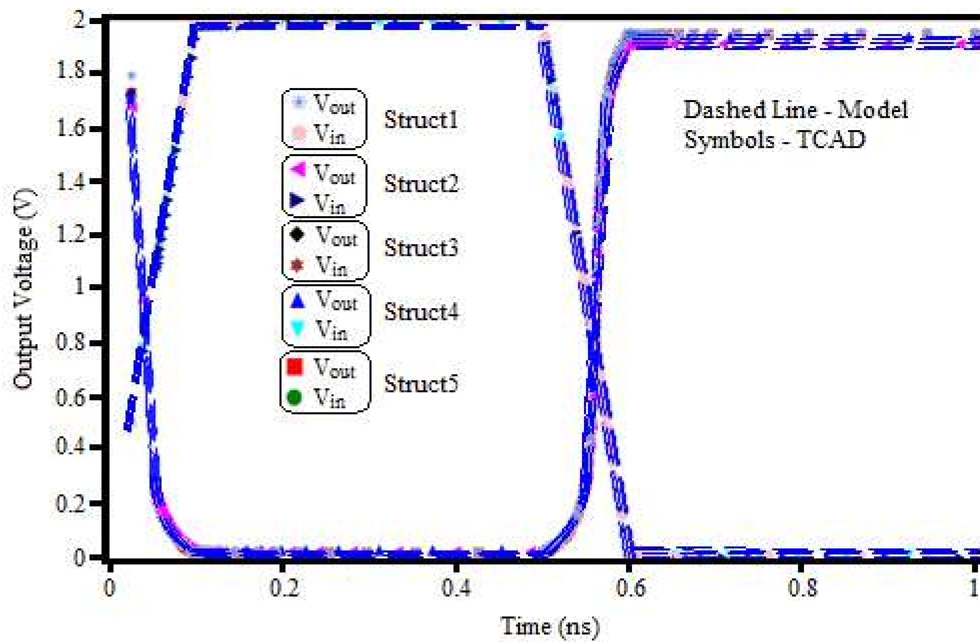

Fig. 6.37: Transient Response for V_{dd}=2V

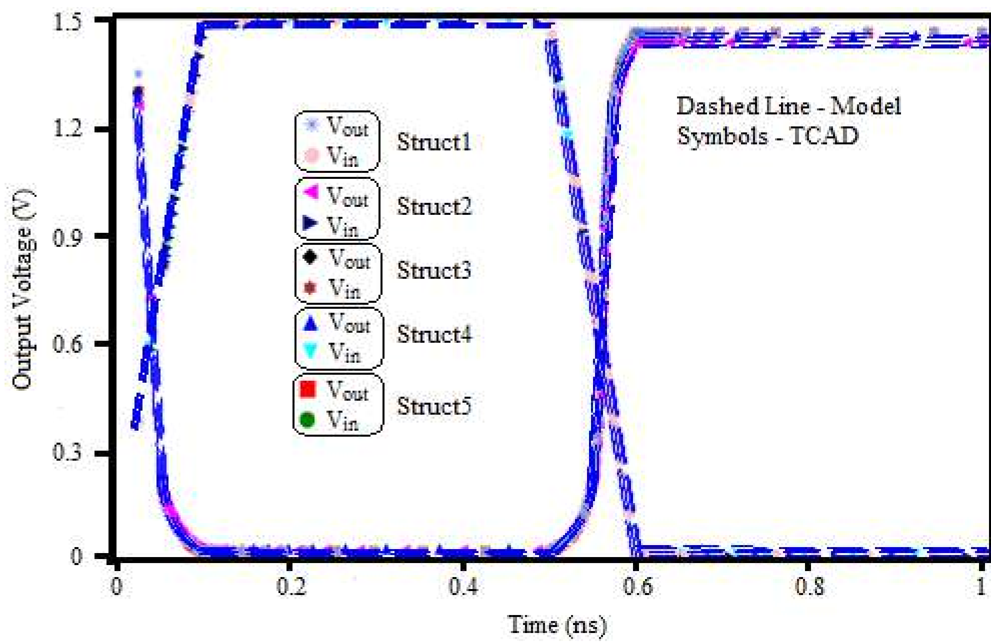

Fig. 6.38: Transient Response for V_{dd}=1.5V

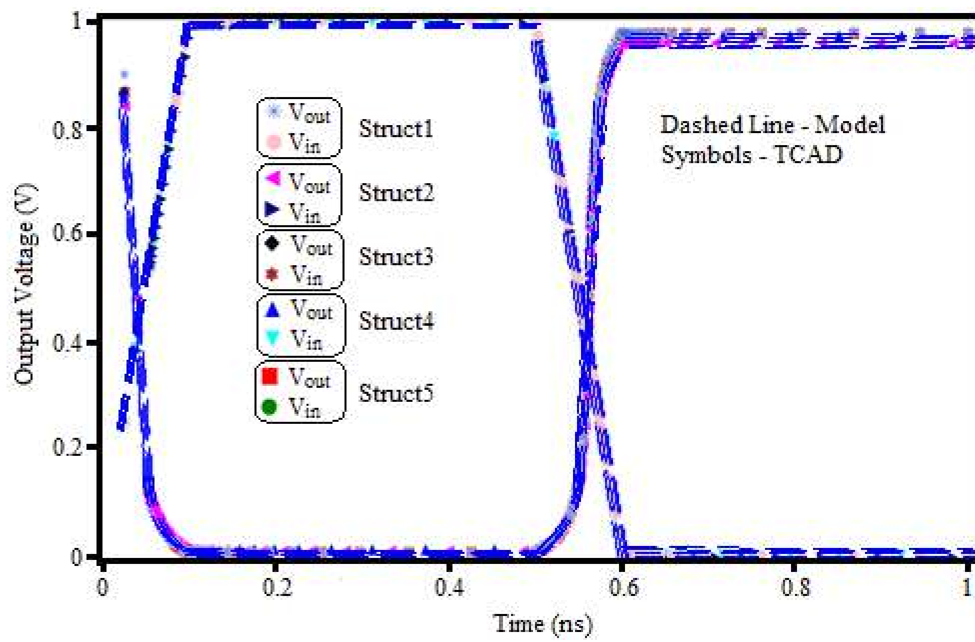

Fig. 6.39: Transient Response for V_{dd}=1V

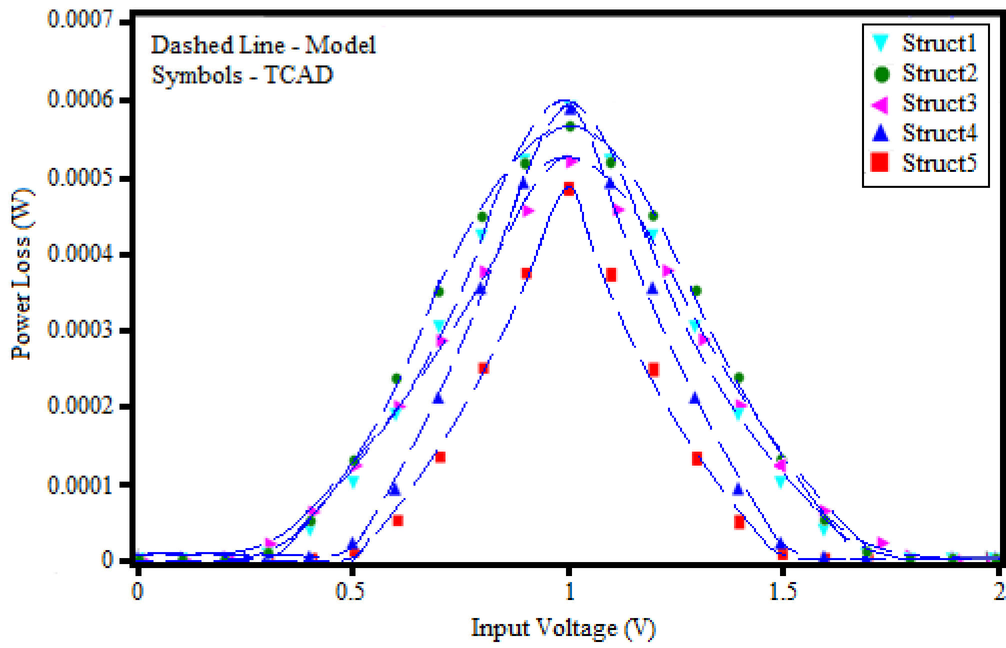

Fig. 6.40: Power Loss Variation with Input Voltage at V_{dd}=2V

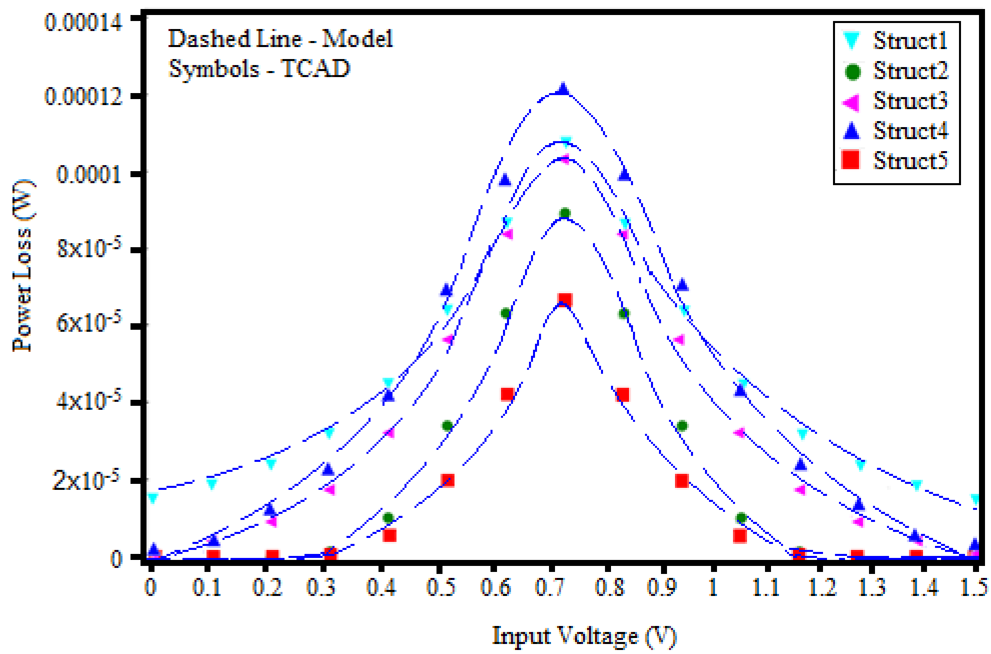

Fig. 6.41: Power Loss Variation with Input Voltage at V_{dd}=1.5V

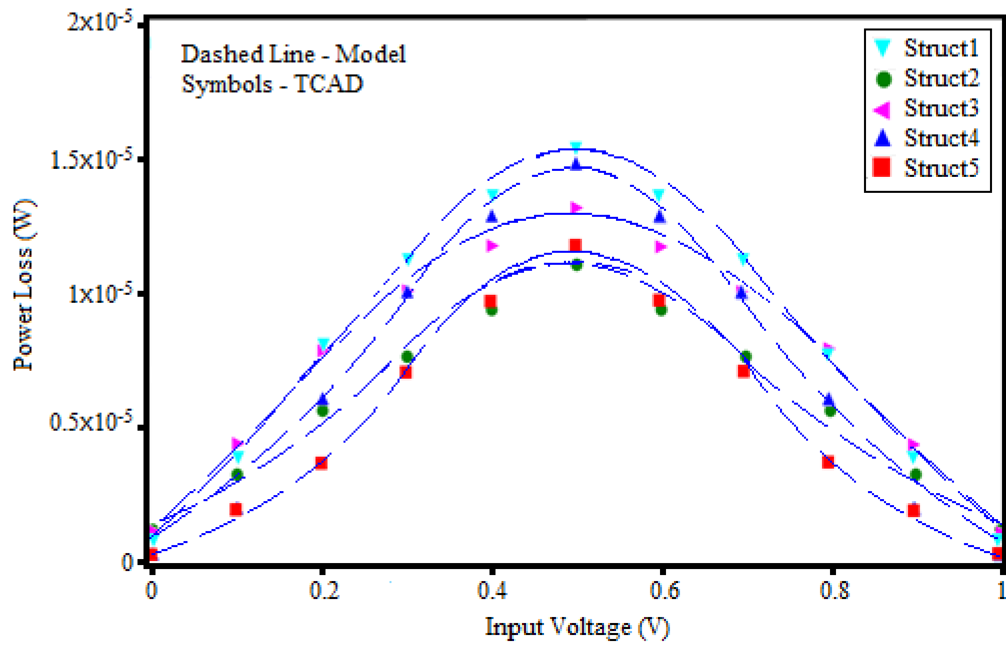

Fig. 6.42: Power Loss Variation with Input Voltage at V_{dd}=1V

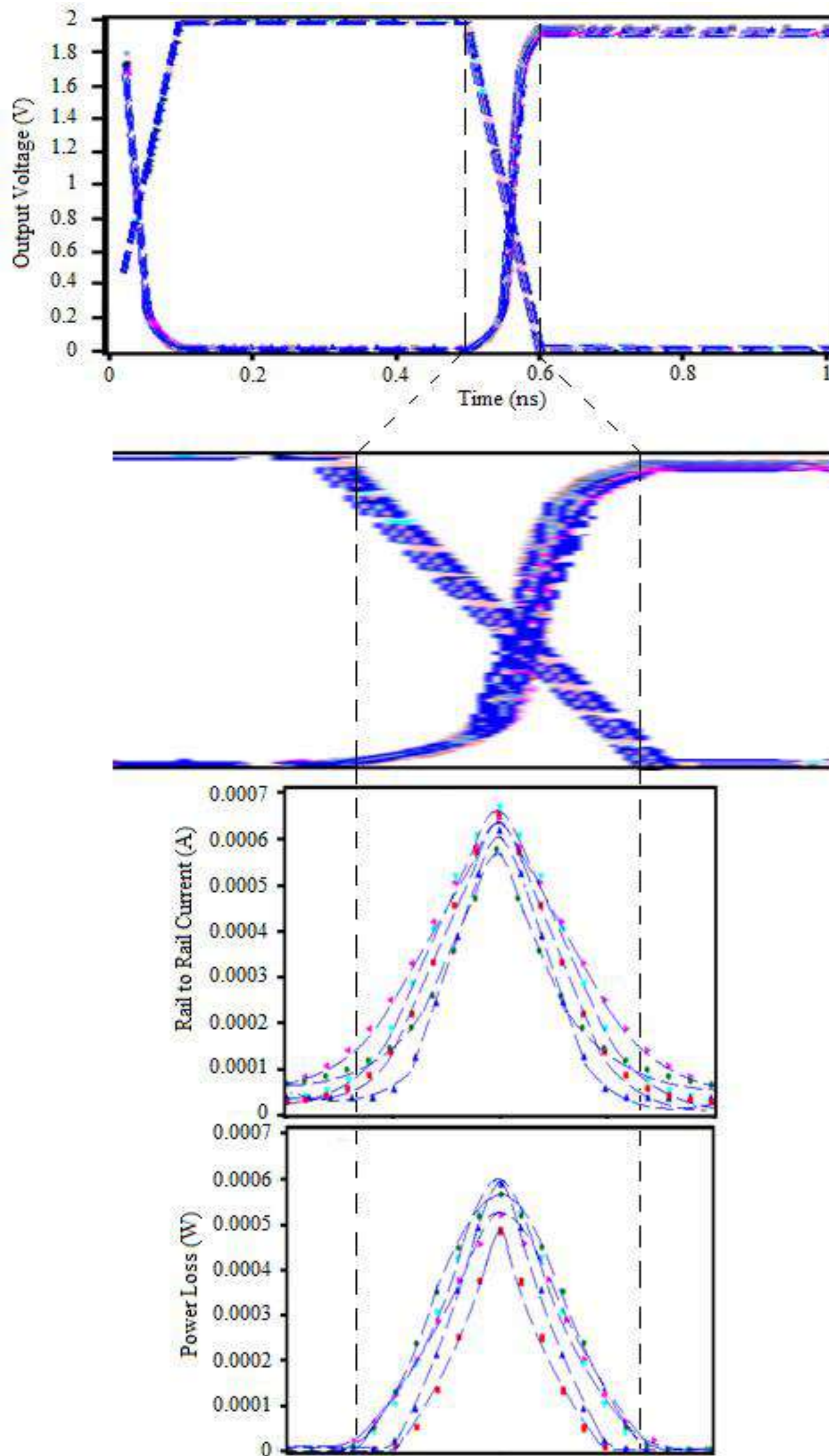

Fig. 6.43: Transient Response Along with Power Loss at V_{dd}=2V

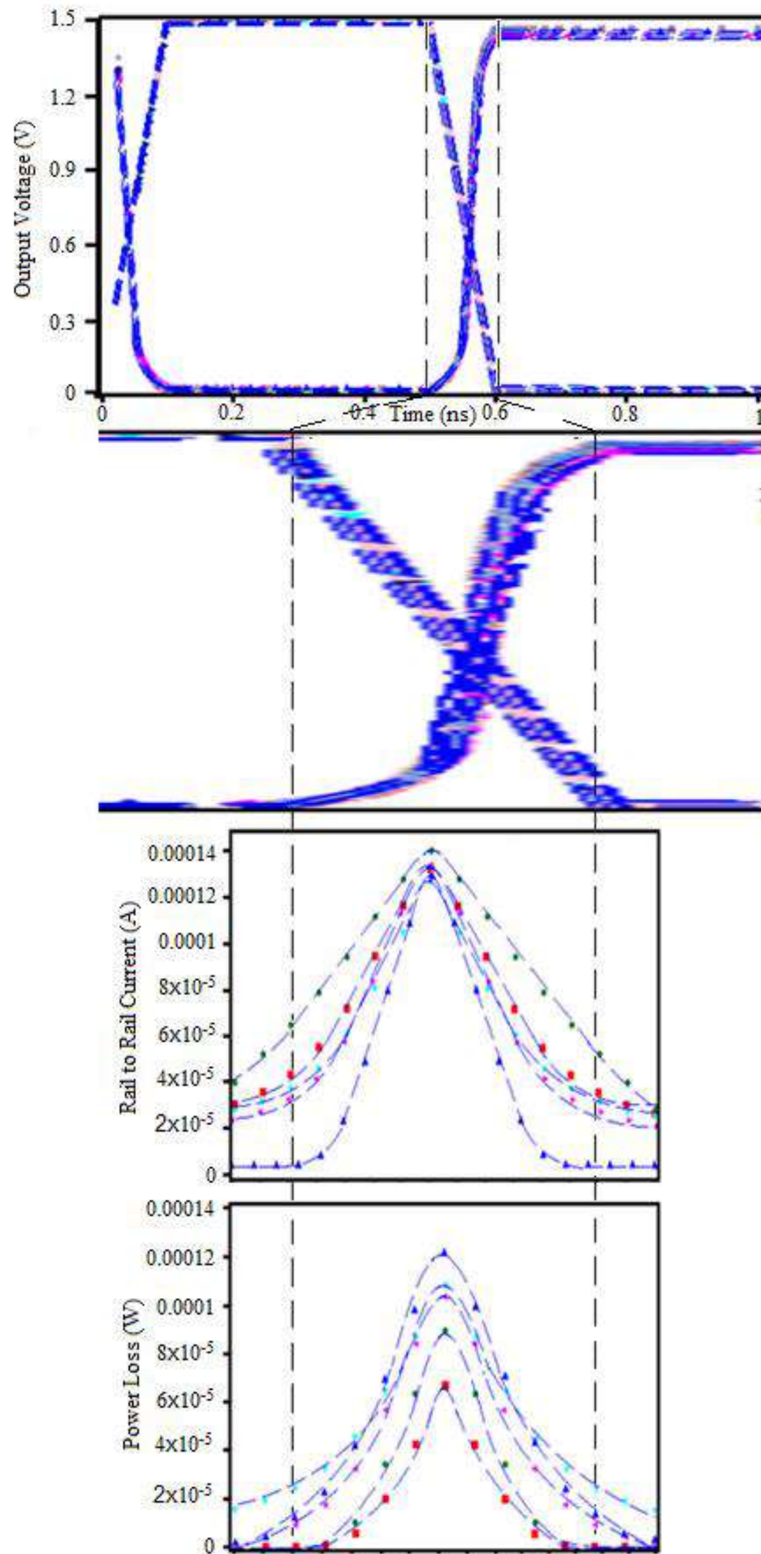

Fig. 6.44: Transient Response Along with Power Loss at V_{dd}=1.5V

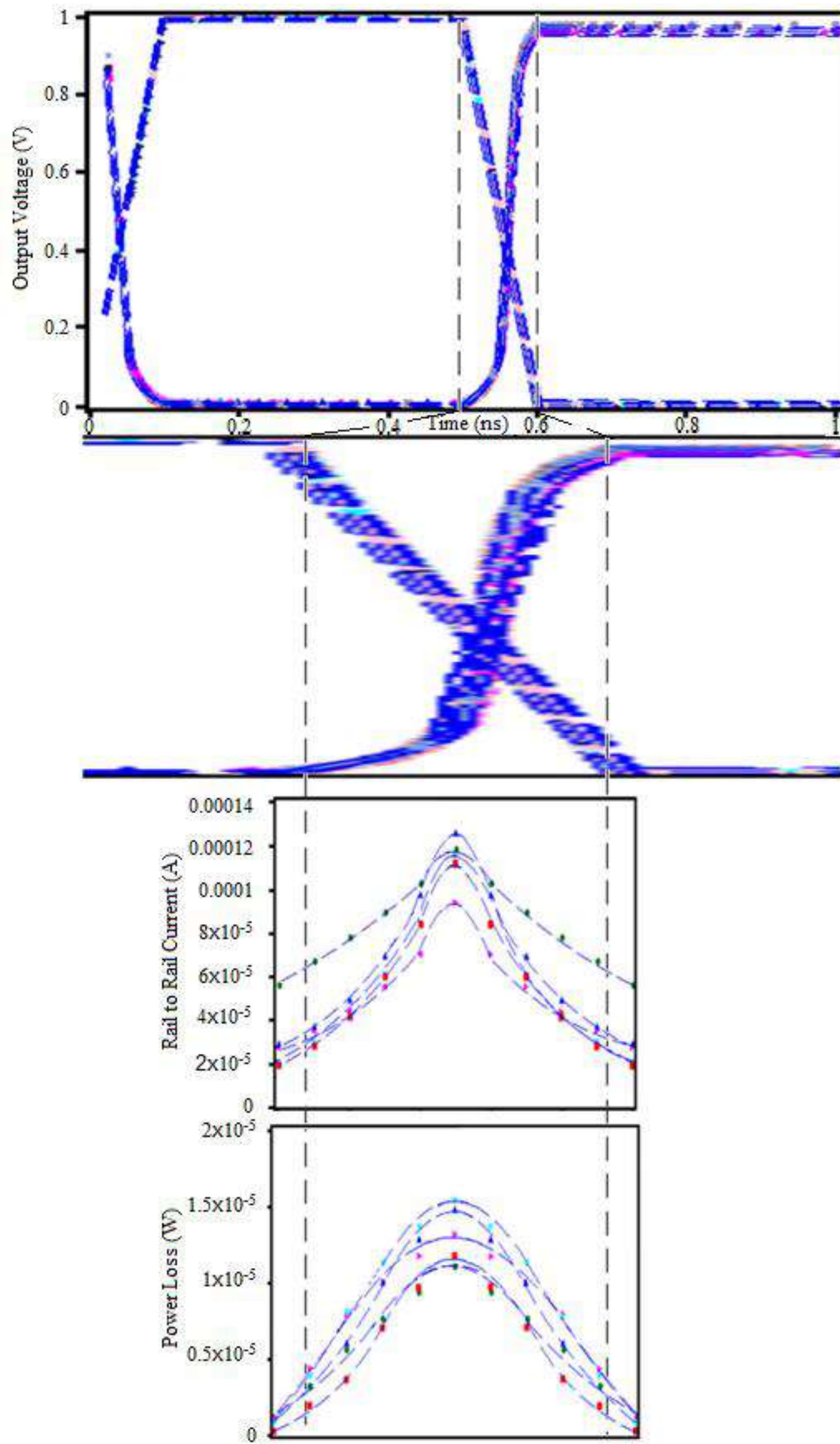

Fig. 6.45: Transient Response Along with Power Loss at V_{dd}=1V

Table 6.6 : Rise Time and Fall Time of CMOS inverter of different structures of JLT

Structure	V_{dd}=2V				V_{dd}=1.5V				V_{dd}=1V			
	Rise Time (ns)		Fall Time (ns)		Rise Time (ns)		Fall Time (ns)		Rise Time (ns)		Fall Time (ns)	
	Model	TCAD	Model	TCAD	Model	TCAD	Model	TCAD	Model	TCAD	Model	TCAD
Struct1	0.059	0.055	0.054	0.052	0.043	0.044	0.042	0.041	0.029	0.034	0.028	0.0036
Struct2	0.053	0.056	0.051	0.047	0.041	0.04	0.038	0.039	0.021	0.021	0.023	0.025
Struct3	0.076	0.78	0.080	0.079	0.073	0.75	0.077	0.074	0.062	0.063	0.064	0.063
Struct4	0.042	0.043	0.043	0.041	0.031	0.033	0.026	0.023	0.018	0.017	0.016	0.017
Struct5	0.061	0.063	0.060	0.062	0.049	0.047	0.043	0.041	0.035	0.031	0.038	0.039

Table 6.7 : Propagation delay of CMOS inverter for different structures of JLT

Structure	V_{dd}=2V		V_{dd}=1.5V		V_{dd}=1V	
	Model	TCAD	Model	TCAD	Model	TCAD
Struct1	0.031 ns	0.033 ns	0.023 ns	0.024 ns	0.012 ns	0.014 ns
Struct2	0.029 ns	0.026 ns	0.021 ns	0.021 ns	0.011 ns	0.012 ns
Struct3	0.046 ns	0.048 ns	0.029 ns	0.27 ns	0.015 ns	0.016 ns
Struct4	0.022 ns	0.023 ns	0.018 ns	0.019 ns	0.008 ns	0.007 ns
Struct5	0.029 ns	0.028 ns	0.022 ns	0.024 ns	0.013 ns	0.01 ns

6.5 Corner Effect

In this section a study corner effect found in four structures of JLT viz. rectangular, pentagonal, hexagonal and octagonal has been presented. A technique for reduction of corner effect has also been presented, where the gate width is reduced than the actual requirement. This is commonly known as gate underlap technique. After application of this method in these structures the gate does not remain a single piece of metal or a single piece of polycrystalline Silicon. Instead it becomes a set of gate with a number of segments. The number of segments depend upon geometry of JLT. Since the corner effect arises due to

superposition of the electric fields emanated from two adjacent gate segments, the effect can be obtained by vector addition of these electric fields at the corner.

6.5.1 Mathematical Formulation of Corner Effect of Different Structures

The corner effect in different structures can be formulated by formulating the electric field at the corners of the structures. The electric field at the corner is obtained by taking the vector addition of two components from two adjacent gates.

For a rectangular JLT the resultant lateral electric field obtained by vector addition of x and y component of the electric field is given as,

$$E_{rect}(x,y)=\sqrt{(E_{rect}(x))^2+(E_{rect}(y))^2} \tag{6.70}$$

Where,

$$E_{rect}(x)=-\frac{8\in_{ox}}{a_{si}(4\in_{si}t_{ox}+\in_{ox}a_{si}+\in_{ox}b_{si})}(\phi_{gs}-\phi_0(z))x \tag{6.71}$$

$$E_{rect}(y)=-\frac{8\in_{ox}}{b_{si}(4\in_{si}t_{ox}+\in_{ox}a_{si}+\in_{ox}b_{si})}(\phi_{gs}-\phi_0(z))y \tag{6.72}$$

for pentagonal JLT the resultant electric field is

$$E_{pent}(x,y)=\sqrt{(E_{pent}(x))^2+(E_{pent}(y))^2-0.62E_{pent}(x)E_{pent}(y)} \tag{6.73}$$

$$E_{pent}(x)=\frac{4.98t_{ox}\in_{si}}{4.98\in_{si}t_{ox}+1.9\in_{ox}t_{si}}(\phi_{gs}-\phi_0(z))-\frac{19.92\in_{ox}}{t_{si}(4.98\in_{si}t_{ox}+1.9\in_{ox}t_{si})}(\phi_{gs}-\phi_0(z))x$$

$$E_{pent}(y)=\frac{4.98t_{ox}\in_{si}}{4.98\in_{si}t_{ox}+1.9\in_{ox}t_{si}}(\phi_{gs}-\phi_0(z))-\frac{22.6\in_{ox}}{t_{si}(4.98\in_{si}t_{ox}+1.9\in_{ox}t_{si})}(\phi_{gs}-\phi_0(z))y$$

for hexagonal JLT the resultant electric field is

$$E_{hex}(x,y)=\sqrt{(E_{hex}(x))^2+(E_{hex}(y))^2-E_{hex}(x)E_{hex}(y)} \tag{6.74}$$

$$E_{hex}(x)=-\frac{4\in_{ox}}{\sqrt{3}t_{si}(2t_{ox}\in_{si}+\in_{ox}t_{si})}(\phi_{gs}-\phi_0(z))x \tag{6.75}$$

$$E_{hex}(y)=-\frac{2\in_{ox}}{t_{si}(2t_{ox}\in_{si}+\in_{ox}t_{si})}(\phi_{gs}-\phi_0(z))y \tag{6.76}$$

for octagonal JLT the resultant electric field is

$$E_{oct}(x,y)=\sqrt{(E_{oct}(x))^2+(E_{oct}(y))^2-1.41E_{oct}(x)E_{oct}(y)} \tag{6.77}$$

$$E_{oct}(x)=-\frac{2\in_{ox}}{2.42t_{si}(\in_{si}t_{ox}+0.6t_{si}\in_{ox})}(\phi_{gs}-\phi_0(z))x \tag{6.78}$$

$$E_{oct}(y)=-\frac{2\in_{ox}}{2.42t_{si}(\in_{si}t_{ox}+0.6t_{si}\in_{ox})}(\phi_{gs}-\phi_0(z))y \tag{6.79}$$

6.5.2 Corner Effect Reduction Technique

A technique for reduction of corner effect in the structures mentioned above using gate underlap [30] is shown in Fig. 6.46. Here the width of the gate is reduced from both ends for all the sides of the structures.

Rectangular JLT

The electric field at the corner with gate underlap,

$$E_{cornerrect}(x)=E_{rect}(x)\cos\theta=-\frac{8\in_{ox}}{a_{si}(4\in_{si}t_{ox}+\in_{ox}a_{si}+\in_{ox}b_{si})}(\phi_{gs}-\phi_0(z))x\cos\theta \tag{6.80}$$

$$E_{cornerrect}(y)=E_{rect}(y)\cos\theta=-\frac{8\in_{ox}}{a_{si}(4\in_{si}t_{ox}+\in_{ox}a_{si}+\in_{ox}b_{si})}(\phi_{gs}-\phi_0(z))y\cos\theta \tag{6.81}$$

The resultant electric field at the corner is

$$E_{cornerrect}(x,y)=E_{rect}(x,y)\cos\theta \tag{6.82}$$

where, $\theta=\tan^{-1}(\frac{x}{t_{ox}})=\tan^{-1}(\frac{y}{t_{ox}})$ (6.83)

Drain current model for the rectangular JLT can be obtained following similar approach as in chapter 5.

The resistance of the non depleted region without gate underlap

$$R_{ndrect}(z,V_{gs},V_{ds})=\frac{1}{q\mu_{nrect}n}\frac{\Delta L}{\frac{4t_{si}\in_{si}t_{ox}qN_d+\in_{ox}t_{si}^2qN_d-8\in_{ox}\in_{si}(\phi_0-\phi_{gs})}{\in_{ox}qN_d}}$$

The resistance of the depleted region without gate underlap

$$R_{drect}(z,V_{gs},V_{ds})=\frac{1}{q\mu_{prect}p}\frac{\Delta L}{\left(t_{si}-\sqrt{\frac{4t_{si}\in_{si}t_{ox}qN_d+\in_{ox}t_{si}^2qN_d-8\in_{ox}\in_{si}(\phi_0-\phi_{gs})}{\in_{ox}qN_d}}\right)^2}$$

The resistance of the non depleted region with gate underlap

$$R_{ndcornerrect}(z,V_{gs},V_{ds})=\frac{1}{q\mu_{ncornerrect}n}\frac{\Delta L}{\frac{4t_{si}\in_{si}t_{ox}qN_d+\in_{ox}t_{si}^2qN_d-8\in_{ox}\in_{si}(\phi_0-\phi_{gs})}{\in_{ox}qN_d}}$$

The resistance of the depleted region with gate underlap

$$R_{dcornerrect}(z,V_{gs},V_{ds})=\frac{1}{q\mu_{pcornerrect}p}\frac{\Delta L}{\left(t_{si}-\sqrt{\frac{4t_{si}\in_{si}t_{ox}qN_d+\in_{ox}t_{si}^2qN_d-8\in_{ox}\in_{si}(\phi_0-\phi_{gs})}{\in_{ox}qN_d}}\right)^2}$$

The effective mobility at the corner without gate underlap,

$$\mu_{nrect}(x,y) = -1.55\times10^{3}\left[\frac{1}{1+(\frac{E_{rect}(x,y)}{6.91\times10^{3}})^{1.11}}\right]^{0.9} \tag{6.84}$$

$$\mu_{prect}(x,y) = -5.75\times10^{2}\left[\frac{1}{1+(\frac{E_{rect}(x,y)}{1.45\times10^{4}})^{2.637}}\right]^{0.38} \tag{6.85}$$

The effective mobility at the corner with gate underlap,

$$\mu_{ncornerrect}(x,y) = -1.55\times10^{3}\left[\frac{1}{1+(\frac{E_{cornerrect}(x,y)}{6.91\times10^{3}})^{1.11}}\right]^{0.9} \tag{6.86}$$

$$\mu_{pcornerrect}(x,y) = -5.75\times10^{2}\left[\frac{1}{1+(\frac{E_{cornerrect}(x,y)}{1.45\times10^{4}})^{2.637}}\right]^{0.38} \tag{6.87}$$

The equivalent resistance at the corner without and with gate underlap is given as

$R_{rect}(z,V_{gs},V_{ds}) = R_{drect}(z,V_{gs},V_{ds}) \,||\, R_{ndrect}(z,V_{gs},V_{ds}) \,||\, R_{drect}(z,V_{gs},V_{ds})$

and

$R_{cornerrect}(z,V_{gs},V_{ds}) = R_{dcornerrect}(z,V_{gs},V_{ds}) \,||\, R_{ndcornerrect}(z,V_{gs},V_{ds}) \,||\, R_{dcornerrect}(z,V_{gs},V_{ds})$

The drain current at the corner without gate under lap

$$I_{drect} = \frac{\phi((m+1)\Delta L) - \phi(m\Delta L)}{R_{rect}(V_{gs},V_{ds})} \tag{6.88}$$

The drain current at the corner with gate under lap

$$I_{dcornerrect} = \frac{\phi((m+1)\Delta L) - \phi(m\Delta L)}{R_{cornerrect}(V_{gs}, V_{ds})} \tag{6.89}$$

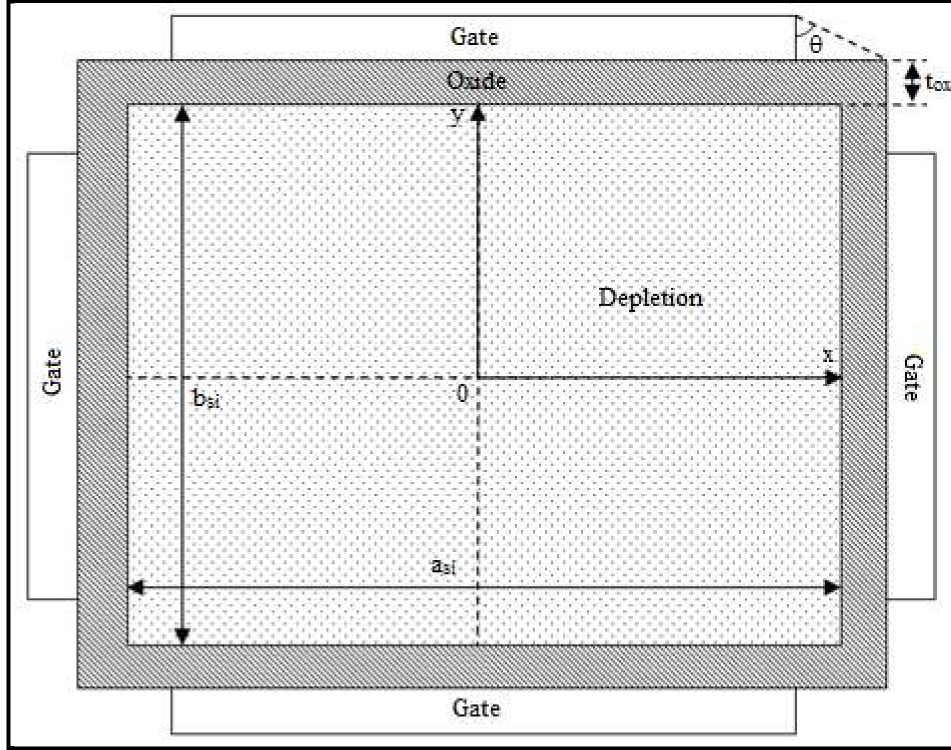

Fig. 6.46: Cross-sectional view of a rectangular JLT with lateral gate underlap

Pentagonal JLT

The electric field at the corner with gate underlap,

$$E_{cornerpent}(x) = E_{pent}(x)\cos\theta =$$
$$\left[\frac{4.98t_{ox}\in_{si}}{4.98\in_{si}t_{ox}+1.9\in_{ox}t_{si}}(\phi_{gs}-\phi_0(z)) - \frac{19.92\in_{ox}}{t_{si}(4.98\in_{si}t_{ox}+1.9\in_{ox}t_{si})}(\phi_{gs}-\phi_0(z))x\right]\cos\theta$$

$$E_{cornerpent}(y) = E_{pent}(y)\cos\theta =$$
$$\left[\frac{4.98t_{ox}\in_{si}}{4.98\in_{si}t_{ox}+1.9\in_{ox}t_{si}}(\phi_{gs}-\phi_0(z)) - \frac{22.6\in_{ox}}{t_{si}(4.98\in_{si}t_{ox}+1.9\in_{ox}t_{si})}(\phi_{gs}-\phi_0(z))y\right]\cos\theta$$

The resultant electric field at the corner is

$$E_{cornerpent}(x,y)=E_{pent}(x,y)\cos\theta\,, \tag{6.90}$$

where, $\theta=\tan^{-1}(\frac{x}{t_{ox}})=\tan^{-1}(\frac{y}{t_{ox}})$

Drain current model for the rectangular JLT can be obtained following similar approach as in chapter 5.

The resistance of the non depleted region without gate underlap

$$R_{ndpent}(z,V_{gs},V_{ds})=\frac{1}{q\mu_{npent}n}\frac{\Delta L}{\frac{4t_{si}\in_{si}t_{ox}qN_d+\in_{ox}t_{si}^2qN_d-8\in_{ox}\in_{si}(\phi_0-\phi_{gs})}{\in_{ox}qN_d}}$$

The resistance of the depleted region without gate underlap

$$R_{dpent}(z,V_{gs},V_{ds})=\frac{1}{q\mu_{ppent}p}\frac{\Delta L}{\left(t_{si}-\sqrt{\frac{4t_{si}\in_{si}t_{ox}qN_d+\in_{ox}t_{si}^2qN_d-8\in_{ox}\in_{si}(\phi_0-\phi_{gs})}{\in_{ox}qN_d}}\right)^2}$$

The resistance of the non depleted region with gate underlap

$$R_{ndcornerpent}(z,V_{gs},V_{ds})=\frac{1}{q\mu_{ncornerpent}n}\frac{\Delta L}{\frac{4t_{si}\in_{si}t_{ox}qN_d+\in_{ox}t_{si}^2qN_d-8\in_{ox}\in_{si}(\phi_0-\phi_{gs})}{\in_{ox}qN_d}}$$

The resistance of the depleted region with gate underlap

$$R_{dcornerpent}(z,V_{gs},V_{ds})=\frac{1}{q\mu_{pcornerpent}p}\frac{\Delta L}{\left(t_{si}-\sqrt{\frac{4t_{si}\in_{si}t_{ox}qN_d+\in_{ox}t_{si}^2qN_d-8\in_{ox}\in_{si}(\phi_0-\phi_{gs})}{\in_{ox}qN_d}}\right)^2}$$

The effective mobility at the corner without gate underlap,

$$\mu_{npent}(x,y)=-1.55\times10^3\left[\frac{1}{1+(\frac{E_{pent}(x,y)}{6.91\times10^3})^{1.11}}\right]^{0.9} \tag{6.91}$$

$$\mu_{ppent}(x,y) = -5.75\times10^{2}\left[\frac{1}{1+(\frac{E_{pent}(x,y)}{1.45\times10^{4}})^{2.637}}\right]^{0.38} \quad (6.92)$$

The effective mobility at the corner with gate underlap,

$$\mu_{ncornerpent}(x,y) = -1.55\times10^{3}\left[\frac{1}{1+(\frac{E_{cornerpent}(x,y)}{6.91\times10^{3}})^{1.11}}\right]^{0.9} \quad (6.93)$$

$$\mu_{pcornerpent}(x,y) = -5.75\times10^{2}\left[\frac{1}{1+(\frac{E_{cornerpent}(x,y)}{1.45\times10^{4}})^{2.637}}\right]^{0.38} \quad (6.94)$$

The equivalent resistance at the corner without and with gate underlap is given as

$R_{pent}(z,V_{gs},V_{ds}) = R_{dpent}(z,V_{gs},V_{ds}) \,||\, R_{ndpent}(z,V_{gs},V_{ds}) \,||\, R_{dpent}(z,V_{gs},V_{ds})$

and

$R_{cornerpent}(z,V_{gs},V_{ds}) = R_{dcornerpent}(z,V_{gs},V_{ds}) \,||\, R_{ndcornerpent}(z,V_{gs},V_{ds}) \,||\, R_{dcornerpent}(z,V_{gs},V_{ds})$

The drain current at the corner without gate under lap

$$I_{dpent} = \frac{\phi((m+1)\Delta L)-\phi(m\Delta L)}{R_{pent}(V_{gs},V_{ds})} \quad (6.95)$$

The drain current at the corner with gate under lap

$$I_{dcornerpent} = \frac{\phi((m+1)\Delta L)-\phi(m\Delta L)}{R_{cornerpent}(V_{gs},V_{ds})} \quad (6.96)$$

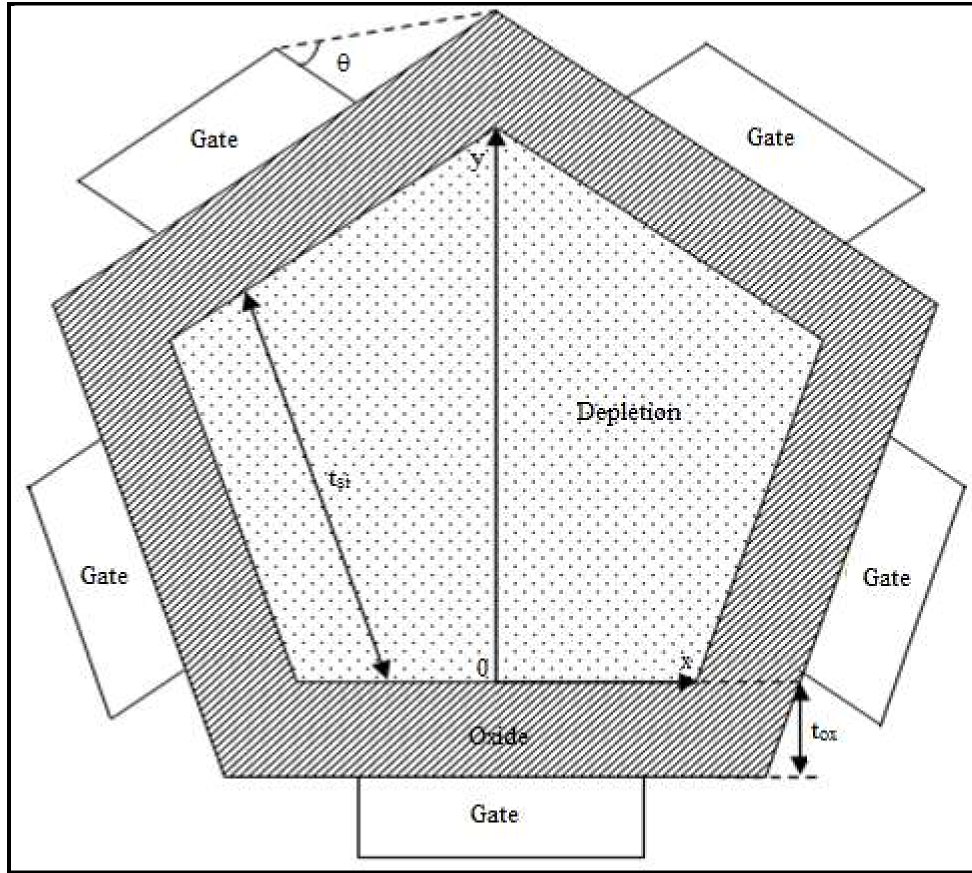

Fig. 6.47: Cross-sectional view of a pentagonal JLT with lateral gate underlap

Hexagonal JLT

The electric field at the corner with gate underlap,

$$E_{cornerhex}(x) = E_{hex}(x)\cos\theta = -\frac{4\in_{ox}}{\sqrt{3}t_{si}(2t_{ox}\in_{si} + \in_{ox} t_{si})}(\phi_{gs} - \phi_0(z))x\cos\theta$$

$$E_{cornerhex}(y) = E_{hex}(y)\cos\theta = -\frac{2\in_{ox}}{t_{si}(2t_{ox}\in_{si} + \in_{ox} t_{si})}(\phi_{gs} - \phi_0(z))y\cos\theta$$

The resultant electric field at the corner is

$$E_{cornerhex}(x, y) = E_{hex}(x, y)\cos\theta \tag{6.97}$$

where, $\theta = \tan^{-1}(\frac{x}{t_{ox}}) = \tan^{-1}(\frac{y}{t_{ox}})$

Drain current model for the rectangular JLT can be obtained following similar approach as in chapter 5.

The resistance of the non depleted region without gate underlap

$$R_{ndhex}(z,V_{gs},V_{ds}) = \frac{1}{q\mu_{nhex}n}\frac{\Delta L}{\frac{4t_{si}\in_{si}t_{ox}qN_d + \in_{ox}t_{si}^2 qN_d - 8\in_{ox}\in_{si}(\phi_0-\phi_{gs})}{\in_{ox}qN_d}}$$

The resistance of the depleted region without gate underlap

$$R_{dhex}(z,V_{gs},V_{ds}) = \frac{1}{q\mu_{phex}p}\frac{\Delta L}{\left(t_{si} - \sqrt{\frac{4t_{si}\in_{si}t_{ox}qN_d + \in_{ox}t_{si}^2 qN_d - 8\in_{ox}\in_{si}(\phi_0-\phi_{gs})}{\in_{ox}qN_d}}\right)^2}$$

The resistance of the non depleted region with gate underlap

$$R_{ndcornerhex}(z,V_{gs},V_{ds}) = \frac{1}{q\mu_{ncornerhex}n}\frac{\Delta L}{\frac{4t_{si}\in_{si}t_{ox}qN_d + \in_{ox}t_{si}^2 qN_d - 8\in_{ox}\in_{si}(\phi_0-\phi_{gs})}{\in_{ox}qN_d}}$$

The resistance of the depleted region with gate underlap

$$R_{dcornerhex}(z,V_{gs},V_{ds}) = \frac{1}{q\mu_{pcornerhex}p}\frac{\Delta L}{\left(t_{si} - \sqrt{\frac{4t_{si}\in_{si}t_{ox}qN_d + \in_{ox}t_{si}^2 qN_d - 8\in_{ox}\in_{si}(\phi_0-\phi_{gs})}{\in_{ox}qN_d}}\right)^2}$$

The effective mobility at the corner without gate underlap,

$$\mu_{nhex}(x,y) = -1.55\times10^3\left[\frac{1}{1+(\frac{E_{pent}(x,y)}{6.91\times10^3})^{1.11}}\right]^{0.9} \tag{6.98}$$

$$\mu_{phex}(x,y) = -5.75\times10^{2}\left[\frac{1}{1+(\frac{E_{pent}(x,y)}{1.45\times10^{4}})^{2.637}}\right]^{0.38} \tag{6.99}$$

The effective mobility at the corner with gate underlap,

$$\mu_{ncornerhex}(x,y) = -1.55\times10^{3}\left[\frac{1}{1+(\frac{E_{cornerhex}(x,y)}{6.91\times10^{3}})^{1.11}}\right]^{0.9} \tag{6.100}$$

$$\mu_{pcornerhex}(x,y) = -5.75\times10^{2}\left[\frac{1}{1+(\frac{E_{cornerhex}(x,y)}{1.45\times10^{4}})^{2.637}}\right]^{0.38} \tag{6.101}$$

The equivalent resistance at the corner without and with gate underlap is given as

$R_{hex}(z,V_{gs},V_{ds})= R_{dhex}(z,V_{gs},V_{ds}) \parallel R_{ndhex}(z,V_{gs},V_{ds}) \parallel R_{dhex}(z,V_{gs},V_{ds})$

and

$R_{cornerhex}(z,V_{gs},V_{ds})= R_{dcornerhex}(z,V_{gs},V_{ds}) \parallel R_{ndcornerhex}(z,V_{gs},V_{ds}) \parallel R_{dcornerhex}(z,V_{gs},V_{ds})$

The drain current at the corner without gate under lap

$$I_{dhex} = \frac{\phi((m+1)\Delta L)-\phi(m\Delta L)}{R_{hex}(V_{gs},V_{ds})} \tag{6.102}$$

The drain current at the corner with gate under lap

$$I_{dcornerhex} = \frac{\phi((m+1)\Delta L)-\phi(m\Delta L)}{R_{cornerhex}(V_{gs},V_{ds})} \tag{6.103}$$

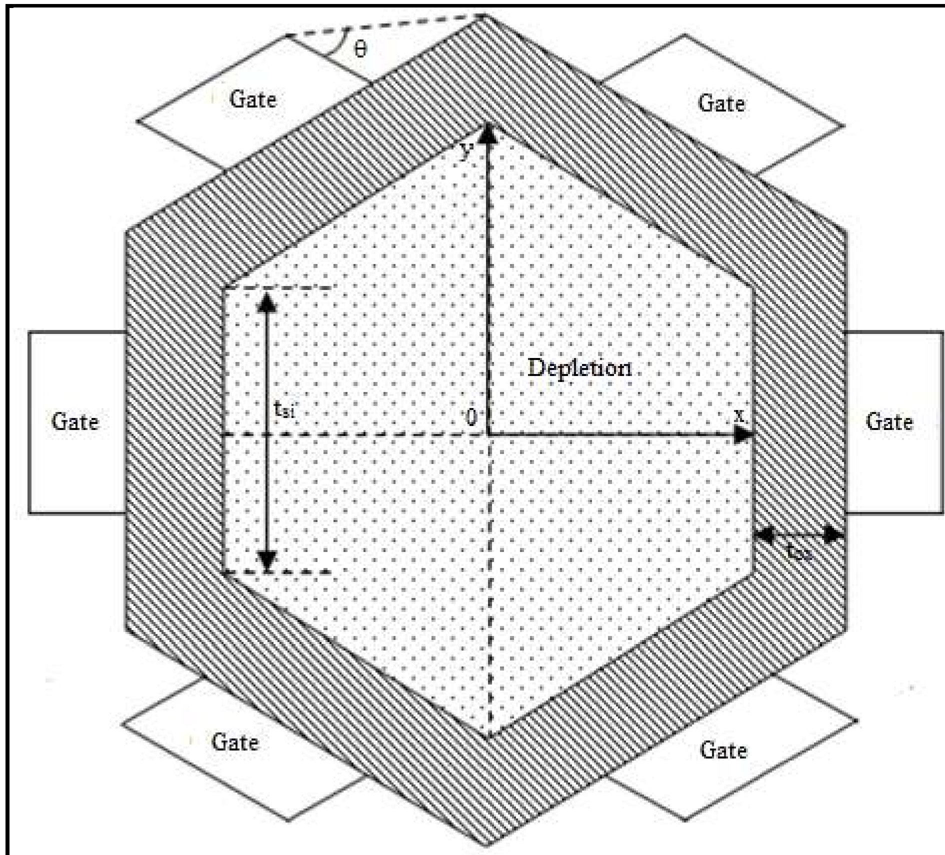

Fig. 6.48: Cross-sectional view of a hexagonal JLT with lateral gate underlap

Octagonal JLT

The electric field at the corner with gate underlap,

$$E_{corneroct}(x) = E_{oct}(x)\cos\theta = -\frac{2\in_{ox}}{2.42t_{si}(\in_{si} t_{ox} + 0.6t_{si}\in_{ox})}(\phi_{gs} - \phi_0(z))x\cos\theta$$

$$E_{corneroct}(y) = E_{oct}(y)\cos\theta = -\frac{2\in_{ox}}{2.42t_{si}(\in_{si} t_{ox} + 0.6t_{si}\in_{ox})}(\phi_{gs} - \phi_0(z))y\cos\theta$$

The resultant electric field at the corner is

$$E_{corneroct}(x, y) = E_{oct}(x, y)\cos\theta \qquad (6.104)$$

where, $\theta = \tan^{-1}(\frac{x}{t_{ox}}) = \tan^{-1}(\frac{y}{t_{ox}})$

Drain current model for the rectangular JLT can be obtained following similar approach as in chapter 5.

The resistance of the non depleted region without gate underlap

$$R_{ndoct}(z, V_{gs}, V_{ds}) = \frac{1}{q\mu_{noct} n} \frac{\Delta L}{\frac{4t_{si} \in_{si} t_{ox} qN_d + \in_{ox} t_{si}^2 qN_d - 8 \in_{ox} \in_{si} (\phi_0 - \phi_{gs})}{\in_{ox} qN_d}}$$

The resistance of the depleted region without gate underlap

$$R_{doct}(z, V_{gs}, V_{ds}) = \frac{1}{q\mu_{poct} p} \frac{\Delta L}{\left(t_{si} - \sqrt{\frac{4t_{si} \in_{si} t_{ox} qN_d + \in_{ox} t_{si}^2 qN_d - 8 \in_{ox} \in_{si} (\phi_0 - \phi_{gs})}{\in_{ox} qN_d}}\right)^2}$$

The resistance of the non depleted region with gate underlap

$$R_{ndcorneroct}(z, V_{gs}, V_{ds}) = \frac{1}{q\mu_{ncorneroct} n} \frac{\Delta L}{\frac{4t_{si} \in_{si} t_{ox} qN_d + \in_{ox} t_{si}^2 qN_d - 8 \in_{ox} \in_{si} (\phi_0 - \phi_{gs})}{\in_{ox} qN_d}}$$

The resistance of the depleted region with gate underlap

$$R_{dcorneroct}(z, V_{gs}, V_{ds}) = \frac{1}{q\mu_{pcorneroct} p} \frac{\Delta L}{\left(t_{si} - \sqrt{\frac{4t_{si} \in_{si} t_{ox} qN_d + \in_{ox} t_{si}^2 qN_d - 8 \in_{ox} \in_{si} (\phi_0 - \phi_{gs})}{\in_{ox} qN_d}}\right)^2}$$

The effective mobility at the corner without gate underlap,

$$\mu_{noct}(x, y) = -1.55 \times 10^3 \left[\frac{1}{1 + (\frac{E_{oct}(x, y)}{6.91 \times 10^3})^{1.11}} \right]^{0.9} \tag{6.105}$$

$$\mu_{poct}(x,y) = -5.75\times10^{2}\left[\frac{1}{1+(\frac{E_{oct}(x,y)}{1.45\times10^{4}})^{2.637}}\right]^{0.38} \quad (6.106)$$

The effective mobility at the corner with gate underlap,

$$\mu_{ncorneroct}(x,y) = -1.55\times10^{3}\left[\frac{1}{1+(\frac{E_{corneroct}(x,y)}{6.91\times10^{3}})^{1.11}}\right]^{0.9} \quad (6.107)$$

$$\mu_{pcorneroct}(x,y) = -5.75\times10^{2}\left[\frac{1}{1+(\frac{E_{corneroct}(x,y)}{1.45\times10^{4}})^{2.637}}\right]^{0.38} \quad (6.108)$$

The equivalent resistance at the corner without and with gate underlap is given as

$R_{oct}(z,V_{gs},V_{ds})= R_{doct}(z,V_{gs},V_{ds}) \,||\, R_{ndoct}(z,V_{gs},V_{ds}) \,||\, R_{doct}(z,V_{gs},V_{ds})$

and

$R_{corneroct}(z,V_{gs},V_{ds})= R_{dcorneroct}(z,V_{gs},V_{ds}) \,||\, R_{ndcorneroct}(z,V_{gs},V_{ds}) \,||\, R_{dcorneroct}(z,V_{gs},V_{ds})$

The drain current at the corner without gate under lap

$$I_{doct} = \frac{\phi((m+1)\Delta L)-\phi(m\Delta L)}{R_{oct}(V_{gs},V_{ds})} \quad (6.109)$$

The drain current at the corner with gate under lap

$$I_{dcorneroct} = \frac{\phi((m+1)\Delta L)-\phi(m\Delta L)}{R_{corneroct}(V_{gs},V_{ds})} \quad (6.110)$$

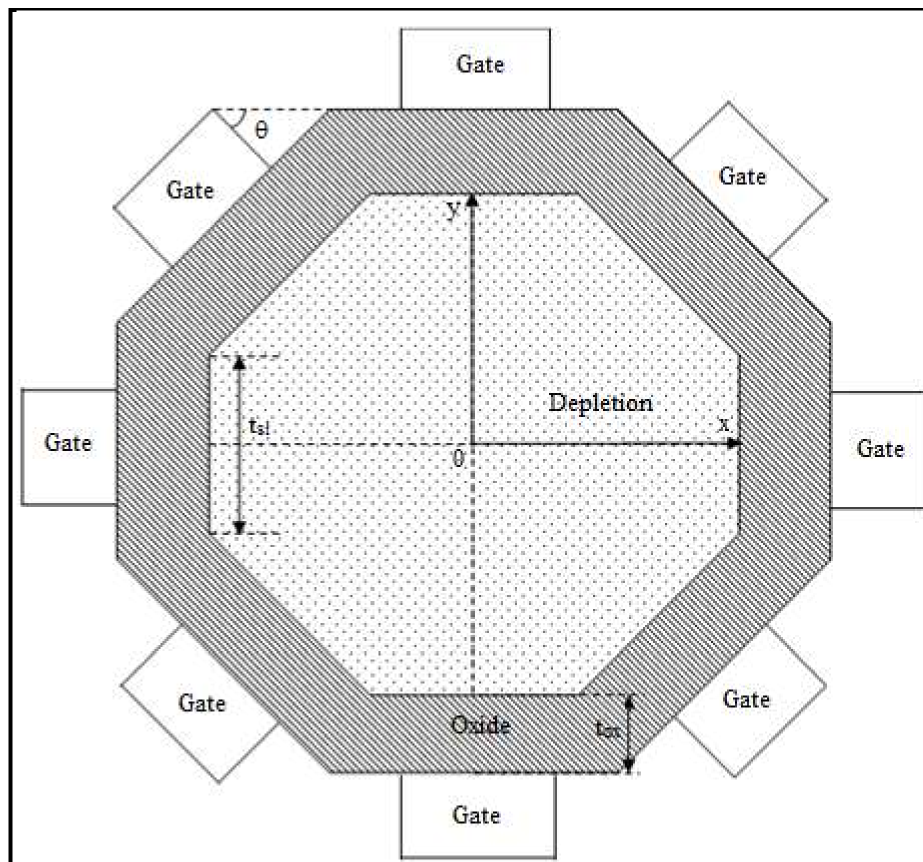

Fig. 6.49: Cross-sectional view of a octagonal JLT with lateral gate underlap

6.4.3 Results, Discussion and Validation

The proposed method for corner effect reduction in different structures of JLT has been modelled and the same has been simulated in MATLAB simulation environment. Result obtained in the MATLAB simulation has been compared with the simulation result obtained from Cogenda VisualTCAD 1.8.2 2D device simulator. Fermi-Dirac statistics is used throughout all the simulations.

Comparison of corner effect in the structures is shown in Fig. 6.50 by varying the resultant electric field with channel position. It is seen that electric field is minimum at the centre and increases linearly towards the corner. This may cause premature turn on with a large localized current at the corners. The electric field variation is maximum for the

rectangular structure and decreases with increase in the vertex angle. In other words corner effect decreases with increasing vertex angle.

In Fig. 6.51-6.54 the comparison of electric field variation is shown for different structures of JLT with and without gate underlap. For a JLT with gate underlap the electric field variation is much lower compared to the complete gate all around device.

A comparison of output characteristics of different structures is shown in Fig. 6.55-6.58 and transfer characteristics is shown in Fig. 6.59-6.62 with and without gate underlap. Though the use of gate underlap technique reduces the on-state current but it is highly effective in reducing the subthreshold leakage current by reducing the corner effect.

In all the cases the channel length is taken as L=20nm, source and drain lengths are taken as L_s=L_d=5nm, the gate dielectric thickness is taken as, t_{ox}=2nm, the length of one side is taken as, t_{si}=10nm, the drain to source voltage is taken as, V_{ds}=0.1V and the work function of the gate material is taken as, Φ_M=5.4eV.

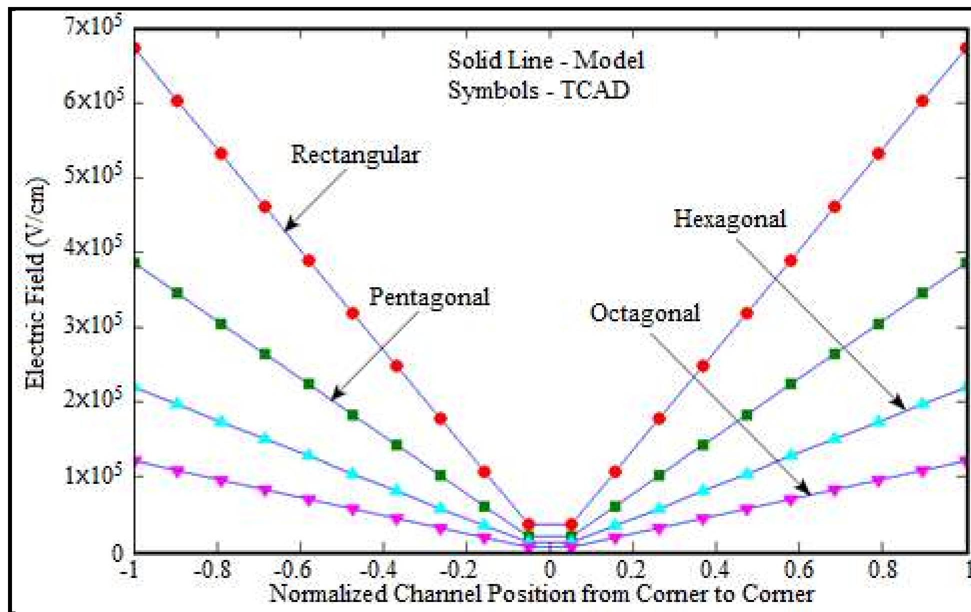

Fig. 6.50: Electric field variation with channel position for rectangular, pentagonal, hexagonal and octagonal JLT

Average error = 0.7%
Maximum error =1.1%
Minimum error =0%

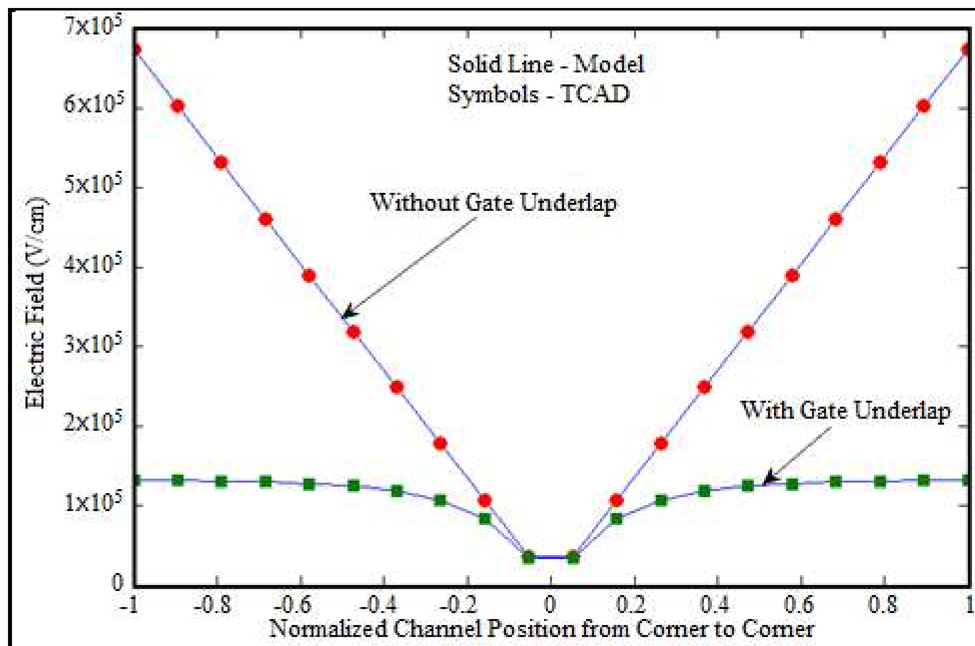

Fig. 6.51: Comparison of electric field variation with channel position for rectangular JLT with and without gate underlap

Average error = 0.9%
Maximum error =1.3%
Minimum error =0%

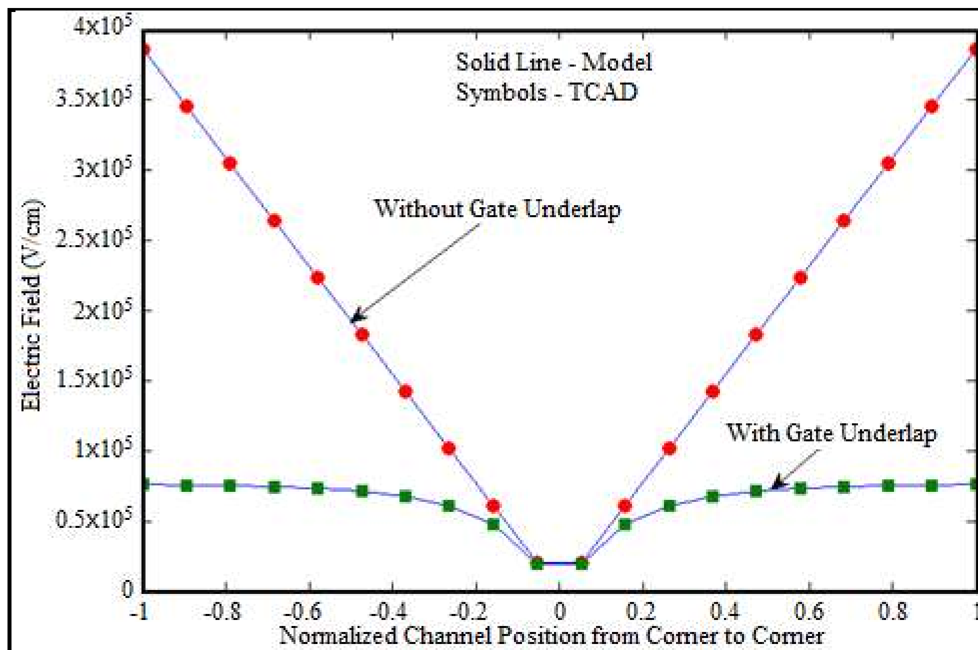

Fig. 6.52: Comparison of electric field variation with channel position for pentagonal JLT with and without gate underlap

Average error = 0.9%
Maximum error =1.3%
Minimum error =0%

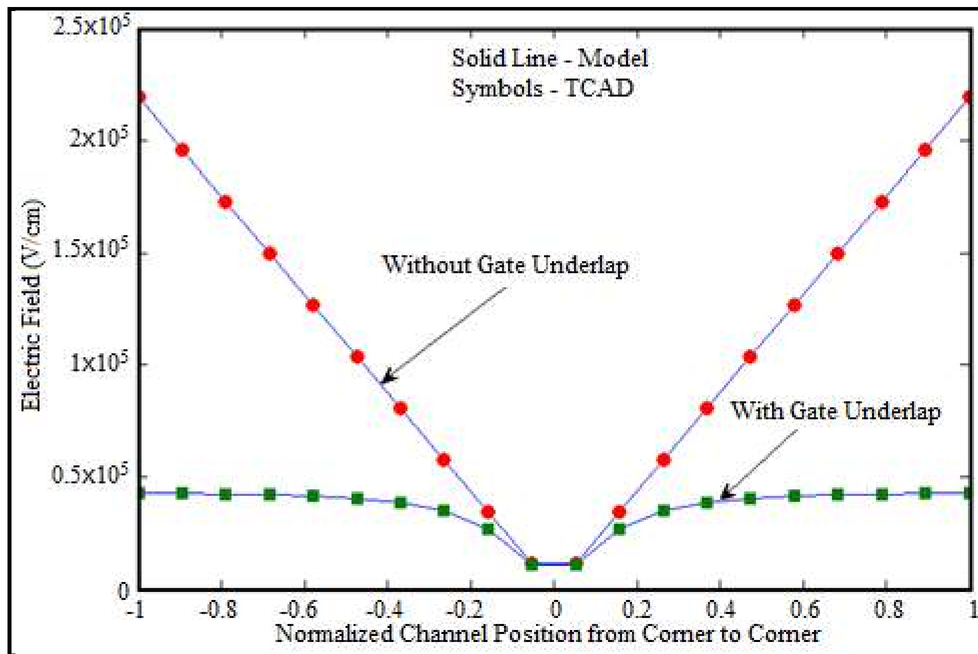

Fig. 6.53: Comparison of electric field variation with channel position for hexagonal JLT with and without gate underlap

Average error = 0.9%

Maximum error =1.3%

Minimum error =0%

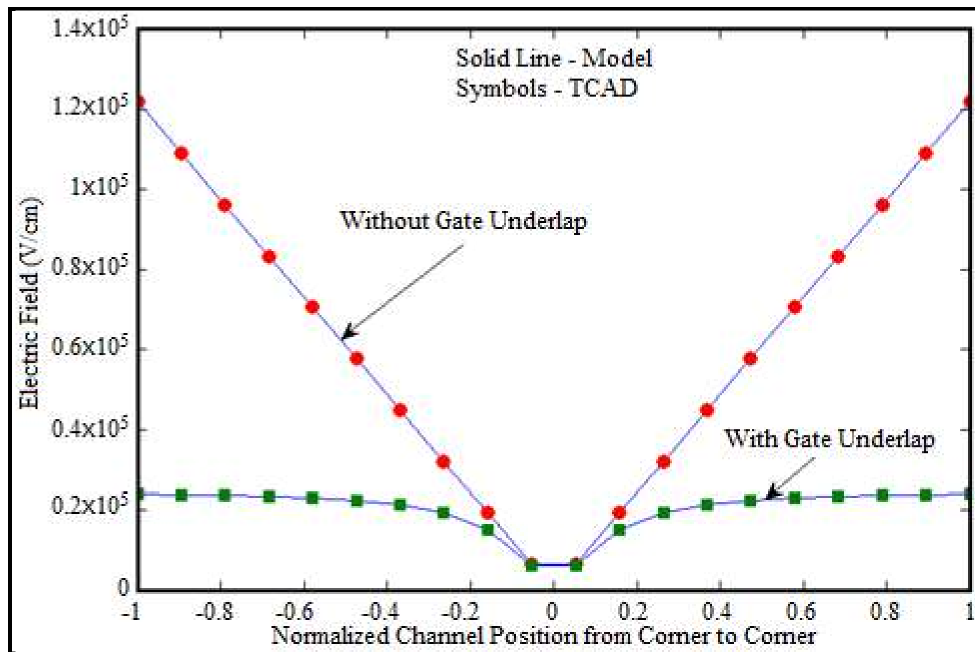

Fig. 6.54: Comparison of electric field variation with channel position for octagonal JLT with and without gate underlap

Average error = 0.9%

Maximum error =1.3%

Minimum error =0%

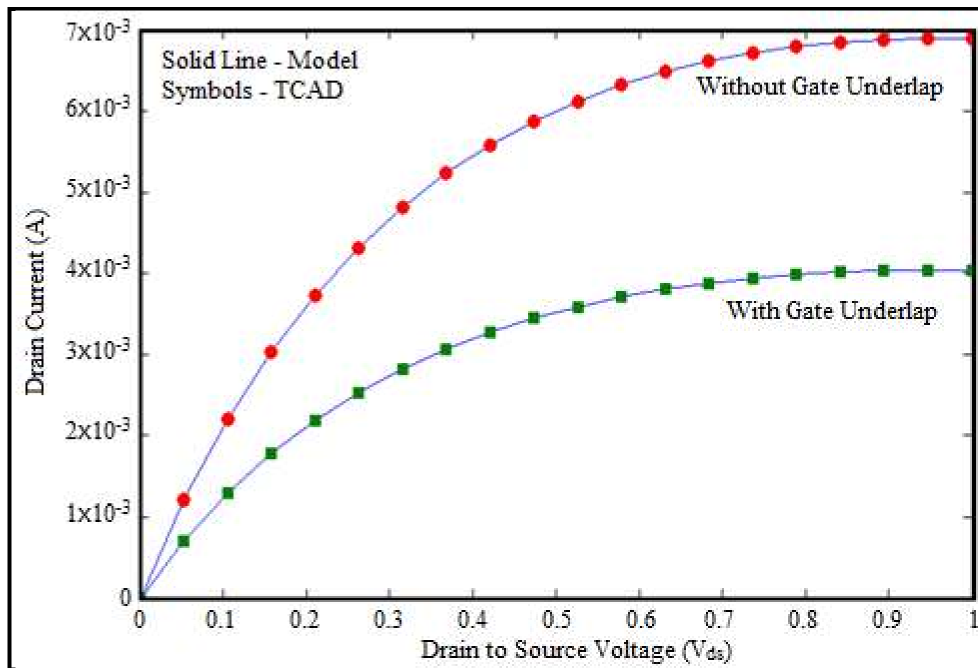

Fig. 6.55: Comparison of output characteristics for rectangular JLT with and without gate underlap

Average error = 0.8%
Maximum error =1.1%
Minimum error =0%

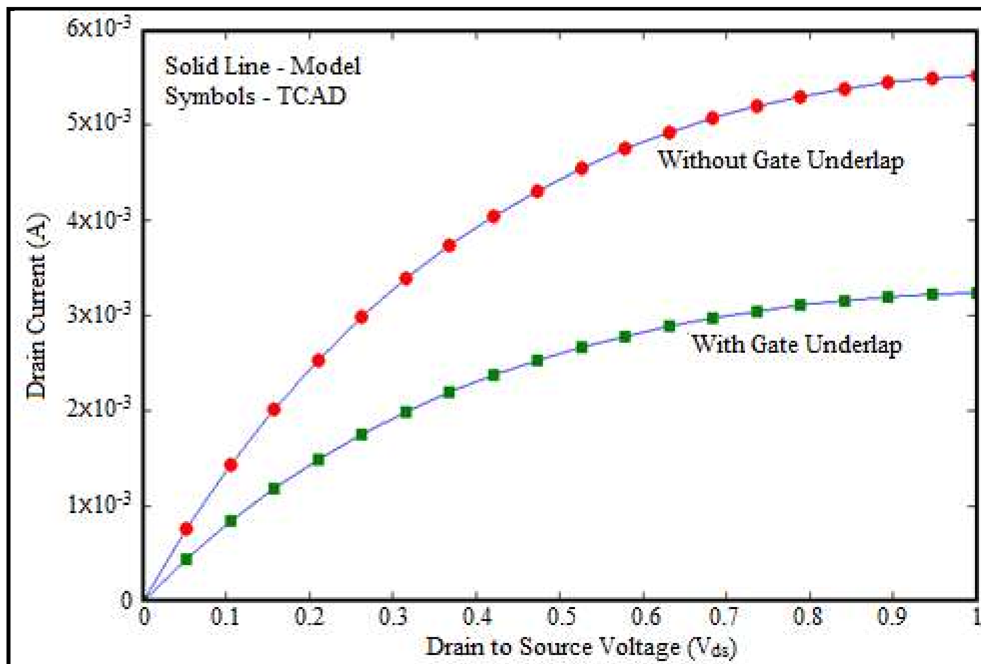

Fig. 6.56: Comparison of output characteristics for pentagonal JLT with and without gate underlap

Average error = 0.9%
Maximum error =1.3%
Minimum error =0%

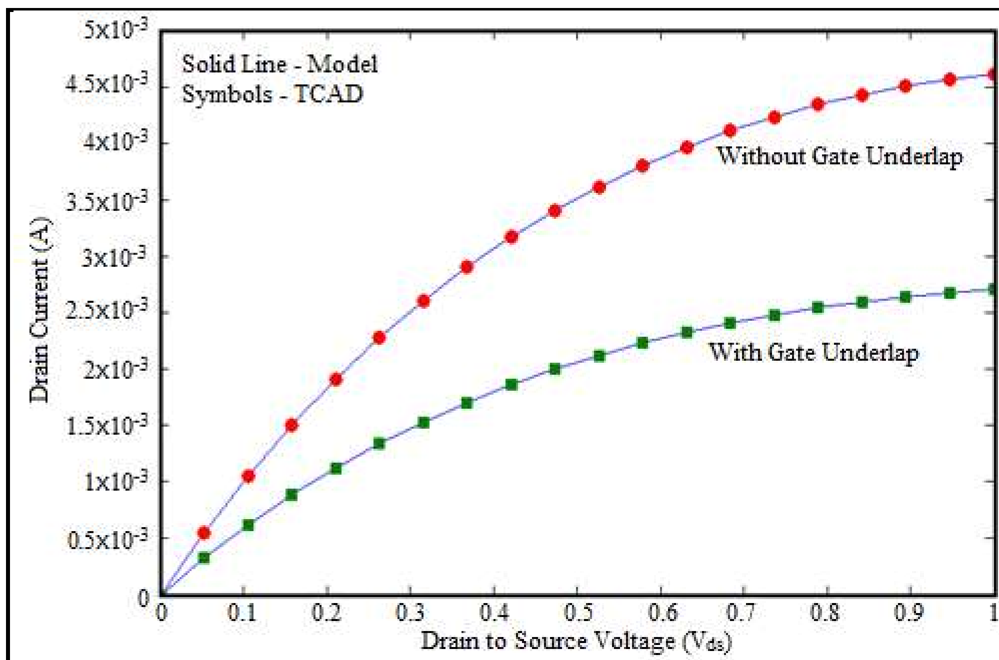

Fig. 6.57: Comparison of output characteristics for hexagonal JLT with and without gate underlap

Average error = 1.1%
Maximum error =1.4%
Minimum error =0%

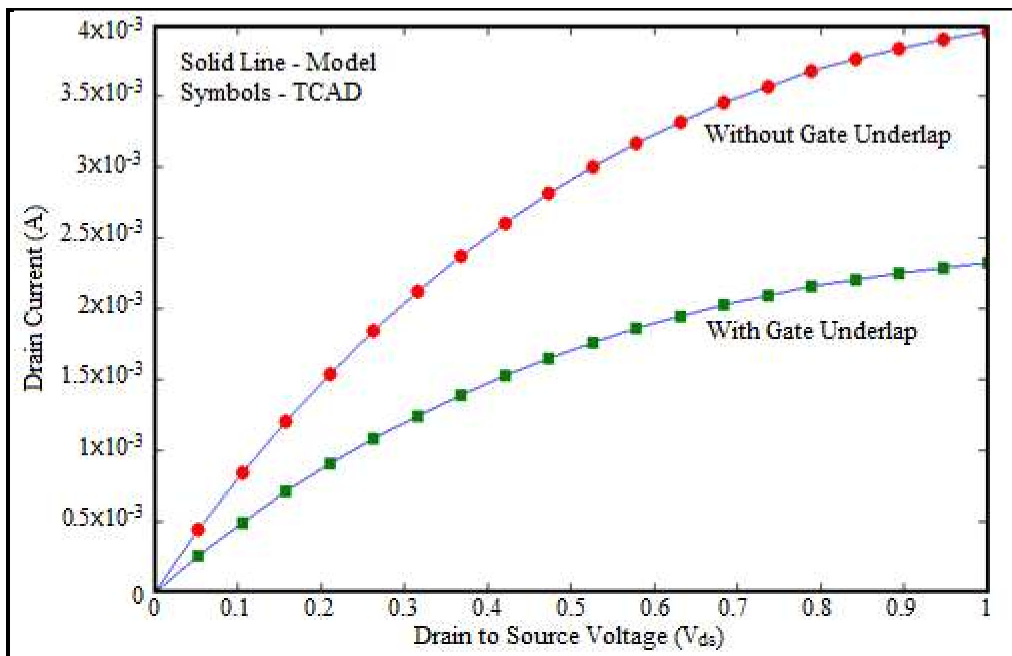

Fig. 6.58: Comparison of output characteristics for octagonal JLT with and without gate underlap

Average error = 0.9%
Maximum error =1.2%
Minimum error =0%

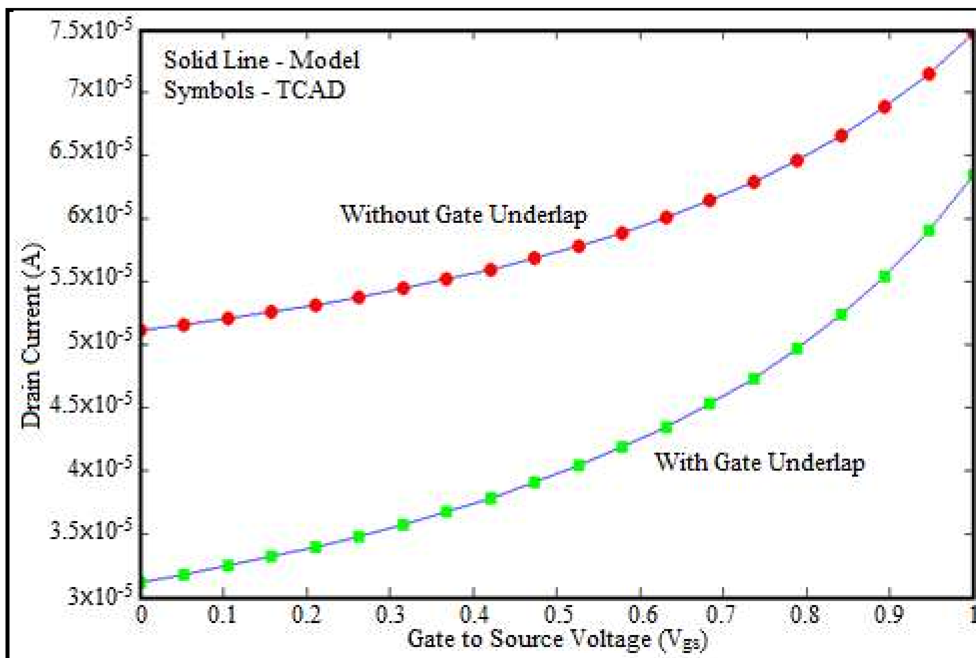

Fig. 6.59: Comparison of transfer characteristics for rectangular JLT with and without gate underlap

Average error = 0.7%
Maximum error =1.2%
Minimum error =0%

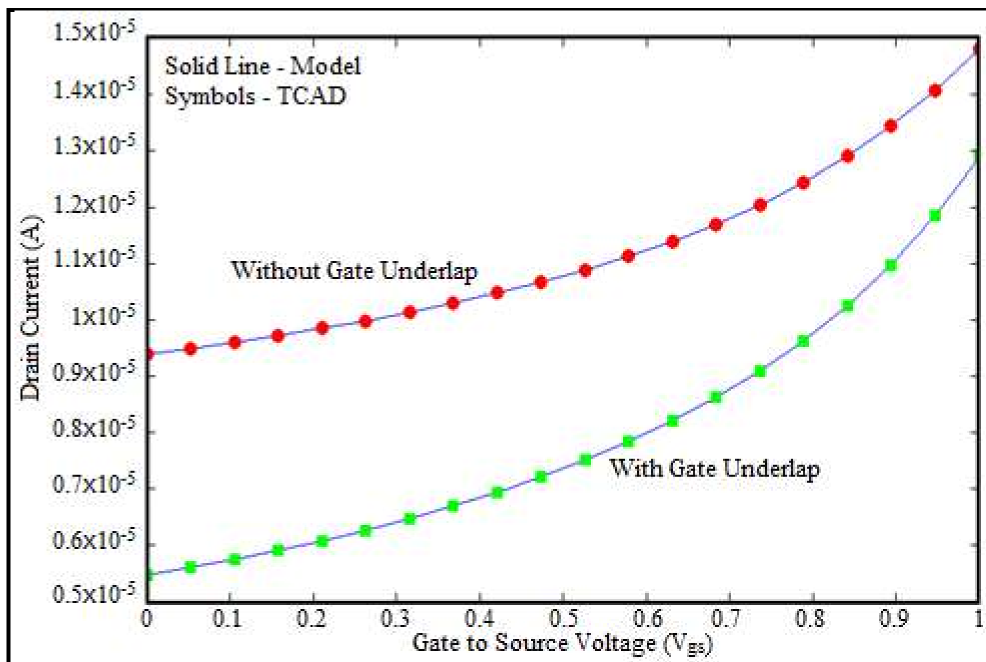

Fig. 6.60: Comparison of transfer characteristics for pentagonal JLT with and without gate underlap

Average error = 0.8 %
Maximum error =1.3%
Minimum error =0%

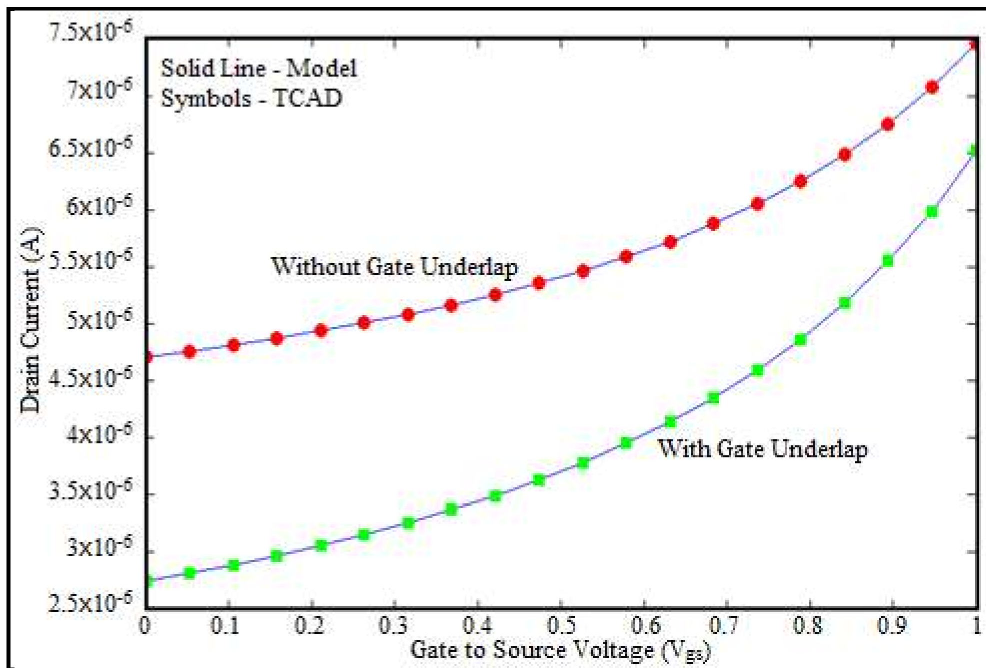

Fig. 6.61: Comparison of transfer characteristics for Hexagonal JLT with and without gate underlap

Average error = 0.9%
Maximum error =1.3%
Minimum error =0%

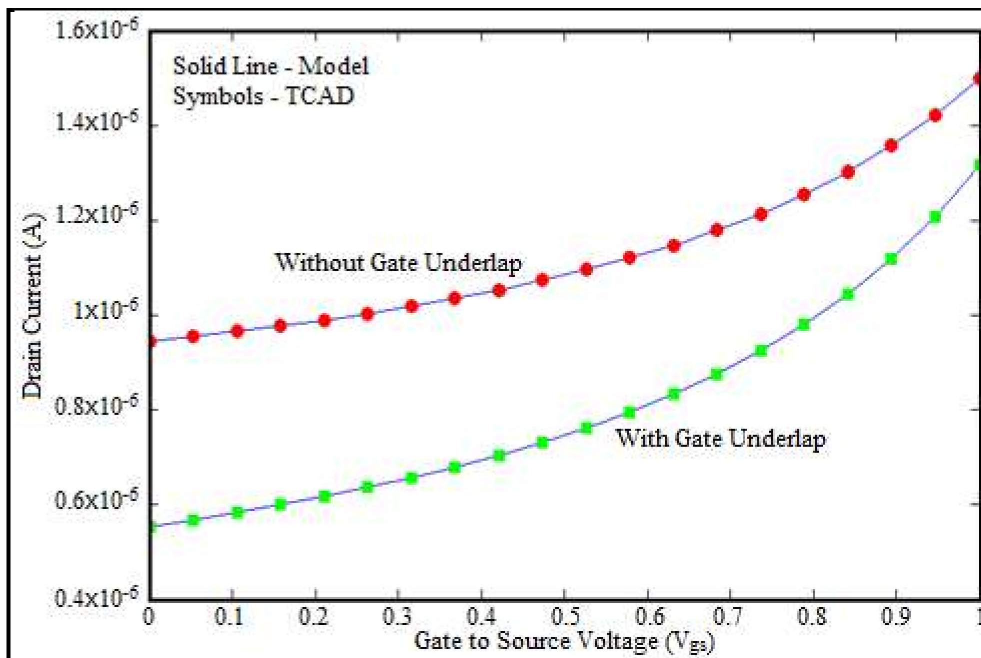

Fig. 6.62: Comparison of transfer characteristics for octagonal JLT with and without gate underlap

Average error = 1.1%
Maximum error =1.5%
Minimum error =0%

6.6 Conclusions

A method for reducing the off state leakage current of a double gate JLT by placing a dielectric layer at the centre has been proposed. The model for the proposed structure has been obtained and compared with simulation results obtained from TCAD. It is seen that the JLT with dielectric layer has lower subthreshold current compared to the conventional JLT. So by using this technique we can achieve proper turnoff even with a lower K gate dielectric and lower work function gate material.

Two techniques for enhancement of carrier mobility are also proposed and the analytical model for the same has also been developed. Simulation study shows that the mobility in the subthreshold region for the proposed structures are less compared to the conventional one while in the on state the proposed structures show much higher mobility as compared to the conventional one. Among the proposed structures the structure with gradual variation of channel doping concentration shows the best results. Transfer characteristics comparison shows that the structure has better subthreshold characteristic also.

A study on corner effect in rectangular, pentagonal, hexagonal and octagonal structures of Gate All Around JLT has also been presented by comparing the electric field variation with position from centre to corner. The study shows that octagonal JLT exhibits minimum corner effect while rectangular JLT exhibits maximum corner effect. A technique for reduction of corner effect has also been presented for the above mentioned structures. The analytical model for the technique proposed has been obtained. The same has been simulated in MATLAB. The results obtained from MATLAB has been compared with the results obtained from TCAD. The simulation shows a reduced corner effect in the structures with gate underlap.

Contributions

This chapter provides a method for reduction of off-state current using dielectric layer of appropriate dimension along the central axis of the device. This chapter also presents technique for carrier mobility enhancement with a function based doping profile. In this

chapter it has been attempted to look at a particular problem found in some non-conventional structures of JLT. A method for corner effect reduction has also been presented in this chapter.

Bibliography

[1] Gundapaneni, S., Ganguly, S., and Kottantharayil, A. Enhanced Electrostatic Integrity of Short-Channel Junctionless Transistor With High-κ Spacers. *IEEE Electron Device Letters*, 32(10), pages 1325-1327, 2011

[2] Baruah, R. K. and Paily, R. A Dual-Material Gate Junctionless Transistor With High-k Spacer for Enhanced Analog Performance. *IEEE Transactions on Electron Devices,* 61 (1), pages 123-128, 2014

[3] Lou, H., Zhang, L., Zhu, Y., Lin, X., Yang, S., He, J., and Chan M. A Junctionless Nanowire Transistor with A Dual-material Gate. *IEEE Transactions on Electron Devices*, 59(7), pages 1829–1836, 2012.

[4] Colinge J. P., Lee, C. W., Afzalian, A., Dehdashti, N., Yan, R., Ferain, I., Razavi, P., O'Neill, B., Blake, A., White, M., Kelleher, A. M., McCarthy B., and Murphy R. SOI Gated Resistor: CMOS without Junctions. In *IEEE International SOI Conference*, pages 1-2, Foster City, California, USA , 2009

[5] Lee, C. W., Afzalian, A., Akhavan, N. D., Yan, R., Ferain, I., and Colinge. J. P. Junctionless Multigate Field Effect Transistor. *Applied Physics Letters*, 94(5), pages 053511, 2009

[6] Nazarov, A., Balestra, F., Raskin, J. P., Gamiz, F., and Lysenko, V.S. *Semiconductor-On-Insulator Materials for Nanoelectronics Applications*, Springer, 2011

[7] Gnani, E., Gnudi, A., Reggiani, S., and Baccarani, G. Theory of The Junctionless Nanowire FET. *IEEE Transactions on Electron Devices*, 58(9), pages 2903-2910, 2011

[8] Colinge, J. P., Lee, H. W., Afzalian, A., Akhavan, N. D., Yan, R., Ferain, I., Razavi, P., O'Neill, B., Blake, A., White, M., Kelleher, A. M., McCarthy, B., and Murphy, R. Nanowire Transistors without Junctions. *Nature Nanotechnology*, 5, pages 225-229, 2010

[9] Colinge, J. P. Junctionless Transistors. In *IEEE International Meeting for Future of Electron Devices*, pages 1-2, Kansai (IMFEDK), 2012

[10] Colinge, J. P., Kranti, A., Yan, R., Lee, C. W., Ferain, I., Yu, R., Akhavan, N. D., and Razavi P. Junctionless Nanowire Transistor (JNT): Properties and design guidelines. *Solid- State Electronics*, 65–66, pages 33-37, 2011

[11] Park, C. H., Ko, M. D., Kim, K. H., Baek, R. H., Sohn, C. W., Baek, C. K., Park, S., Deen, M. J., Jeong, Y. H., and Lee, J. S. Electrical Characteristics of 20-nm Junctionless Si Nanowire Transistors. *Solid-State Electronics,* 73, pages 7-10, 2012

[12] Gnudi, A., Reggiani, S., Gnani, E. and Baccarani, G. Analysis of Threshold Voltage Variability Due to Random Dopant Fluctuations in Junctionless FETs. *IEEE Electron Device Letters*, 33(3), pages. 336–338, 2012.

[13] Duarte J. P., Kim M. S., Choi S. J. and Choi Y. K. A Compact Model of Quantum Electron Density at The Subthreshold Region for Double-gate Junctionless Transistors, *IEEE Transactions on Electron Devices*, 59(4), pages 1008–1012, 2012.

[14] Gnudi, A., Reggiani, S., Gnani, E. and Baccarani, G. Semi Analytical Model of The Subthreshold Current in Short-Channel Junctionless Symmetric Double-Gate Field-Effect Transistors, *IEEE Transactions on Electron Devices*, 60(4), 2013

[15] Li, C., Zhuang, Y., Di, S., and Han, R. Subthreshold Behaviour Models for Nanoscale, Short-Channel Junctionless Cylindrical Surrounding-Gate MOSFETs. *IEEE Transactions on Electron Devices*, 60(11), pages 3655-3662, 2013

[16] Holtij, T., Schwarz, T., Kloes, A., and Iñiguez, B. 2D Analytical Potential Modelling of Junctionless DG MOSFETs in Subthreshold Region Including Proposal for Calculating the Threshold Voltage. In *13th International Conference on ULIS*, pages 81-84, MINATEC Grenoble, France, 2012

[17] Chiang, T. K., A New Subthreshold Current Model for Junctionless Tri-gate MOSFETs to Examine Interface Trapped Charge Effects, *IEEE Transactions on Electron Devices*, 62 (9), pages 2745–2750, 2015

[18] Chiang, T. K., A Quasi-two-dimensional Threshold Voltage Model for Short-Channel Junctionless Double-gate MOSFETs. *IEEE Transactions on Electron Devices*, 59 (9), pages 2284–2289, 2012

[19] Chiang, T. K., A New Quasi-2-D Threshold Voltage Model for Short Channel Junctionless Cylindrical Surrounding Gate (JLCSG) MOSFETs. *IEEE Transactions on Electron Devices*, 59(11), pages 3127–3129, 2012

[20] Trevisoli, R. D., Doria, R. T., de Souza, M., Das, S., Ferain, I., and Pavanello, M. A. Surface Potential Based Drain Current Analytical Model for Triple Gate Junctionless Nanowire Transistors. *IEEE Transactions on Electron Devices*, 59(11), pages 3510–3518, 2012

[21] Baidya, A., Lenka, T. R. and Baishya, S. Performance Analysis and Improvement of Nanoscale Double Gate Junctionless Transistor based Inverter using High-K Gate Dielectrics. In *TENCON 2015 - 2015 IEEE Region 10 Conference*, pages 1-4, Macau, 2015

[22] Colinge, J. P. *FinFET and Other Multi-Gate Transistors*, Springer 2008.

[23] Fossum, J. G., Yang, J. W. and Trivedi, V. P. Suppression of Corner Effects in Triple-Gate MOSFETs, *IEEE Electron Device Letters*, 24, pages 745-747, 2003.

[24] Kumar, M. P., Gupta, S. K. and Paul, M. Corner Effects in SOI-Tri gate FinFET structure by Using 3D Process and Device Simulations. In *3rd IEEE International Conference on Computer Science and Information Technology (ICCSIT)*, 9, pages 704 – 707, 2010.

[25] Xiong, W., Park, J. W. and Colinge, J. P. Corner Effect in Multiple-gate SOI MOSEFT. *IEEE International SOI Conference*, pages 111-113, 2003.

[26] Michielis, L. D., Moselund, K. E., Selmi, L. and Ionescu, A. M. Corner Effect and Local Volume Inversion in SiNW FETs. *IEEE Transactions on Nanotechnology*, 10(4), pages 810-816, 2011.

[27] International Technology Roadmap for Semiconductors 2.0, 2015

[28] Muller, R. S. and Kamins, T.I. *Device Electronics for Integrated Circuits.* Willey, 2002

[29] Uyemera, J. P. *CMOS Logic Circuit Design*, Kluwer Academic Publishers, 2002

[30] Sharma, S. and Chaudhury, K. A Novel Technique for Suppression of Corner Effect in Square Gate All Around Mosfet. *Electrical and Electronic Engineering* ,2, pages 336-341, 2012